QATAR UNIVERSITY

COLLEGE OF ENGINEERING

UV STABILIZATION AND FLAME RETARDANCY OF POLYETHYLENE FOR PIPING APPLICATIONS

BY

REEM MOUDAR ALJINDI

A Thesis Submitted to

the Faculty of the College of Engineering

in Partial Fulfillment of the Requirements for the Degree of

Masters of Science in Mechanical Engineering

June 2019

COMMITTEE PAGE

The members of the Committee approve the Thesis of
Reem Moudar Aljindi defended on 23/04/2019.

Prof. Abdelmagid Hammuda
Thesis Supervisor

Prof. Adriaan Luyt
Thesis Co-supervisor

Prof. Ramesh Singh
Committee Member

Dr. Asan Gani Bin Abdul Muthalif
Committee Member

Dr. John-John Cabibihan
Committee Member

Approved:

Abdel Magid Hamouda , Dean, College of Engineering

ABSTRACT

ALJINDI, REEM, M, Masters: June: 2019, Masters of Science in Mechanical Engineering

Title: UV Stabilization and Flame Retardancy of Polyethylene for Piping Applications

Supervisors of Thesis: Prof. Abdelmagid S. Hammuda, Prof. Adriaan S. Luyt

This work presented an investigation of the ultra violet (UV) stability and flame retardancy of linear low-density polyethylene (LLDPE) and low-density polyethylene manufactured in autoclave process (LDPE-A), that are used widely in irrigation pipes. Two formulations based on new combinations of hindered amine light stabilizers (HALS) and UV absorbers were developed and implemented in LLDPE and LDPE-A for UV stabilization, and six halogen-free flame retardant (FR) formulations were implemented in the two polyethylene (PE) grades for enhancing flame retardancy. The UV-stabilized compounds were tested through an artificial UV weathering experiment that simulated the harsh environmental conditions that irrigation pipes face, and the FR-containing compounds were assessed in terms of fire retardancy through a standard flammability test (UL-94 V0). Mechanical and thermal characterization techniques were employed for both compounds. In terms of UV stability, LDPE-A compounds exhibited a higher stability against UV aging than LLDPE compounds. In terms of flammability, the addition of a triazine derivative and ammonium polyphosphate at a loading of 35 % wt. was found to be the most efficient, leading to UL-94 V0 ranking in LDPE-A.

DEDICATION

I dedicate this work to my loving soulmate, for none of this would have been possible without them by my side.

To my parents, whose love and support knew no bounds.

To my amazing siblings, who were the comforting sunshine in my hardest hours.

ACKNOWLEDGMENTS

First and foremost, I want to sincerely thank my two wonderful supervisors, Prof. Abdelmagid and Prof. Adriaan, for all their help and guidance that have allowed me to finish this piece of work and grow as a person and a researcher.

I wish from the deepest depth of my heart to thank Prof. Elsadig Mahdi and the rest of the faculty and staff at the Department of Mechanical & Industrial Engineering for making my experience as a Masters student a truly unforgettable one.

I dearly send the warmest thank you to my dear friends and colleagues, Eng. Soumia Gasmi and Eng. Sara Shahid, for their support, guidance and fruitful companionship to me during my tenure at the Centre of Advanced Materials.

Finally, I would like the acknowledge the role of Qatar National Research Fund (a member of Qatar Foundation) in financially supporting this study through the National Priorities Research Program NPRP9-161-1-030.

TABLE OF CONTENTS

LIST OF TABLES

LIST OF FIGURES

Chapter 1: Introduction

1.1 Background

Polymers are indispensable contemporary materials used in nearly all areas of daily life. Their application fields comprise commodity products, as well as engineering materials, and they have become essential to modern economy. The global plastics production in 2013 rose to 299 million tons, corresponding to almost 4% increase compared to 2012. The consumption of plastics is expected to reach 540 million tons in 2020 [1]. Among the different types of polymers, polyolefins – specifically polyethylene (PE) – represent the most widely used commodities. Polyolefins consumption reached 170 million tons in 2018, and the Middle East has been reported to be the second fastest growing polyolefins market world-wide [2]. The production of PE amounts to more than one third of the market share of thermoplastics. Polyethylene grades comprise several attractive properties that make them suitable for many applications. Polyethylenes have excellent mechanical and chemical resistance, good electrical insulation, excellent processability, and are low in cost. They are extensively employed in outdoor applications like agriculture applications, specifically the low-density grades of polyethylene; LLDPE and LDPE that are used in irrigation pipes [1,3,4]. However, despite the superior properties that polyethylene possesses, having them continuously exposed to harsh climatic conditions, specifically ultraviolet (UV) radiation, can alter most of their features and significantly reduce their mechanical and physical integrity [5–12].

Polyethylene pipelines are the basic component of irrigation networks in farm-level irrigation systems [1,4,13,14]. In Qatar, there are kilometers of PE pipes that are replaced every six months due to degradation as a result of heat, humidity and UV radiation (Figure 1.1). Weathering initiates photo-degradation, that can lead to a

significant loss of mechanical strength and reduction of ductility and physical properties. As a result, the useful lifetime of the product can be drastically reduced. Furthermore, replacing these pipes should be very expensive, and disposing the used pipes adds to the already serious environmental problem which faces the earth. Qatar produces 400 tons landfill per day [15]. which counts amongst the highest in the world. A significant part of this landfill consists of disposed plastics that could have been in use for longer periods of time if properly treated.

Figure 1.1 Polyethylene (PE) thin irrigation pipes, used in Qatar.

Several factors dictate the severity and rate of photo-degradation; exposure to sunlight, temperature, moisture (i.e. rain and humidity) and the geographical location. The last factor is important, since there are fewer negative effects where the intensity of the radiation is low, and the number of sunlight hours per year is less. For example, a period of exposure in Arizona is more damaging than in New Hampshire because of the additional hours of UV exposure and, to the higher ambient temperatures faced [16]. In this perspective, it is important to mention that most of the polymer weathering studies, involving evaluation of polymers' durability with the addition of UV stabilizers, are mainly based on climate conditions deviating significantly from the particular case of Middle East countries, like Qatar. Accordingly, the relevant systems can be further developed to lie within

the higher requirements for countries with high temperature, humidity and sunlight exposure, like Qatar.

Moreover, as there is a periodical replacement of PE irrigation pipes, the new pipes are always stored in warehouses, which may pose a serious flammability problem. Polyethylenes are among the most flammable polymers, with a high heat of combustion, low limited oxygen index (LOI), and high heat release, leaving little or no residual char. To improve the flame resistance, halogen-containing flame retardants (HFRs), such as various brominated FRs are mainly used in combination with antimony oxide, due to their efficiency at low loadings (1-2 % wt) and their low cost [17,18]. Nevertheless, HFRs present significant disadvantages, namely corrosion of the equipment during processing, production of toxic and potentially carcinogenic gases during combustion, and environmentally unsafe disposal for water and soil. On the other hand, other flame retardant solutions such as aluminum hydroxide and magnesium hydroxide are more environmentally friendly, but need to be added to the polymer in high loadings (above 50 wt.%). These high levels impair negatively on the mechanical, physical and rheological properties as well as the processing ability of polyolefins [17]. On the other hand, halogen-free FRs such as phosphorus- and nitrogen-based compounds, including intumescent flame retardant systems (IFRs), present a viable alternative [19–21]. The halogen-free FRs can be tested on polyethylene to replace the conventional halogen-containing compounds, at suitable loadings, without compromising flame retardancy and overall material performance, like mechanical properties.

1.2 Problem Statement

Polyethylene has become an indispensable material that represents the most widely used commodities. One of the essential applications of polyethylene is the irrigation pipes, that are the basic component of farm-level irrigation networks worldwide. The irrigation systems in Qatar employ polyethylene pipes in gardens and farms. However, the outdoor exposure of polyethylene to harsh environmental conditions such as UV radiation and humidity, deteriorates its mechanical durability and alters most of its physical and rheological features. Therefore, the useful lifetime of polyethylene pipes is drastically reduced, imposing periodical replacements (every six months) that are expensive and add to Qatar and the world's current landfill problem. Moreover, the new pipes are always stored in warehouses, which gives rise to flammability concerns, as polyethylene is one of the most flammable materials. Therefore, polyethylene pipes need to exhibit both high weathering resistance and low flammability.

1.3 Aims and Objectives

The proposed project falls under the umbrella of the National Priorities Research Program, NPRP9-161-1-030. The final aim is to design and develop novel, tailor-made polyethylene formulations exhibiting both low flammability and high weathering resistance, suitable to add value to typical commodity plastics and to efficiently penetrate the Qatar and other world markets. The objectives of this masters research project were set towards the achievement of the final aim of the bigger project. This project covers the following objectives:

- Study the effect of UV exposure on the mechanical and thermal properties of linear low-density polyethylene (LLDPE) and a low-density polyethylene grade (LDPE-A).

- Investigate two UV stabilization formulations for the LLDPE and LDPE-A.
- Investigate several halogen-free flame retardant (FR) formulations for the LLDPE and LDPE-A.
- Evaluate the effect of the FR formulations on the mechanical properties of the LLDPE and LDPE-A.

1.4 Thesis Outline

The thesis is divided into six chapters, including this chapter that introduces the project and gives a brief background to the problem. The second chapter comprises a thorough literature review, which covers various topics and presents several studies related to the UV stabilization and flame retardancy of polyethylenes. The third chapter presents the materials and methods employed in the project, and a description of all the conducted analyses and characterization techniques for both UV and FR stabilized compounds. The fourth chapter presents all the analysis related to UV stabilization of the polyethylenes, along with the results and discussion of all the findings. The fifth chapter outlines all the analysis related to the flame retardancy work. Finally, the sixth chapter concludes and elaborates the findings of chapters 4 and 5 and highlights the optimal solutions that were found. Further recommendations for future work are presented in Chapter 6.

Chapter 2: Literature Review

2.1 Polyethylene

2.1.1 Structure and morphology of polyethylenes

Polyolefins are thermoplastic polymers produced by the polymerization of olefin monomers, such as ethylene, propylene, and butene. Polyolefins are made up of chains of carbon and hydrogen atoms only, that could be with side branches or without. Polyethylene (PE) has a simple repeated chemical structure in a single molecule (-CH_2–CH_2-) as shown in Figure 2.1. It is produced by the polymerization of ethylene monomers. The structure of PE comprises long chainlike molecules of hydrogen atoms connected to a carbon backbone, which can be produced in either branched or linear forms [1,22].

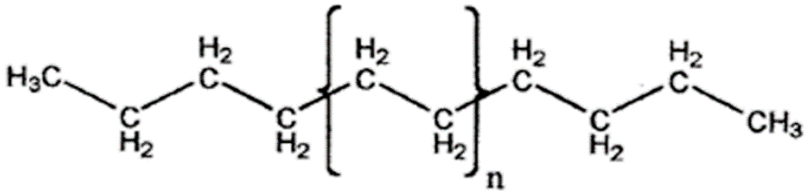

Figure 2.1 Chemical structure of neat polyethylene [22].

The morphology refers to the size and shape of the crystals, which determines most of the properties of the polymer. Crystallinity is a measure of structural order in a solid material. PE is a semi-crystalline polymer, which makes it an excellent option for a variety of applications worldwide. The part of the structure that provides the polymer with strength and integrity is called crystalline lamellae, which is the neat packed chains in the structure of the polymer. The amorphous parts are the other randomly distributed chains, and they are responsible for providing the structure with elasticity and ductility. An illustration of the semi-crystalline structure is shown in Figure 2.2 [23–25].

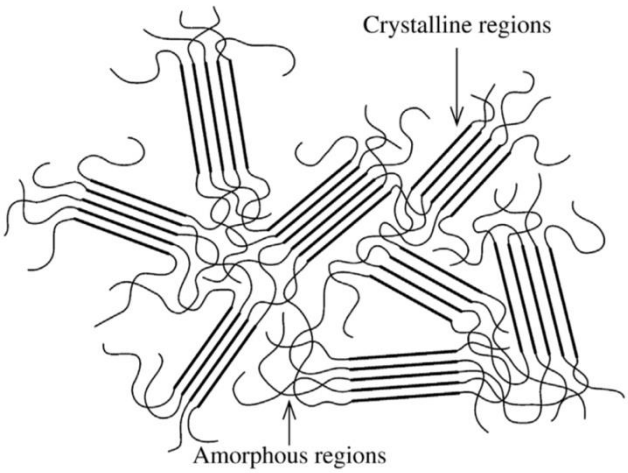

Figure 2.2 Model of the structure of a semicrystalline PE.

Polyethylene is increasingly used in different applications due to its attractive properties. It is a flexible, odorless and non-toxic polymer. It has excellent electrical insulation, and excellent mechanical and chemical resistance. It has good toughness and processability, in addition to being low in cost. It is extensively used in outdoor applications, and load-bearing applications like packaging [1,22].

2.1.2 Grades of polyethylene

Nowadays, polyethylene exists in several grades that vary in mechanical, rheological and thermal properties. Although these variations arise chiefly from chain branching, that are produced during polymerization, there are other factors that dictate the type of a polyethylene. Density, melt flow index (MFI), type of manufacturing process and catalyst used during production, along with degree of branching are used to classify polyethylenes [3,22].

Branching disrupts the packed crystalline regions in the polymer structure. For instance, a higher degree of branching decreases the size of crystalline regions and leads to lower crystallinity. Crystallinity is directly proportional to the polymer's strength and stiffness. A polyethylene structure with high crystallinity is generally

higher in density, stiffness and strength, but lower in impact toughness. Polyethylene branching is controlled mainly by the type of catalyst employed during the polymerization process, and the addition of a monomer during polymerization in some cases like LLDPE. Short chain branching (SCB) and long chain branching (LCB) are two types of branching that dictate the grade of a polyethylene. SCB refers to the branches generated due to the introduction of a comonomer, while LCB refers to the branching formed as a result of side reactions during the polymerization process (i.e. polymerization of ethylene). High-density polyethene (HDPE), low-density polyethylene (LDPE) and linear low-density polyethylene (LLDPE) are three major grades of PE that are widely used for a variety of applications. Figure 2.3 shows a schematic illustration of the structures of the three polyethylene grades. HDPE is the most linear form of the three PE grades with a minimum SCB content. LLDPE is a linear form that has a higher amount of SCB than HDPE, while LDPE is known to have both types of branching; SCB and LCB in high content. However, the SCB formed in LDPE chains are due to the polymerization of ethylene. For instance, ethylene in LDPE polymerizes as chain with branches which are the LCB, and the SCB are formed on the ethylene long branches. The existence of SCB interferes with the formation of the crystalline part of the structure, lamellae. This is because the lamellae are uniformly packed chains, and the presence of branching, especially SCB, does not allow the chains to fold and form packed segments. In contrast, a structure with few SCB is more capable of crystalizing than those with high SCB content. Consequently, HDPE and LLDPE are known to be more crystalline than LDPE [22–24].

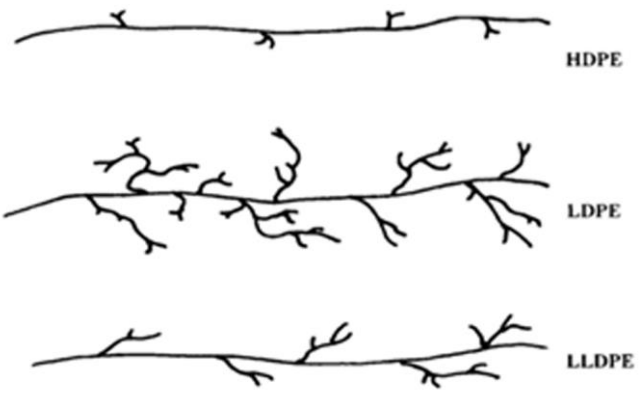

Figure 2.3 Molecular chain characteristics of the three common types of PE [23].

2.1.2.1 Linear low-density polyethylene (LLDPE)

LLDPE is one of the major grades of polyethylene that is made by copolymerization of ethylene with olefins of longer chains; comonomers, such as butene, hexene and octene. The structure of LLDPE comprises short chain branches (SCB) only as shown in Figure 2.4, which makes it more crystalline than LDPE. The increased crystallinity increases the density and hence makes LLDPE stiffer than LDPE. It possesses superior tensile and impact strength, and is considered more ductile and resistant to puncture than LDPE [1]. It is extensively employed in agriculture applications such as greenhouse films and irrigation pipes. It is also used in automotive parts, tubing, packaging bags and bottles [4]. It has been reported that the production capacity of LLDPE has increased more than five times than that in 2000 in the Middle East region only [26].

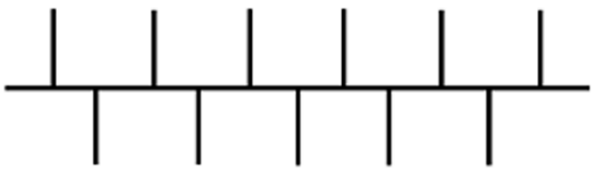

Figure 2.4 LLDPE chain structure [23].

2.1.2.2 Low-density polyethylene (LDPE)

LDPE can be manufactured in an autoclave (batch process) (LDPE-A) or in a tubular reactor (continuous process) (LDPE-T). The two LDPEs differ in the type and level of long-chain branching and in the molecular shape as shown in Figure 2.5 [23]. LDPE-A is produced at a constant temperature and under practically ideal mixing, and presents short- and long-chain branching points that are randomly distributed along the chains regardless of the molecular weight; LDPE-A molecules display tree-like branching and a seemingly globular shape. LDPE-T is produced under variable conditions (not a constant temperature) and demonstrates a relatively narrower distribution of molecular weight, but a considerably wider distribution of both the long- and short-chain branching [24].

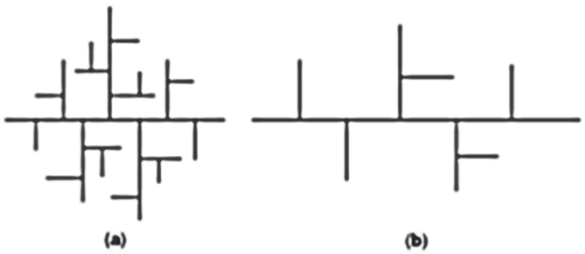

Figure 2.5 Autoclave produced LDPE-A and (b) tubular reactor produced LDPE-T.

2.1.3 Consumption of polyethylene

The production of PE contributes to a grand total of over one third of the market share of commodity thermoplastics. The estimated production capacity of PE in 2010 is shown in Figure 2.6 [1]. In 2012, the production of PE exceeded 70 million tons with 25% LDPE, 30% LLDPE and 45% HDPE [1]. In 2014, the Middle East produced 1.9 million tons of LDPE, compared to the world production of 23.3 million tons. Polyolefins consumption is anticipated to reach 170 million tons by 2018, and the Middle East has been reported to be the second fastest growing

polyolefins market world-wide [27]. In 2009, Qatar produced 549,000 tons of LDPE and 273,000 tons of HDPE. Currently, the annual production of the three grades of PE (LDPE, LLDPE and HDPE) in Qatar is more than 2 million metric tons [28].

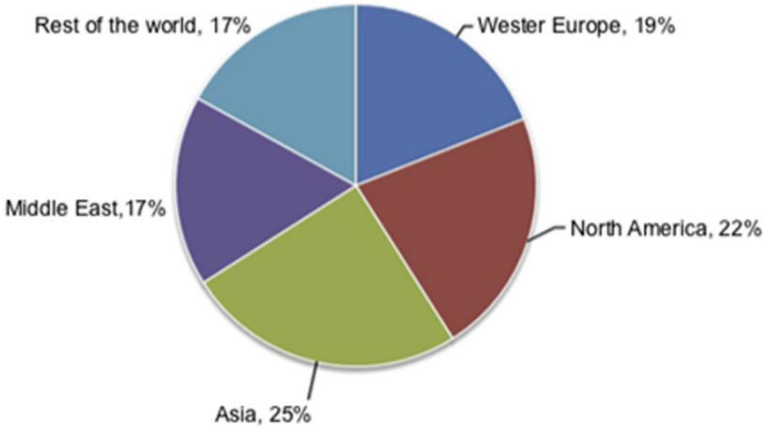

Figure 2.6 Geographical breakdown of production capacity of PE in 2010 [1].

2.2 UV-Weathering and Stabilization of Polyethylenes

2.2.1 Photodegradation of polyethylenes

Despite the high tear strength and stress cracking resistance that both LLDPE and LDPE possess, having them continuously exposed to harsh climatic conditions can alter most of their features and reduce their mechanical integrity [5–7]. It has been shown by several studies that the exposure to ultraviolet (UV) radiation has led to increased crystallinity, density and hardness, coupled with deterioration in mechanical integrity (tensile, flexural, impact and ductility) and physical properties (yellowing, reduced transparency, cracking) in both LLDPE and LDPE [7,8,10–12, 29–33].

Oxidative photodegradation (or photo-oxidation) of polymers is a light-induced degradation that is produced by light radiation – specifically UV radiation, in the presence of oxygen, which is mostly the result of natural weathering. Polymers

exposed to oxygen with the presence of radiation undergo severe and faster degradation than those without a radiation exposure. One of the major differences between oxidation and photo-oxidation is that the second one introduces carbonyl, vinyl, peroxide, carboxyl, and/or hydroxyl groups to the polymer, which propagate and accelerate the degradation. Most of these groups are light-absorbing groups. Hydroperoxide is one of the photodegradation products that is capable of absorbing UV radiation 300-500 times more than pure elastomer [34]. Along with UV radiation, other environmental and climatic conditions play a significant role in accelerating the degradation of polymers. High temperatures, humidity and variations in wind, atmospheric gases, mechanical stresses, and the geographical location influence the weathering significantly and accelerate the photodegradation of polyethylenes [35].

According to [36], one or more of the following chemical processes take place in the polymer chains as a result of photo-degradation:

- Random chain scission – chain scissions at random locations of the chains (splitting of polymer chains into fragments).
- End-chain scission – when monomer units are cleaved up from the chain ends.
- Cross-linking – the generation of bonds between the polymer chains.
- Chain stripping – atoms or groups that are not connected to the polymer backbone are cleaved off.

Polyethylenes are known to undergo chain scissions and cross-linking as a result of photodegradation [33,36].

2.2.1.1 Types of UV-radiation

UV-radiation is classified into three types based on the wavelength of light [35]:

- UV-A (wavelength of 315 - 400 nm)
- UV-B (wavelength of 280 – 315 nm)
- UV-C (wavelength of 200 – 280 nm)

UV-B and UV-C are more energetic radiations due to their shorter wavelengths. Both UV-B and UV-C are absorbed by the atmosphere, but a very little amount of UV-A is absorbed by the ozone layer. Therefore, the type of radiation that is behind the photodegradation of polymers during weathering is UV-A (i.e. radiations with wavelength range of 315-400 nm).

2.2.1.2 Mechanism of polyethylene degradation

The photodegradation of polyethylene due to weathering was explained in a series of initiation, propagation, and chain branching reactions. Generally, the initiation of photodegradation of polymers can be attributed to photolysis of hydroperoxide groups. The photodegradation mechanism is explained as follows:

- Alkyl free radicals ($R\bullet$) are formed as a result of the removal of hydrogen from the polymer chain (RH) by the act of either light, heat, additives, fillers, shear, or catalyst residues. In the case of UV aging, photons are the main initiators of the degradation reaction.
- The free radicals react with oxygen so that new reactive species are formed.

$$O_2 + R\bullet \longrightarrow ROO\bullet + RH$$

$$ROO\bullet + RH \longrightarrow ROOH + R\bullet$$

H_2O , H_2 , H_2O_2 are also formed in the process.

- The primary oxidation product hydroperoxide ($ROOH$) is unstable and reactive. It decomposes into new free radical species like alkoxy and hydroxyl radicals, that later participate in the chain reaction.

$$ROOH \longrightarrow \bullet\mathrm{OH} + RO\bullet$$

- Even a small amount of the free radicals can lead to intense oxidative degradation, as the reaction has a chain nature. This process is usually referred to as autoxidation [37].

The propagation of the reaction in polyethylene leads to either chain scission and/or cross-linking. Chain scission happens when the chains become weak and consequently cut at their reactive points where the free radicals are. The chain scissions lead to increased melt flow index and reduced molecular weight. Crosslinking happens when the free-radicals combine together in the chains, leading to increased viscosity. For example, alkyl free radicals combine when they are close to each other [34,37]. Furthermore, it has been proven that both thermal and photodegradation share the same mechanism, except for the initiation stage of the reaction. Thermal degradation is initiated by heat and is carried out by a homolytic scission of the carbon-hydrogen bonds in methylene groups. On the other hand, photooxidation is initiated by UV radiation of wavelength longer than 290 nm [37].

In summary, the photodegradation of polymers due to outdoor weathering is a set of complex reactions and depends on the structure and morphology of the polymer, the wavelength and intensity of radiation, environmental conditions and other factors like the presence of certain additives or metallic traces during the manufacturing process of the polymer. The UV radiation breaks the C-C and/or C-H bonds in the

polymer which result in the production of free radicals that propagate the chain reaction. As a result of this, one or more of the following chemical changes take place in the polymer: chain scission, crosslinking, photolysis, separation of small molecules (like carbon monoxide, carbon dioxide, water, etc.), and depolymerization [37].

UV-exposed polyethylenes are susceptible to photodegradation by free radicals through chain scissions and/or cross-linking between chains. These two reactions affect the mechanical integrity, crystallinity and molecular weight of polyethylenes. Moreover, localized increases and decreases in density that lead to cracks and macroscopic failure of the polymer are the result of chain scissions and cross-linking reactions. The unbranched (linear) grades of polyethylene are more susceptible to cross-linking reactions as a result of weathering [38].

Different structures of polyethylene react differently to UV radiation. For instance, it has been reported that the highly branched LDPE is more susceptible to degradation than LLDPE, as the amorphous areas of the polymer's structure degrade easily. Hence, a structure with a high amount of crystalline areas is more difficult to degrade [34, 35, 38].

2.2.2 UV-weathering studies

The photodegradation of polyethylene has been investigated for years using different approaches to establish a thorough understanding and assessment of the polymer performance outdoors. Polymer weathering has become one of the established methods for understanding polymers' reaction to real climatic parameters [5]. UV-weathering analysis can be performed outdoors or by using accelerated artificial UV-weathering equipment. Weathering of polyethylenes has been performed in

various trends such as analyzing virgin polyethylene [10,30], polyethylene in blends [10,39,40], polyethylene with different light stabilizing additives [5,10,41–43], or with nanoparticles [12,44–46].

Outdoor natural weathering is exposing samples to real climatic conditions for a long period of time so that the sample experiences the climatic variations throughout the year. The test aims to evaluate a material's resistance to real environmental conditions, which can give an assessment of the product's durability prior to manufacturing. There are several factors influencing the outdoor weathering; temperature, light intensity, level of humidity, wind, and rain. All these factors are affected by geographical locations and seasonal variations [47]. Consequently, to obtain adequate and accurate results from an outdoor weathering test, the weathering should be conducted in a geographical location that allows the sample to experience at least the same level of conditions that it will experience during its service lifetime. Outdoor weathering studies are more expensive and require longer periods of exposure that can last for years to simulate all seasonal changes, unlike the artificial accelerated weathering that can simulate real climatic conditions in shorter periods and at a lower cost [48].

Accelerated weathering tests are done in laboratories in which the samples are exposed to intense artificial conditions to evaluate their durability and resistance to harsh environmental conditions in shorter periods of exposure. Nowadays, different weathering machines are employed to simulate all the critical environmental factors affecting durability; temperature, UV radiation that can be provided by either fluorescent tubes or xenon arc, light/dark cycling, and humidity. Most of the UV weathering machines operate by employing repeated cycles of heating, UV exposure and condensation, to simulate real outdoor conditions as closely as possible.

Moreover, these machines can be set to different standards, allowing the simulation of different climates and varying parameters. Additionally, employing artificial weathering allows effective quality control of the test conditions and samples' status. Typical periods of exposure in artificial weathering experiments are 1000-2000 lamp hours, and can be extended if needed [38,48].

Outdoor and artificial weathering studies were conducted on both LLDPE and LDPE samples to examine their UV and thermal stability in different trends. First of all, samples from both polymers experienced up to 60% reduction in different mechanical properties as a result of outdoor exposure for six months [30], and artificial exposure for 1600 h [7]. The latter study indicated that LLDPE is relatively more stable than LDPE against aging.

Weathering studies were also conducted to assess the performance of different light stabilizers in LLDPE and LDPE. Physical loss of hindered amine light stabilizers (HALS) was reported after 600 days of outdoor exposure of LDPE films [43]. Moreover, [5] conducted an outdoor weathering study to evaluate the performance of light absorbers and HALS in LLDPE and LDPE films. It was observed that a synergistic combination of both types of additives has led to a higher stability. In another study, LLDPE/LDPE blends experienced reduction in tensile properties and formation of carbonyl group after 270 hours of artificial UV weathering [39]. It was also shown that neat LLDPE degrades slower than blended LLDPE [10,39,49].

2.2.3 Mechanisms of photostabilization

Photostabilization or UV stabilization of polymers is meant to prevent or reduce the degradation of polymers caused by the exposure of light and other harsh environmental conditions like heat and humidity. Photostabilization refers to the inhibition or retardation of the photo-oxidation process by interrupting its

mechanism, by reducing the chain length of propagation or/and reducing the rate of photo-initiation. Different additives can be employed to photo-stabilize polymers, like light absorbers, light stabilizers, and nanoparticles [50].

2.2.3.1 Antioxidants

Antioxidants (AOs) operate by interrupting the propagation of the autoxidation reaction; specifically the free-radical reactions. These additives are essential and usually added to the polymer during the polymerization process. AOs are classified by function as primary and secondary. Primary AOs are free radical scavengers as they work by consuming the free radicals, while secondary AOs combine with the secondary hydroperoxide species formed during the oxidation. Primary AOs provide a hydrogen atom to the unpaired election in the free radical. This makes the radical stable, and the AO a radical. The AO has a structure that makes it more stable than other radicals, and this leads to interrupting the propagation of the radical reaction in the polymer chains. Moreover, the radical AO can pair with other free radicals, creating new stable chemical species. Some primary AOs provide stability for melt-processing only, and are not suitable for long term stability [37,50].

One of the most popular and widely used primary antioxidants is hindered-phenol. This family of antioxidants operates using its reactive hydroxyl (OH) group, that allows the structure to stabilize the free radicals by donating a hydrogen atom from the hydroxyl group. This action makes the AO itself stable by transforming it into a phenoxy radical, preventing the formation of new radicals in the chain. These AOS are usually added to the polymer to enhance its performance and thermal stability during processing, especially when the applications employ high temperatures. They can also be employed for improving the long-term thermal stability. However, the use of hindered-phenol antioxidants leads to undesired changes in the polymer's

properties. This happens as the phenolic AOs undergo oxidation to stabilize the chain, leading to yellowing or gas fading that increase with processing. Also, these AOs can under some conditions lead to degradation. For example, at high processing temperatures, they can combine with oxygen to form peroxy radicals which lead to degradation. The remaining metal catalyst residues from the polymerization process can also oxidize hindered phenols and lead to degradation [37].

Phenol-free antioxidants were developed to overcome the discoloration issues of the phenolic-based ones. They also act as free radical scavengers and can be employed in different polymers to enhance the long term thermal stability. These phenol-free stabilizers are referred to as hindered amine light stabilizers (HALS) [34,37].

2.2.3.2 Hindered amine light stabilizers (HALS)

HALS are long-term photo-stabilizers. The development of HALS started when the stable nitroxyl radical (2,2,6,6-tetramethylpiperidine-N-oxyl) was prepared in 1959. This radical was found to be an efficient inhibitor of the oxidation of organic materials. Tinuvin 770 and Sanol LS770 were the trade names of the first HALS structure (HALS-1) released to the market in 1974 [33]. It has been shown that the use of HALS as long-term light and thermal stabilizers lead to gradual deterioration in mechanical and physical properties with aging, unlike the phenolic-based antioxidants that cause a sudden failure [37].

Nowadays, there are different forms of HALS that differ in structure and effectiveness. However, all HALS share the 2,2,6,6-tetramethylpiperidine ring structure that provides them with the ability to scavenge the radicals formed by UV exposure. Generally, the HALS mechanism is based on their participation in the peroxide and hydroperoxide decomposition, and carbon radical trapping [51]. In

fact, a lot of research has been conducted to establish a defined mechanism of action for HALS, in which many different mechanisms were developed. However, there is still no consensus on a specific mechanism of HALS, as it is circumstances dependent. It has been shown that the results may significantly differ depending on the polymer's structure, source of light, and different degradation conditions. from one polymer to another [52].

In the early stages of HALS development, it was found that HALS do not absorb the UV radiation. Denisov cycle was the first proposed mechanism that explained the mode of action of HALS. It stated that HALS can operate by trapping the free radicals generated during photo-oxidation by producing the piperidinoxyl radicals (nitroxide) (Figure 2.7) [33,52].

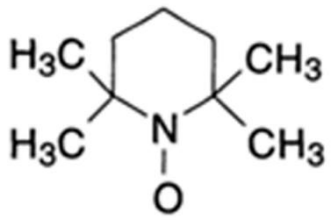

Figure 2.7 Stable 2,2,6,6-tetramethylpiperidine-N-oxide radical [33].

Further experiments showed that the mode of action of HALS comprise a set of complex reactions. In summary, HALS operate by a combination of reactions in which free radical scavenging, generation of charge transfer complexes (CTC) with oxygen, and hydroperoxide deactivation are the main activities taking place. The stabilization efficiency of HALS is affected by the presence of other additives in the polymer, such as halogen flame retardants or thioethers co-stabilizers [33]. It has been concluded that the efficiency of HALS as UV stabilizers is ascribed mainly to their radical scavenging ability, which is achieved by the formation of the nitroxide,

and its ability to regenerate, so it does not get consumed quickly and lasts for longer periods than any ordinary antioxidant [52].

Multiple weathering studies approved the efficiency of HALS as light stabilizers. HALS were examined as stand-alone, and in combination with other additives. An advantage of high molecular weight HALS, except for their low migration rate, is their contribution to long-term thermal stability of polyolefins. Combinations of different HALS have been examined on synergism or antagonism [41,43,53,54], as well as combinations thereof with UV absorbers, in some of which, synergistic effects were observed [5,31,55]. It was found that combining a HALS (Tinuvin 1577) with a UV absorber (Chimassorb 2020) has led to a better UV stability in LDPE films [55]. Moreover, better UV stability was achieved with formulations containing synergistic combinations of HALS and UV absorbers in LLDPE and LDPE films [31]. Besides providing polyolefins with UV stability, high molecular weight HALS was able to also provide long term thermal stability [43,51–54]. HALS-3 or Chimassorb 944 was employed in LLDPE and LDPE films, and provided improved UV and thermal stability in all the studies [43,53,54]. It was also found that Chimassorb 944 was able to reduce the carbonyl index, which is an indicator of photodegradation, in UV exposed LLDPE films [56]. The combination of HALS and antioxidants was also examined in LDPE films, in which a synergistic effect was reported [54].

2.2.3.3 Light absorbers

UV absorbers operate by absorbing the damaging UV radiation before it reaches the photoactive species in the polymer. UV absorbers absorb the damaging part of the light spectrum (300 to 400 nm) and dissipate it in ways that are not harmful and do

not lead to initiation of degradation. One of the mechanisms of dissipating energy is converting the damaging UV radiation into heat that can be released into the polymer matrix, or harmless infrared radiation. UV absorbers should be chemically stable, otherwise they get broken or destroyed during the reaction [38,50]. Carbon black is one of the very effective UV absorbers that is widely employed in stabilizing polymers. Rutile titanium oxide is another effective UV absorber, but it is employed in applications where the radiation to be absorbed is located in the UVB range that is below 315 nm [50].

As far as UV absorbers are concerned, benzophenones, such as Chimassorb 81, and benzotriazoles, such as Tinuvin 1577, are the most extensively studied types. A disadvantage of UV absorbers is that they require a specific absorption depth (sample thickness) to offer a satisfactory level of protection to the plastic [42]. Benzotriazoles were reported to provide the best stabilization compared to other UV absorbers [32]. It has been observed that, when used in films, combinations of high molecular mass HALS with benzotriazole UV absorbers perform better than similar combinations of HALS with benzophenone UV absorbers [42]. Benzotriazoles were also reported as optimal UV absorbers for LLDPE in a study conducted by [32]. Moreover, improved UV and thermal stability was reported when employing a UV absorber that can absorb the same UV range as the polymer does [32,52].

2.2.3.4 Synergism effect

Synergism effect in UV stabilization refers to obtaining a greater UV resistance when combining two or more different types of additives, that cannot be achieved when employing any of the additives as a stand-alone UV stabilizer. On the contrary, antagonism happens when the obtained UV resistance from a mixture of two or more additives is less that the effect of the two additives employed

independently of each other [33]. Combinations of different HALS have been examined on synergism or antagonism [41–43] as well as combinations with UV absorbers, in some of which synergistic effects were observed [5,52,54]. LDPE films that contained combinations of HALS and UV absorbers showed higher thermal stability and less degradation than those with HALS only [55]. Films that employed HALS as a stand-alone light stabilizer lost 50% of their mechanical properties after 205 days of outdoor exposure, while films the contained a combination of UV absorbers and HALS lost 50% of its mechanical properties after 590 days of exposure [5].

2.3 Flame Retardancy of Polyethylenes

The fire loss statistics for some countries and cities were provided by the International Association of Fire and Rescue Services (CTIF). Worldwide statistics on fire loss was not reported. However, according to a report summarizing the fire trends in 51 cities during 2012-2016, the average number of fires per year in all these cities was 3,498,804. Additionally, the average number of fire deaths was found to be 1135 per year during 2012-2016, as per another report that contained data from 41 cities only [57]. In the United Kingdom, it was reported that there are roughly 15,000 fire injuries and 900 fire deaths per year, with up to £1.0 billion annual cost of damage of property and loss of goods. The inhalation of toxic combustion gases and smoke was reported as the reason behind most of the fire deaths [58].

Polymers are considered as flammable materials, due to their chemical structures. The interest in finding solutions to enhance the flame retardancy of polymers goes back to the discovery of the highly flammable cellulose nitrate and celluloid in the nineteenth century. The production of highly flame retarded polymers has become one of the first concerns of plastics industries [19].

Flame retardancy refers to the mechanisms and techniques applied to a material, so that when exposed to flame it either retards the propagation of that flame or slows the flames generated from the material itself after getting ignited. This means that a flame-retardant (FR) material is not the one that will not burn, but it will be harder to burn [59].

One of the useful classifications of polymers that tells about their fire retardancy and thermal decomposition is the one based on their chemical composition. Polymers can be carbon-containing like polyolefins, nitrogen-containing like polyamides, oxygen-containing like polyesters or chlorine-containing like poly(vinyl chloride) [19]. Polyethylenes are among the most flammable materials with a high heat of combustion, low limited oxygen index (LOI) and high heat release, leaving little or no residual char [19,20,36].

2.3.1 Polymer combustion

Combustibility is a measure of the ability of a substance to ignite. Polymers are highly combustible materials, in which the combustion cycle of a polymer starts when it is exposed to a certain amount of heat that is sufficient to start pyrolysis (decomposition). Once a polymer starts decomposing, it generates combustible gases that combine with oxygen to form an ignitable blend. If the temperature is enough for autoignition (i.e. the temperature required to reach the activation energy of the combustion reaction), an impulsive ignition will occur. Otherwise, the ignition will take place at a lower temperature known as the flash point. Heat is released during the combustion, and a part of this heat is transferred to the substrate leading to more decomposition. A self-sustaining combustion cycle begins when the released heat is sufficient to maintain the polymer's decomposition rate above that required to

maintain the concentration of the combustible volatiles (i.e. the reaction's fuel) with respect to the flammability limits of the system [19].

Three elements should be present to maintain a sustained fire; fuel (which is here the combustible volatiles that are released from a carbon-rich polymer being degraded), heat (which is provided by the decomposition of the fuel or externally by another source), and oxygen (which usually comes from the air, or it can be another oxidizing gas). Figure 2.8 represents the combustion cycle of polymers [19].

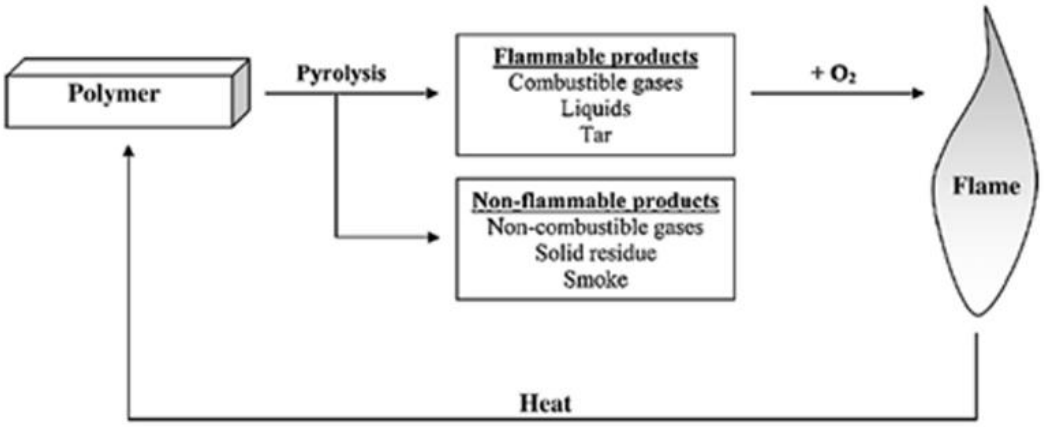

Figure 2.8 The combustion cycle of polymers [19].

Fire evolution happens over multiple phases, as shown in Figure 2.9. The stages of fire evolution can be summarized as follows: [19]

- Ignition: Ignition happens when an ignitable blend has been formed as a result of polymer combustion. Once the lower flammability limit is reached, this blend can either autoignite if the autoignition temperature has been achieved, or flash ignite at a lower temperature with the presence of an external flame source or spark. The ignition leads to the formation of flame that produces heat. A part of this heat is transferred back to the system (surface of fuel) to maintain the flame and the production of volatiles.

- Growth: The fire grows when sufficient amounts of oxygen and fuel are available, leading to a continued increase in the temperature of the system. Materials at this stage that are exposed to flame can ignite when the ambient temperature exceeds 350-500 °C.
- Flashover: Fire grows rapidly at this stage, when all the combustible parts in the compartment are involved in the fire. The ignition of any surrounding materials becomes possible at this stage, and a continued increase in temperature and heat is observed. This stage starts when the average temperature of the upper gas is around 600 °C.
- Fully developed fire: A fully developed fire is the point where both temperature and heat release rate (HRR) are at their peak. The temperature after the flashover ranges between 900 and 1000 °C, and it can reach 1200 °C at this stage. At this stage, the fire may spread to the surrounding rooms and cause building damages.
- Decay: It is the stage at which all the combustible materials or fuels have been burned and consumed. Otherwise, it happens due to the interference of a fire suppression system like sprinklers. Both temperature and HRR decrease during this phase.

Most of the fire deaths are due to the inhalation of toxic gases and fumes that are generated during fire. For polymers, the fire products depend on the chemical composition of the polymer, as well as the conditions under which the burning process happened. Smoke is the main fire product that is produced in most of the fires. It is a combination of complete and incomplete combustion items. Generally, the amount of smoke produced can be related to the thermal stability of the polymer, along with the type of fuel generated during combustion [19,58].

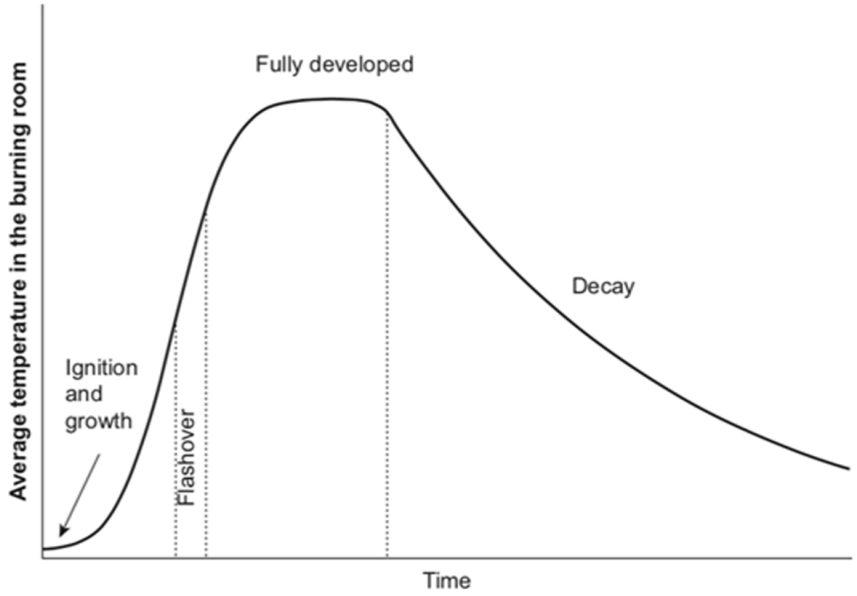

Figure 2.9 Schematic representation of a compartment fire versus time.

2.3.2 Flame retardancy mechanisms

As stated earlier, flame retardancy is the process of reducing the flammability of the material (by slowing the propagation of the fire either after ignition or after the growth of the fire. In other words, it is the process of interrupting the combustion at one or more of its phases, through inhibiting ignition, reducing the rate of burning, or/and modifying the combustion mechanism. This implies the need of excluding one of the elements that should be present to maintain a fire; fuel, heat or oxygen [58].

Research towards enhancing the flame retardancy of polymers is extensive. The production of a flame-retardant polymeric material is basically achieved by either the mechanical blending of suitable flame retardants (FRs) and polymer, or the addition of these FRs chemically during the manufacturing process (copolymerization). The mechanically-added ones are called additive flame retardants, while the chemically-added ones are called reactive flame retardants. The additive FRs are designed not to react with the polymer during the blending process,

but rather at high temperatures when a fire starts. While the reactive FRs react with the polymer during the polymerization process by forming covalent bonds. The reactive FRs have several advantages over the additives; like homogeneous dispersion, and the capability of achieving a desired level flame retardancy at lower concentrations. However, the additive FRs are more applicable to a variety of polymers, and have a lower cost compared to the reactive ones, which make them preferable and widely used for various flame retardancy applications [19].

Flame retardants, regardless of their type, interrupt the combustion through physical or chemical modes of action (Figure 2.10). The physical flame retardancy mechanisms are [19,58]:

- Lowering the temperature of the substrate through generating endothermic reactions (heat sinks) to terminate the combustion.
- Producing inert gases to eliminate the oxidizing agent (usually oxygen), as it will begin diluting once an inert gas is generated.
- Reducing the heat transfer to the fuels by forming a protective coating. This coating acts during the decomposition of the polymer by restraining the spread of oxygen and preventing the flammable volatiles from escaping.

The chemical flame retardancy mechanisms are:

- Producing a carbonaceous char layer that leads to the carbonization of the polymer, at the expense of producing volatiles. This layer is considered as a barrier between the gas and condensed phases.
- Suppression of oxidation reactions by trapping the free radicals that are generated during degradation.

- Accelerating the degradation of the polymer, through causing more dripping and hence withdrawal of the volatiles or fuels to stop the fire. However, additives working with this mode of action are not recommended.

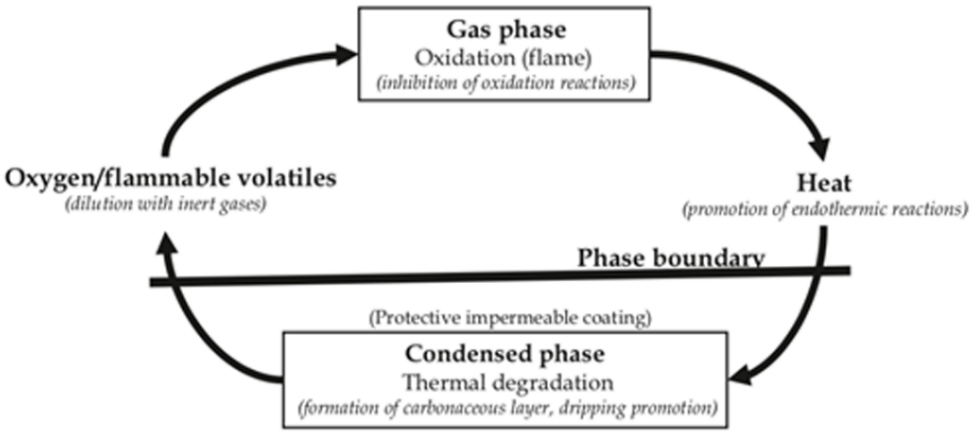

Figure 2.10 Combustion/flame retardation cycle [19].

Generally, the flame retardancy process does not operate through an individual mechanism, but rather in combination of modes of actions. The operation of flame retardants is a complex process that involves multiple stages. The criteria for employing a suitable additive are based on different factors, the most important of which are mentioned below [19,59]:

- The stability of the flame retardant (e.g. thermal stability).
- The cost of the flame retardant.
- The effectiveness of a flame retardant in a specific polymer matrix.
- Maintaining mechanical and other properties of the polymer, along with providing the desired level of flame retardancy.
- The tendency of the flame retardant to cause corrosion or/and migrate.
- The toxicity of the flame retardant.

The flame retardants are classified into two categories; Halogen-containing flame

retardants (HFRs) and halogen-free flame retardants.

2.3.3 Relation between charring processes and flammability

Char formation is one of the main factors governing a polymer's resistance to flammability. A polymer that is able to generate residual char after decomposition has a higher resistance to flammability. This is because the increased amount of char leaves little amount of combustible material that can propagate the flame. Hence, one of the effective mechanisms of improving a polymer's flame retardancy is increasing the amount of char formed during combustion [19,33]. The char formation is executed through four stages: cross-linking, aromatization, fusion of aromatics and graphitization [19].

The ability of a polymer to form char is governed mainly by its structure. It has been reported that the conversion of carbon in the unburnt polymer into carbon in the burnt polymer (char) is more efficient in polymers that are naturally less flammable. For instance, a significant improvement in the flame retardancy of poly(ethylene oxide) was observed after increasing the oxygen and hydrogen content in the chains of the polymer. It was also reported that a higher carbon to oxygen ratio makes a polymeric material less flammable. Moreover, polymers that have short bonds between the aromatic rings tend to cross-link during degradation, and hence form char. However, even the polymers that are not inclined to cross-linking can form char through the incorporation of suitable flame retardants [19].

2.3.4 Fire testing

The flammability characteristics are speed of flame, amount of heat released and ignitability. For evaluating flammability, it is required to evaluate one or more of these characteristics. There are many tests that have been developed to measure

these parameters, either in laboratories or in industry. Limiting oxygen index (LOI) and UL-94 vertical burning test are two popular flammability tests that are widely used to assess the flammability of polymers.

2.3.4.1 Limiting oxygen index (LOI)

The LOI test is a laboratory scale test that follows either ISO 4589 or ASTM D2863 standards. The test aims to measure the polymer's resistance to ignition. For instance, the test measures the minimum amount of oxygen that is required to maintain a combustion for at least 3 minutes or until 5 cm of the sample is consumed. LOI is expressed as $\mathrm{LOI} = 100\ (\frac{[O_2]}{[O_2]+[N_2]})$. The results of the test imply that the higher the LOI value (i.e. higher amount of oxygen is required), the more flame resistant the material is. As air contains 21% of oxygen, any polymer that scores lower than 21 is considered to be combustible. Polymeric materials with scores above 21 are categorized as self-extinguishing, as they cannot maintain the combustion without an external source of energy. Figure 2.11 shows the apparatus of the test. The sample is placed vertically in a glass tube and a stream mixture of oxygen and nitrogen is applied at the bottom, with an applied flame at the top of the sample to ignite it. The dimensions of the samples are usually 100 mm x 65 mm x 3 mm. One of the drawbacks of this test is that it does not provide a real fire scenario and is sometimes considered unsophisticated. However, it is considered a strong tool for assessing flame retardancy in plastic industries, and the fact that it gives a numerical value as a classification makes is preferable [19].

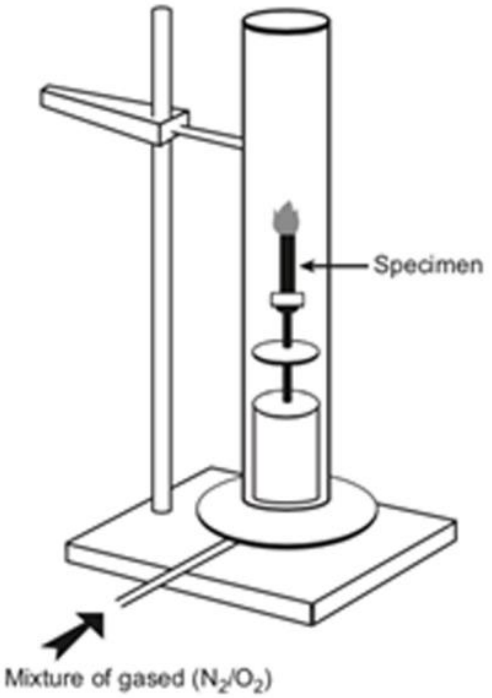

Figure 2.11 Schematic view of the limiting oxygen index test apparatus.

2.3.4.2 UL-94 vertical burning test

The UL-94 test is one of the most common flammability tests for verifying the regulatory compliance of plastic products in either bulk or foam form. The test aims to measure the spread of flame and ignitability of polymers when exposed to a small flame. Usually, the samples undergo a pre-treatment process that includes exposing the samples to heat and humidity for a few days, before conducting the test. The test samples are sets of five rectangular bars with thickness of either 0.8, 1.6 or 3.2 mm (depending on the application). Each bar is held vertically from the top, with a cotton layer placed at the bottom, as shown in Figure 2.12.

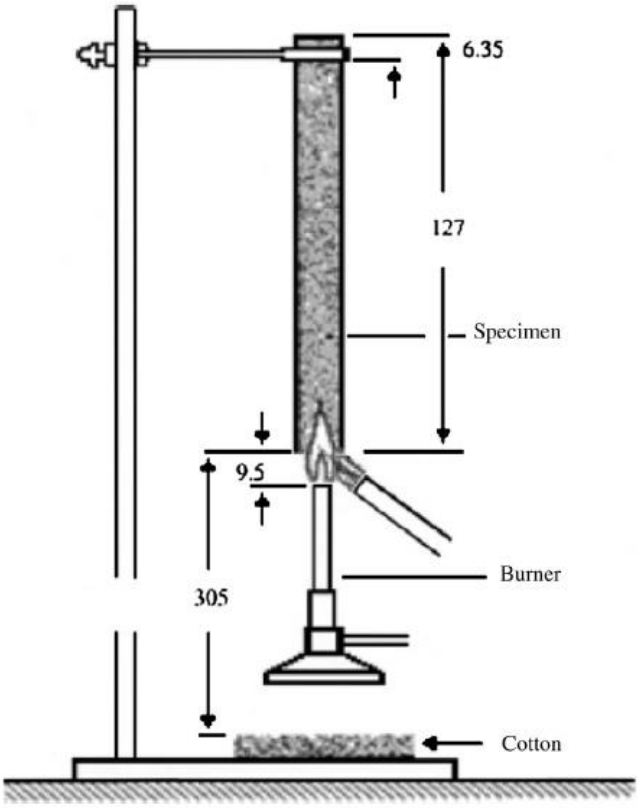

Figure 2.12 Schematic view of the UL94 vertical burning test.

The flame is applied at the lower end of the sample for 10 seconds. If the sample self-extinguishes, the flame is applied again for 10 seconds. Then the sample is classified according to the burning duration, the presence of burning drips, and the total burning time for the five specimens. The categories are V-0, V-1 and V-2; where V-0 is the highest score in terms of the flame retardancy characteristics [19]. The criteria for classifications are summarized in Figure 2.13.

	V-0	V-1	V-2
Total flaming combustion for each specimen	≤10 s	≤30 s	≤30 s
Total flaming combustion for all five specimens of any set	≤50 s	≤250 s	≤250 s
Flaming and glowing combustion for each specimen after second burner flame application	≤30 s	≤60 s	≤60 s
Cotton ignited by flaming drips from any specimen	No	No	Yes
Glowing or flaming combustion of any specimen to holding clamp	No	No	No

Figure 2.13 Criteria for UL 94 Classifications

2.3.5 Halogen-containing flame retardants (HFRs)

Halogen-containing flame retardants (HFRs) suppress the propagation of flame in the vapor phase. Their mechanisms are based on free-radical scavenging that leads to interrupting the combustion cycle. This happens during the chain-branching reactions, where the halogenated FRs react with the generated free radicals during combustion (OH• and H•) to inhibit the chain branching. This is achieved by the formation of hydrogen halides during the combustion that act as flame inhibitors. Moreover, HFRs operate as heat sinks by lowering the heat released during the combustion, which restrains the thermal decomposition. HFRs are also able to separate the oxygen on the surface from the polymer under decomposition. Finally, HFRs can catalyze the oxidation reaction through generating products that can form a protective solid layer of the surface of the degrading polymer. Bromine-, iodine-, chlorine- and fluorine- containing compounds are the major types of HFRs. Generally, bromine and chlorine- based HFRs are more thermally stable and cost effective, than the other two types [19,20].

The toxicity issues related to flame retardants have become a serious concern in the recent years. Halogenated FRs, especially the bromine- and chlorine- based compounds, produce highly toxic gases (carbon monoxide and acidic gases) during

combustion that can be fatal and can lead to serious environmental contaminations. Moreover, the evolution rate of the toxic combustion products during fire is faster for materials that are enhanced with HFRs, which increases the hazard and leads to issues with recycling. In addition, HFRs can lead to corrosion of the equipment during processing, production of toxic gases Many restrictions regarding the production and use of halogenated FRs were raised in Europe and USA as a result of these concerns [19,58]. Therefore, halogenated flame retardants are often phased out and replaced through halogen-free alternatives [19,60].

2.3.6 Halogen-free flame retardants

The need to substitute HFRs by halogen-free alternatives is increasing due to environmental legislations and EU directives, and also due to industrial initiatives and public consciousness [60]. Among alternatives, inorganic flame retardants, such as aluminum hydroxide and magnesium hydroxide, need to be added in high loadings (>50 % wt.) in order for polyethylene to pass various fire standards tests. These high levels impair negatively on the mechanical, physical and rheological properties as well as the processing ability of polyolefins [17]. On the other hand, phosphorus- and nitrogen-based flame retardants, as well as intumescent flame retardant systems (IFRs), present a viable alternative [19,61].

2.3.6.1 Phosphorus-based flame retardants

Phosphorus-based flame retardants can be used as either additive and reactive fillers to enhance the flame retardancy of polymeric materials. They can be used in thermoplastics, thermosets, coatings and other polymeric materials. Their mode of action can vary according to the polymer’s structure, type of phosphorus compound

and conditions under which fire occurs. They can also operate in either the gas phase or the condensed phase, or concurrently in both of them [19,20].

Regarding the condensed phase, these FRs are more effective in polymers that contain either oxygen or nitrogen. This is because they produce dehydrating agents like anhydrides of phosphoric, which initiates the reaction with the polymer and leads to char formation. The generation of char happens when a dehydration reaction takes place, forming double bonds and leading to carbonized structures at high temperatures. They can also be employed in poor char forming materials, with the aid of a char forming additive. Moreover, when these FRs start to degrade, some acids are released, promoting the formation of a thin glassy layer on the condensed phase. This layer acts as a protective coating that reduces the spread of oxygen and the heat transfer between the condensed and gas phases. Additionally, this coating enhances the strength of the char layer and hence delays its breakdown. It also acts as a heat sink, by restraining the complete oxidation of carbon to carbon monoxide [19].

Phosphorus-based FRs can also function effectively in the gas phase, through trapping free radicals and hence slowing the oxidative degradation. This is explained by their ability to reduce the concertation of hydrogen atoms and hence quench the flame. This process is usually referred to as inhibition of combustion, and phosphorous-based FRs are known to be effective combustion inhibitors [20].

Both organic and inorganic phosphorous-based flame retardants are available. Most of the organic ones have not met commercial success. On the other hand, red phosphorous and ammonium polyphosphate (APP) are inorganic phosphorous-based FRs that are widely used. APP is employed in intumescent FR systems. It is generally agreed that APP, a precursor of polyphosphoric acid, promotes the acid

hydrolytic reaction of the substrates, while it also serves as a blowing agent [62–[66]. Red phosphorus is a reddish-black powder that can be mechanically blended with the polymer in small amounts and is known to be an effective FR in polyolefins and other polymeric materials. However, it has a poor thermal stability which promotes a reaction with water molecules during the blending process. This leads to the production of phosphine which is highly toxic. An approach to minimizing the release of phosphine could be the addition of metal oxides, which transfers the toxic phosphine to phosphoric acid [19].

2.3.6.2 Nitrogen-based flame retardants

Nitrogen-based flame retardants are one of the most environment-friendly FRs that produce less smoke, and do not release dioxin products during combustion. They also possess several advantages over the phosphorous-based and the halogen-based FRs. One of their main features is they share a similar chemistry with most of the polymers. Moreover, polymers with nitrogen-based FRs can be recycled. On the other hand, nitrogen-based FRs are mainly effective in polyamides and polyolefins, but are usually not used alone in other polymers [19].

Melamine and melamine derivatives are nitrogen-based FRs of principal interest. Melamine is low in cost and contains 67% of nitrogen (by mass) and melts at 345 °C. It operates by absorbing the heat (when reaching its melting temperature) and reducing the temperature of the polymer's surface during combustion in the condensed phase. At higher temperatures, it releases ammonia that is capable of diluting oxygen and other combustible gases. This leads to the formation of three thermally stable condensates of melamine known as melem, melon and melam, as well as the release of residues that lead to endothermic processes. Melamine is usually not employed alone as an FR, but it is often used as a blowing agent or as an

adjuvant with other FR additives [19,20].

Melamine forms thermally stable salts as it is a weak base. Salts, in general, are known to possess flame retardant features. Three commonly used salts are: melamine phosphate and melamine pyrophosphate that have a mode of action similar to intumescent FRs, and melamine cyanurate. Most of the salts function as FRs in the condensed phase [19].

N-alkoxy is one of the melamine derivatives that act as a flame retardant by creating radical species during the combustion. N-alkoxy compounds, such as alkoxyamines, were found to be efficient FRs in polyolefins, especially polyethylene and polypropylene films. In fact, alkoxyamines were firstly introduced as light stabilizers for polymers and they were employed in agriculture films and coatings to slow down the oxidation. They were also, unexpectedly, found by Ciba Specialty Chemicals, currently known as BASF, to have flame retardant features. Flamestab NOR 116 was one of the first alkoxyamine products launched to the market as a flame retardant and a UV stabilizer [19].

2.3.6.3 Intumescent systems

Intumescent fire retardancy systems (IFRs) play an effective role mainly by the condensed-phase mechanism forming a carbonaceous foam residue (swollen char) on the surface of the polymer that acts as a heat insulator and a physical barrier to the transport of oxygen and pyrolysis products. Commonly used IFRs consist of three main ingredients, namely an acid source, a carbon source (char forming agent, CFA) and a gas source (blowing agent). The acid source decomposes at a low temperature and generates inorganic acid, such as phosphoric acid, polyphosphoric acid and metaphosphoric acid. An esterification reaction takes place between the

inorganic acid and the carbon source, and the carbon source turns into the protective char layer after the dehydration temperature. The blowing agent releases gases (e.g. water vapor, NH_3) causing the ester to create a foam that forms an insulating barrier which adheres to the substrate. Finally, the ester decomposes to form a tough carbon matrix acting as a shield for the polymer [21]. In each case, the ratio of acid source, charring source and blowing agent should be optimized per polymer type.

A widely used and effective IFR system is based on ammonium polyphosphate (APP), pentaerythritol (PER) and melamine (MA). It is generally agreed that APP, a precursor of polyphosphoric acid, promotes the acid hydrolytic reaction of the substrates, while it also serves as a blowing agent [62-66]. In addition, new CFAs, i.e. triazines and their derivatives, have attracted more and more attention; they are good carbon sources and potential gas sources, because of their abundant nitrogen and structure of tertiary nitrogen, presenting also water resistance [62,63,65].

Chapter 3: Materials and methods

3.1 Materials

3.1.1 Polymers

Linear low density polyethylene (LLDPE) (density = 918 kg/m^3, MFI = 1 g/10 min, co-monomer 1-butene) and low density polyethylene, manufactured in the autoclave process (LDPE-A) (density = 920 kg/m^3, MFI = 0.3 g/10 min). Both polymers were provided by Qatar Petrochemical Company (QAPCO, Doha, Qatar). LLDPE was received as a powder, and LDPE-A was received as pellets and powderized by Weaver Trading Company in South Africa.

Table 3.1 List of Examined Polyethylene Grades

Polyethylene grade	**Manufacturing company**	**Density (23 °C) kg/m^3**	**MFI (g/10 min)**	**Melting temperature (°C)**
LLDPE	QAPCO	918	1	122
LDPE-A	QAPCO	920	0.3	109

3.1.2 UV stabilization additives

Both UV absorbers and HALS were employed as UV stabilization additives. Chimassorb 81, Tinuvin 1577, and Chimassorb 944 were provided by BASF, and Sabostab 119 was provided by Sabo Company.

(a) Chimassorb 81

Chemical name: 2-hydroxy-4-(octyloxy)phenyl]phenylmethanone

Chimassorb 81 is a benzophenone UV light absorber (UVA). It comes as a slightly yellow powder. It protects a range of polymers against UV degradation. It provides

good light stability when combined with a HALS of the Chimassorb or Tinuvin range. It has shown good compatibility with plasticized PVC and polyolefins. It can be used with other light stabilizers, antioxidants and phosphites. Additive loss during processing is minimal due to the low vapor pressure of the additive. It can be used in thick films, molded items and packages for industrial and consumer applications. The melting temperature range of this additive is 100-135 °C and it starts decomposing at 275 °C (0.2% weight loss at 275 °C). According to the guidelines for use, typical addition levels are 0.10-0.5 % by weight in thick sections and 0.15-0.5% by weight in films [67]. Chimassorb 81 was supplied by BASF.

(b) Tinuvin 1577

Chemical name: 2-(4,6-Diphenyl-1,3,5-triazin-2-yl)-5-hexyloxyphenol

Tinuvin 1577 is a UV light absorber of the hydroxyphenyl triazine class (UVA) – modified version of benzotriazole UV absorbers. It provides a higher UV stabilization and resistance to weathering than the conventional benzotriazoles. It has a very strong absorbance in the 300-400 nm region. It comes as yellowish granules. It has a minimum volatility and very good compatibility with a range of polymers, including polyethylenes. It can also be used in flame-retarded compounds, as it is very suitable for processing conditions with high loadings. It can also be employed successfully in polymers having catalyst residues as it has a minimal tendency to chelate. It is very suitable for aging and processing applications requiring low volatility and high loadings, and these requirements are essential in co-extruded and co-injected items. Moreover, combinations of Tinuvin 1577 with HALS and antioxidants has shown a synergistic performance. It can also be used as a stand-alone additive, and in lower concentrations than the other UV absorbers due to its high UV screen activity. The melting point of this additive is 148 °C and it

starts decomposing at 300 °C (1% weight loss at 300 °C). According to the guidelines for use, addition level can vary from 0.2- 6% by weight according to the application [68]. Tinuvin 1577 was supplied by BASF.

(c) Chimassorb 944

Chemical name: Poly[[6-[(1,1,3,3-tetramethylbutyl)amino]-1,3,5-triazine-2,4-diyl][(2,2,6,6-tetramethyl-4-piperidinyl)imino]-1,6-hexanediyl[(2,2,6,6-tetramethyl-4-piperidinyl)imino]]).

Chimassorb 944 is a high molecular weight hindered amine light stabilizer (HALS). It provides different polymers with an excellent light stability, along with a very effective long-term thermal stability. It is widely and successfully employed in polyethylenes. It is also effective in polypropylene, polyacetals, PVC, and polyamides. It can also be used in thin films and thick cross sections. In thick items, it is specifically effective in polyethylenes. The additive comes in the form of white to slightly yellowish granules. It is a highly compatible additive with a low volatility, and a very good resistance to extraction. It is recommended to be accompanied with a UV absorber such as Chimassorb 81 or Tinuvin 326/328 to maintain high light stability. The melting range is 100-135 °C and it starts decomposing at 275 °C (0.2% weight loss at 275 °C). According to the guidelines for use, the addition level is 0.05-1% by weight in thick cross sections of LLDPE and LDPE [69]. Chimassorb 944 was supplied by BASF.

(d) Sabostab 119

Chemical name: 2,4,6-triamine,N2,N2"-1,2-ethanediylbis[N2-[3-[[4,6-bis[butyl(1,2,2,6,6-pentamethyl-4-piperidinyl)amino]-1,3,5-triazin-2-yl]amino]propyl]-N',N”-dibutyl-N',N"-bis(1,2,2,6,6-pentamethyl-4-piperidinyl)-1,3,5-triazine.

Sabostab 119 is a hindered amine light stabilizer (HALS) that provides excellent

light and thermal stability for a wide range of polymers and coatings. It provides excellent light and thermal oxidative stability in polyolefins. A synergistic performance was reported for combinations with low and high weight molecular HALS, and UV absorbers. According to the guidelines for use, the addition levels vary from 0.05-1% by weight, depending on the applications [70]. Sabostab 119 was supplied by Sabo.

Table 3.2 summarizes the main properties of the four additives. The TGA weight loss specifies the temperature at which the additive starts to decompose. Therefore, the processing temperatures should remain below the decomposition temperature of all the additives in a compound by at least 20-30 °C to prevent any decomposition of the additives.

Table 3.2 Properties of the Examined UV Additives

UV Additive	**Category**	**Molecular weight (g/mol)**	**Melting temperature (°C)**	**TGA weight loss (%)**
Chimassorb 81	Benzophenone UV absorber	326.4	47 – 49	0.8% (200 °C)
Chimassorb 944	HALS	2000-3100	100 – 135	0.2% (275 °C)
Sabostab 119	HALS	2286	115 - 150	5% (362 °C)
Tinuvin 1577	Low volatile hydroxyphenyl triazine UV absorber	425	148	1% (300 °C)

3.1.3 Flame retardants

The examined halogen-free flame retardants (FRs) were provided by BASF, MCA Technologies GmbH, Clariant and Perstorp.

(a) Flamestab NOR 116

Chemical name: Triazine derivative

Flamestab NOR 116 is a monomeric N-alkoxy hindered amine (NOR HAS). It is a halogen-free flame retardant that provides flame retardancy as well as UV stabilization in polyolefins. It comes as off-white granules and it has a high resistance to extraction as well as to high polymer compatibility. It can be employed in films, fibers and thick articles to provide long term flame retardancy. Unlike the usual halogen-free flame retardants, it is used in low concentrations which conserves the mechanical properties of the polymer. It also provides good thermal and UV stability and can be combined with HALS or UV absorbers to improve the UV stability. The melting range of the additive is 108-123 °C, and it starts decomposing at 260 °C. Flamestab NOR 116 is added to polyolefins in 0.5-5% by weight, according to the application and the product's thickness [71]. This additive was supplied by BASF.

(b) PPM Triazine 765

Chemical name: Ammonium polyphosphate (APP) + poly-[2, 4-(piperazine-1, 4-yl)-6-(morpholine-4-yl)-1, 3, 5-triazine]/Piperazin (PPM triazine HF).

PPM Triazine 765 is a synergistic blend of ammonium polyphosphate and PPM triazine HF, which acts as a very good carbon source, as well as blowing agent in halogen-free intumescent FR system. Triazines and their derivatives are good carbon sources and potential blowing agents (gas sources), because of their abundant nitrogen and structure of tertiary nitrogen, presenting also water resistance. PPM Triazine 765 is derived from the synergism between phosphorus and nitrogen. It

operates by creating a protective layer of solid char on the surface under combustion. It provides heat-insulation and reduces permeability of oxygen to slow down the combustion. It also prohibits dripping of the molten polymer. This FR system provides low levels of toxic fumes, and low density of smoke. It is recommended to be used in polyolefins, especially polypropylene and low density polyethylenes in loadings of 20-25% by weight. It can be successfully blended with most of the additives, particularly HALS additives. PPM Triazine 765 comes as off-white crystalline powder and it is considered as infusible with a melting temperature higher than 290 °C. It starts decomposing at 300 °C (2% weight loss at 300 °C). This additive was supplied by MCA Technologies GmbH [72].

(c) PPM Triazine HF

Chemical name: Poly[2,4-(piperazine-1,4-yl)-6-(morpholine-4-yl)-1,3,5-triazine]/ Piperazin.

PPM Triazine HF is a halogen-free flame retardant, derived from the synergism between phosphorus and nitrogen. It is one of the triazine derivatives that are considered as good carbon sources and potential blowing agents (gas sources) in intumescent halogen-free FR systems. It is very suitable for polyolefins, and for extruded and injection molded products. Its mechanism and properties are similar to those for PPM Triazine 765. It forms a protective char layer to slow down the combustion and reduce oxygen permeability. It also leads to low smoke density and low levels of toxic fumes. It is infusible (melts above 290 °C) and starts decomposing at 300°C. A blend of 75% ammonium polyphosphate and 25% PPM Triazine HF is recommended to be used at a loading of 20-25% to achieve high flame retardancy [73]. This additive was supplied by MCA Technologies GmbH.

(d) Exolit AP422

Chemical name: Ammonium polyphosphate (APP) $[NH_4PO_3]_n$

Exolit AP422 is a halogen-free flame retardant with a very low water solubility, low viscosity in aqueous suspensions and low acid number. It is generally agreed that APP, a precursor of polyphosphoric acid, promotes the acid hydrolytic reaction of the substrates, while it also serves as a blowing agent. It is widely used as an acid source and a blowing agent in halogen-free intumescent FR systems in thermoplastics. It is also very effective in intumescent coatings due to its ability to donate acid. It is suitable for polyurethane foams and it is usually added to other polymers with the presence of other flame retardants, in loadings of 10-20%. It is a biodegradable additive that comes as fine-grained white powder. It starts decomposing at 275 °C [74]. This additive was supplied by Clariant.

(e) ADK Stab FP-2200

ADK Stab FP-2200 is a halogen-free flame retardant based on a nitrogen-phosphorus flame retardancy system. It has been recently developed, and it is employed mainly in polyolefins. This additive works by generating intumescences that in return reduces the carbon dioxide emissions and smoke levels during combustion. It comes as a white powder and it has a nitrogen content of 19-23% and a phosphorous content of 16-21%. The recommended extrusion and injection molding temperatures are below 230 °C [75]. This additive was supplied by Adeka Corporation.

(f) Charmor DP40

Charmor DP40 is a dipentaerythritol derivative that is extensively employed in halogen-free intumescent FR systems as a char forming agent (CFA). It is considered as a rich carbon source, and it allows the FR system to produce lower levels of smoke. It has a low water solubility and designed to be effectively used in

outdoor application. Generally, the Charmor DP grade is very suitable for outdoor applications. Its melting point is 222 °C [76]. This additive was supplied by Perstorp.

(g) Charmor PP100

Charmor PP100 is a pentaerythritol derivative that is used as a CFA in halogen-free intumescent FR systems. It is a rich source of carbon that operates by forming a thick char layer during polymer combustion. The Charmor PP grade is very effective in thermoplastics. It melts in the range 160-180 °C [77]. This additive was supplied by Perstorp.

Table 3.3 summarizes the properties for the examined flame retardants (FRs). As stated earlier, the TGA weight loss information were used to specify the processing temperatures for the formulations. In case the provided data sheet for the additive does not specify processing conditions, the temperatures during extrusion and injection molding should be significantly below the specified TGA weight loss temperature.

Table 3.3 Properties of the Examined Halogen-Free Flame Retardants (FRs)

FR additive	**Category**	**Molecular weight (g/mol)**	**Melting temperature (°C)**	**TGA weight loss (%)**
Flamestab NOR 116	Monomeric N-alkoxy hindered amine (triazine derivative)	2261	108-123	1% (260 °C)
PPM Triazine 765	Ammonium polyphosphate (APP) + poly-[2,4-(piperazine-1,4-yl)-6-(morpholine-4-yl)-1,3,5-triazine]/Piperazin (PPM triazine HF)	>2500	Infusible (>290°C)	< 2% (300°C)
PPM Triazine HF	poly-[2,4-(piperazine-1,4-yl)-6-(morpholine-4-yl)-1,3,5-triazine]/Piperazin			< 2% (300 °C)
Exolit AP422	Ammonium polyphosphate (APP) $[NH_4PO_3]_n$	n>1000		5% (350 °C)
ADK Stab FP-2200	Nitrogen-phosphorus FR (blend)		Not observed (< 270 °C)	1% (260 °C)
Charmor DP40	Pentaerythritol derivative, dimer		222 °C	
Charmor PP100	Pentaerythritol derivative, polymer		160-180 °C	

3.1.4 Lubricant

Calcium stearate is a non-wettable powder that is based on stearic acid. It can be manufactured in different particle sizes and shapes. It is generally used in plastics industries as it aids the processing of elastomers and rubbers. It is also considered as a release agent. It promotes a full product dispersion in the elastomers. Calcium stearate was employed in all the formulations as a lubricant to facilitate the processing and ensure uniformity of additives dispersion [78].

3.2 Methods

3.2.1 Sample preparation

UV formulations and FR formulations were prepared as per the selected additives that were discussed in the previous section. This section presents the compositions of all the formulations, the practical methods of preparing the samples and the list of tests and analysis techniques performed throughout the study.

3.2.1.1 UV stabilized compounds

Two UV stabilized formulations were prepared using the two polyethylene grades and the selected additives. As stated earlier in section 2.2.3.4, the examined UV formulations were based on a combination of HALS and UV absorbers. Table 3.4 summarizes the compositions of the four UV formulations that were used in LLDPE and LDPE-A. Calcium stearate was added to all the compounds in 0.05 wt.% to facilitate the extrusion process.

Table 3.4 Composition of UV Formulations in wt.% for Polyethylene Grades.

Formulation	**LLDPE/ LDPE-A (wt.%)**	**Chimassorb 81 (UV absorber) (wt.%)**	**Chimassorb 944 (HALS) (wt.%)**	**Sabostab 119 (HALS) (wt.%)**	**Tinuvin 1577 (UV absorber) (wt.%)**
UV-1	99.75	0.1	0.1		
UV-2	99.75			0.1	0.1

All formulations contained 0.05 wt.% calcium stearate.

The compounds were prepared through thorough bag mixing of the specified amounts of powdered polyethylene and selected additives for 20 minutes to ensure homogeneity. A lab compounder with twin screw extruder KETSE 20/40 EC model no. 838106 was used to melt extrude the mixed powder at a speed of 90 rpm, and the temperatures of the respective zones from feeding to die were 170-195 °C, considering the melting and decomposition temperatures of all the polymers and additives. The extruded mixture was pelletized using a pelletizer to facilitate injection molding. Tensile and impact specimens were prepared by injection molding of the extruded mixture using an ARBURG All-Rounder 570 C golden edition injection molding machine, with temperatures within the range of 180-215 °C. The tensile test samples were injection molded as dumbbell shaped specimens with dimensions 160 mm x 13 mm x 3 mm as per ISO 527 standard. Impact test specimens were produced with dimensions of 63.5 mm x 12.7 mm x 3 mm for impact testing, as per the ASTM D256 standard.

3.2.1.2 Flame retarded compounds

The applied FR formulations involved a nitrogen-based compound (FR1), two intumescent systems with triazine derivatives (FR2, FR3), a commercial blend of phosphorus-nitrogen compounds (FR4) and two intumescent systems with pentaerythritol derivatives (FR5, FR6). Table 3.5 summarizes the categories of the implemented FR formulations and the ratios of the char forming agent (CFA) to the acid source (APP), that were specified for the formulations with intumescent FR systems. The CFA:APP was set to 1:3 in FR3, and 1:1.5 in FR5 and FR6. FR2 was based on PPM triazine 765, which is a combination of ammonium polyphosphate (APP), an acid source, and PPM triazine HF, a char forming agent (CFA) and a blowing agent. Single phosphorus-based FRs were not examined since it is well-known that they are efficient in oxygen-containing polymers, such as polyamides [79].

The halogen-free FR systems were examined in a total content of 5-35 wt.%. All the formulations contained 0.05 wt.% calcium stearate, except FR4 that contained a higher amount of the lubricant, 0.1%, due to the high viscosity of the additive employed in this formulation (Table 3.6).

The preparation of the FR compounds was similar to the UV compounds. After the manual bag-mixing of the specified amounts of powdered polyethylene and additives, the compounds were prepared in the same previously described twin-screw extruder. The process was performed at a speed of 70 rpm, and the temperatures of the respective zones from feeding to die were 170-200 °C. The extruded mixture was pelletized and then injection molded, with temperatures in the range of 180-215 °C. Specimens for UL-94 testing were prepared with dimensions 127 cm x 12.7 cm x 1.6 mm. Tensile and impact specimens were later prepared for

the successful formulations that passed the flammability test, using the same dimension as those for the UV compounds.

Table 3.5 Categories of the Examined FR Formulations

Formulation	**FR System Category**	**CFA:APP**
FR1	Nitrogen-based	-
FR2	Intumescent with triazine	-
FR3	Intumescent with triazine	1:3
FR4	Phosphorus/ Nitrogen	-
FR5	Intumescent with pentaerythritol	1:1.5
FR6	Intumescent with pentaerythritol	1:1.5

The FR additive were numbered foe easier labelling in Table 3.6 as follows:

[1] Flamestab NOR116

[2] PPM Triazine 765

[3] PPM Triazine HF

[4] Charmor DP40

[5] Char-mor PP100

[6] Exolit AP422

[7] ADK Stab FP2200

Table 3.6 Composition of FR Formulations in wt.% for Polyethylene Grades.

Formulation	**PE (wt.%)**	**[1]**	**[2]**	**[3]**	**[4]**	**[5]**	**[6]**	**[7]**	**Total FR (wt.%)**
FR1	94.95	5							5
FR2	69.95		30						30
FR3	64.95			8.75			26.25		35
FR4*	69.95							30	30
FR5	64.95				7		21	7	35
FR6	64.95					7	21	7	35

All formulations contained 0.05 wt.% calcium stearate, except for FR4 that contained 0.1 wt.%

3.2.2 Accelerated UV-aging

The accelerated UV-weathering experiments were performed using an Accelerated Weathering Tester Model QUV-se equipped with Solar Eye Irradiance Control and a UVA lamp. The procedure was in accordance to Cycle-K based on the ISO 4892-3 standard, which exposes the samples to climatic conditions similar to those observed in the geographical location of Qatar. According to this standard, the samples were exposed to repetitive cycles of UV exposure and condensation. UV radiation was set for 8 hours with an irradiance level of 0.76 W/m^2 at a wavelength of 340 nm, with a maximum temperature of 60 °C. Then a 4-hour dark condensation was applied at 50 °C.

The sampling times applied were 0, 500, 1500 and 2500 hours for the LLDPE compounds, and 0, 1000, 1500 and 2000 hours for the LDPE-A compounds, for

tensile and impact samples. The samples were swopped regularly so that the two sides of each sample were equally exposed to the radiation. For example, if a sample was set for 500 hours, it was swopped once 250 hours have elapsed so that each side is directed to the lamp for 250 hours. The same approach was followed for all the sampling times. Sampling times were chosen based on the availability of the weathering machine, the observed stability of the polymer and the time constraint of the project.

3.2.3 UL-94V testing

The flammability of the FR compounds was assessed according to UL 94 vertical burning tests (ASTM D3801) on injection molded bars, following a pretreatment of the specimens for 45 h at 23 °C and 50% RH. The test procedure is described in detail in section 2.3.4.2.

3.2.4 Sample characterization

3.2.4.1 Tensile testing

The tensile properties of the UV and FR compounds were measured using a quasi-static tensile testing machine Lloyd LR50K Plus. The testing procedure followed ISO 527 (Plastics - Determination of tensile properties) standard. An elongation speed of 10 mm/min was used and no pre-load was applied to the sample. The gauge length of the dumbbells was 50 mm. The determination of the Young's modulus (E) was calculated from the slope of the stress-strain curve for strain values between 0.2 and 2.2%. Other tensile properties were measured from the stress-strain curves: tensile strength, elongation at break and stress at break. A minimum of five specimens were tested for each measurement.

3.2.5.2 Impact testing

The Izod impact strength was measured for both UV and FR compounds, according to the ASTM D256 standard. The aim of the test was to assess the toughness of the samples, which refers to the ability of a material to absorb energy before fracturing. Impact testing specimens were produced with dimensions of 63.5 mm x 12.7 mm x 3 mm as stated earlier. The specimens were notched in the center (45° notch and 2 mm depth) to meet the ASTM D256 definitions. The test was performed in an Instron Wolpert PW5 impact testing apparatus and the Izod impact strength (a_{iN} in kJ m^{-2}) was calculated according to Equation 1, where E_c is the corrected measured absorbed energy during impact in J, h is the thickness of the tested specimen in mm and b_N is the remaining width of the tested specimen in mm. A minimum of five specimens were tested for each measurement.

$$a_{iN} = \frac{E_c}{h \times b_N} \times 10^3 \quad (1)$$

3.2.5.3 Scanning electron microscopy (SEM)

SEM was performed on injection molded specimens with 3 mm thickness in FEI Quanta 200 electron microscope at an accelerating voltage of 2–5 kV. The samples were sputter gold coated for 30 s using an Agar sputter coater. SEM images were taken for the neat polymers, UV compounds after different exposure times, and FR compounds.

3.2.5.4 Differential scanning calorimetry (DSC)

Non-isothermal crystallization analysis was performed on all the UV compounds, including the neat polymers, in a Perkin Elmer 8500 differential scanning calorimeter (DSC) under nitrogen atmosphere. The analysis was performed on samples of 5-10 mg. Aluminum pans were used to seal the samples, and a closed, empty aluminum pan was used as a reference. The samples were first heated from 30

to 180 °C at a heating rate of 10 °C/min. After that the temperature was held for 1 min. and then cooled down to 30 °C at the same rate. The melting enthalpy $\Delta H°$ and peak melting temperature T_m were determined in the first heating, while the crystallization temperature T_c and crystallization enthalpy were calculated in the cooling stage.

3.2.5.5 Thermogravimetric analysis (TGA)

Thermogravimetric analysis (TGA) is a common technique to evaluate the thermal stability of various polymers giving information on weight loss, but no chemical information [80,81]. A Perkin-Elmer TGA 4000 thermogravimetric analyzer (TGA) was used to analyze the thermal stability of the samples. For the UV compounds, approximately 15-30 mg of sample was heated from 30 to 600 °C at a heating rate of 10 °C/min under nitrogen flow. The degradation temperature T_d, which was determined at the maximum rate of weight loss (T_d), was measured for the pure polymers and the UV formulated compounds at all the sampling times. The onset of decomposition temperature refers to the temperature where it is assumed that a significant amount of fuel consumption has begun, or in other words the beginning of decomposition. The onset of decomposition temperature was defined as the temperature at 5% weight loss ($T_{d,5\%}$).

For the FR formulated compounds, about 15-30 mg of sample was heated from 30 to 800 °C at 10 °C/min under nitrogen thermal decomposition atmosphere. The onset of decomposition temperature was defined as the temperature at 5% weight loss ($T_{d,5\%}$), the degradation temperature (T_d) was determined at the maximum rate of weight loss, and the char yield as the % residue at 600 and 800 °C. The pure FR additives, pure polymers and the relevant FR-containing compounds were accordingly analyzed.

3.2.5.6 Melt Flow rate (MFR)

The melt flow rate (MFR) is a measure of a thermoplastic polymer's ability to flow under specific conditions over a period of time. Generally, it is expressed as the weight flowing (in grams) in 10 minutes through a die of certain size by an applied pressure, at specific weight and temperature. The melt flow rate is inversely proportional to the polymer's viscosity (i.e. a low MFR refers to a higher viscosity).

The MFR (g/10min) was measured for selected FR-containing compounds at 190 °C and 2.160 kg, according to the ASTM D1238, using a Dynisco model 4004 capillary rheometer.

3.2.5.7 Fourier-transform infrared spectroscopy (FTIR)

Fourier-transform infrared spectroscopy (FTIR) is a technique employed to obtain information about the changes in the polymers' chemical composition during degradation. Infrared (IR) spectroscopy identifies the spectral frequency and intensity of absorbed radiation that come from the molecular transitions between quantum states associated with the vibrations and rotations of specific chemical groups. The test works by dispersing the light and analyzing each wavelength separately. This analysis was performed to evaluate the degree of degradation by measuring the amount of one of the major photo-degradation products, the carbonyl group in the aged samples.

FTIR spectra of the exposed surfaces of the samples were recorded by using a Perkin Elmer Frontier FT-IR spectrometer with 16 scans in the range of 4000 - 550 cm^{-1}. The carbonyl index (CI) was calculated by the integral of the carbonyl peak (1650-1800 cm^{-1}) and the C-H peak (1420 - 1480 cm^{-1}) using equation 2 [31].

$$CI = \frac{Absorption\ of\ carbonyl\ species_{1650-1800\ cm^{-1}}}{Absorption\ of\ C-H\ peak_{1420-1480\ cm^{-1}}} \quad (2)$$

Chapter 4: Comparison Between UV-Stabilization of LLDPE and LDPE-A

4.1 Visual Inspection

Visual observations on the physical appearance of the samples were made after removing them from the weathering machine. The presented images (Figures 4.1-4.4) show the samples after being tensile tested.

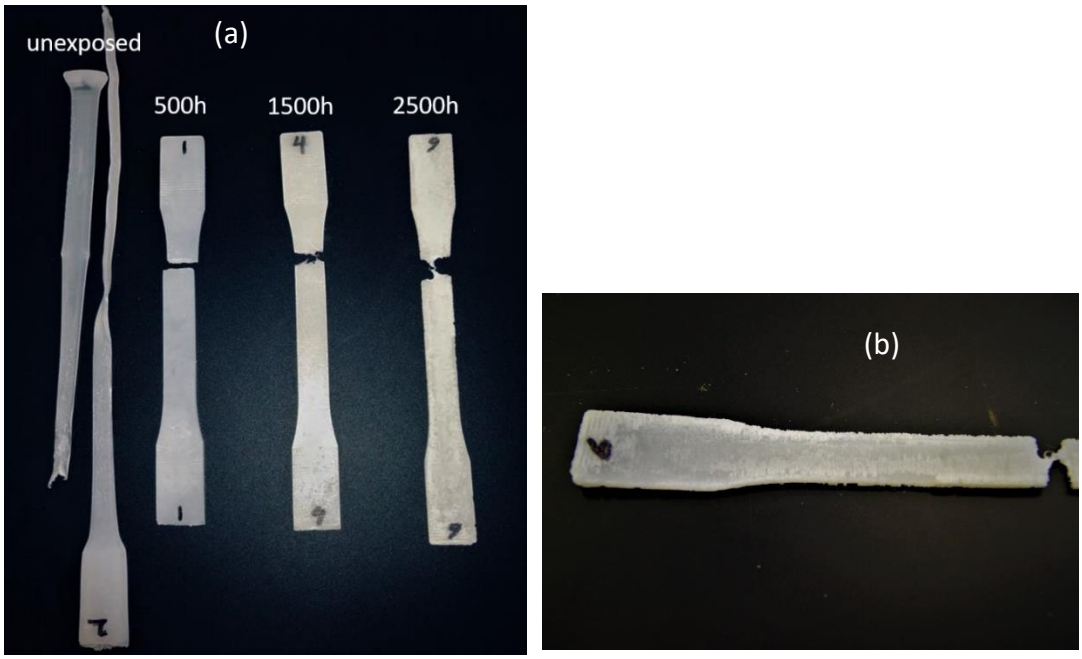

Figure 4.1 Effect of UV-weathering on neat LLDPE at (a) all exposure periods and (b) 2500h

First, the effect of UV-aging on the surface integrity and physical appearance was clear on the neat versions of the polymers (Figures 4.1 and 4.2). In the case of LLDPE, small cracks were observed after 500h of exposure, and became more severe at longer exposure periods. At 1500h and 2500h, the samples started to flake, and the cracks looked deeper as shown in a close-up image (Figure 4.1(b)). It can be seen that the ductility of LLDPE was significantly reduced as a result of UV-aging, as the exposed samples did not elongate and broke quickly during the test, compared

to the unexposed samples. Moreover, the transparency of the samples was reduced with exposure, as shown in Figure 4.1 (a). The same observations were also made on LDPE-A samples. Cracks and flakes began to form after 1000h of exposure (Figure 4.2), and the transparency of the samples was reduced. Also, the exposed samples broke faster than the unexposed samples during the tensile test.

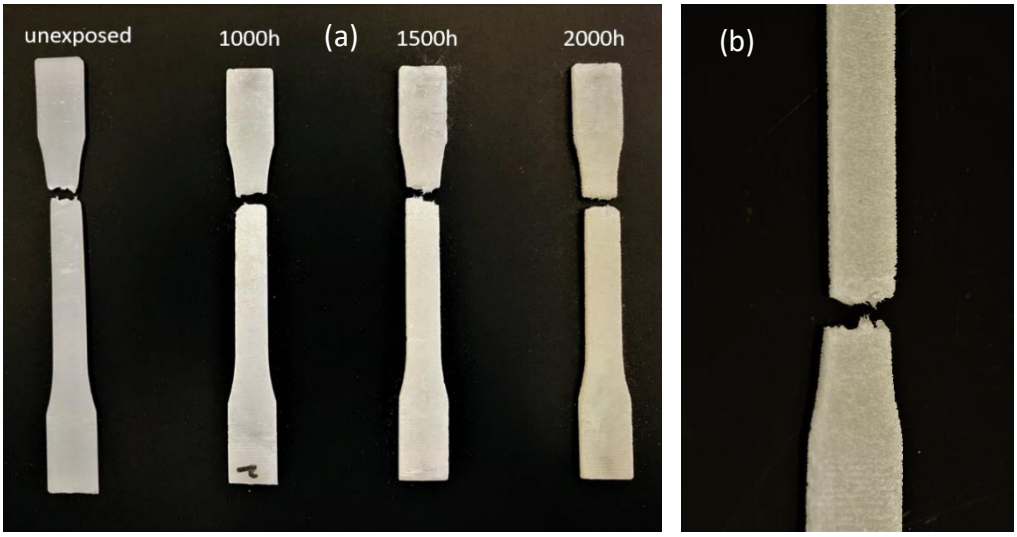

Figure 4.2 Effect of UV-weathering on neat LDPE-A at (a) all exposure periods and (b) 2000h

On the other hand, all the stabilized samples presented a different physical appearance than the neat versions. LLDPE stabilized samples maintained their ductility at all exposure periods, as shown in Figure 4.3. Moreover, no significant cracks were visible, and the samples did not flake as shown in the neat samples. One interesting observation was the color change of the exposed LDPE-A/ UV1 samples, as they turned into a pale yellow at all exposure periods (Figure 4.4(a)).

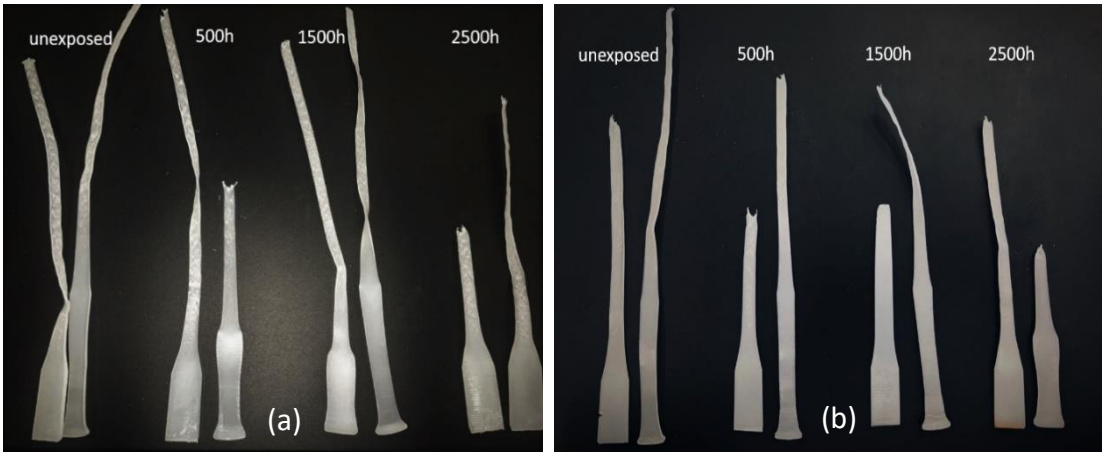

Figure 4.3 Effect of UV-weathering on stabilized LLDPE compounds (a) UV1 and (b) UV2

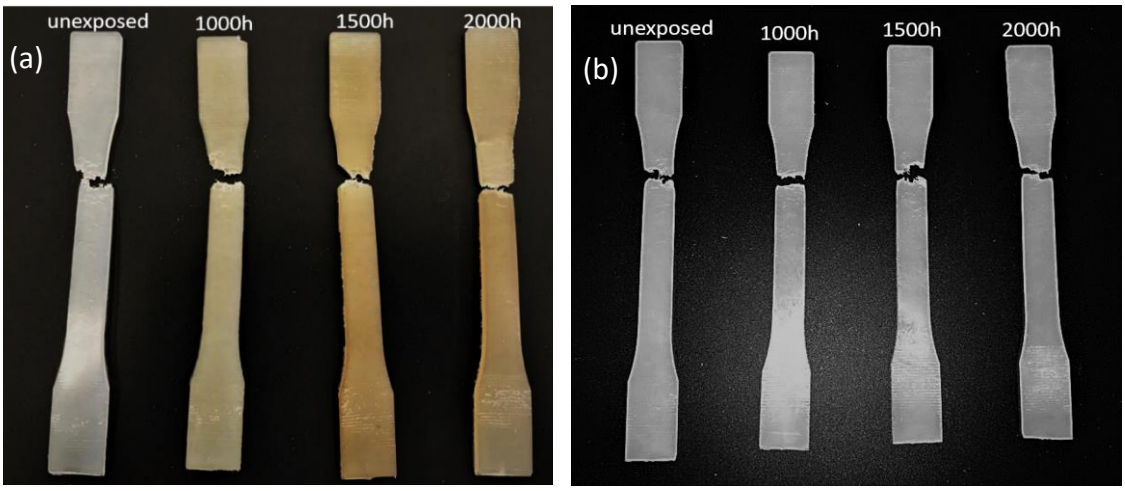

Figure 4.4 Effect of UV-weathering on stabilized LDPE-A compounds (a) UV1 and (b) UV2

4.2 Microscopic Analysis

SEM analysis was used to examine the surface morphology of the neat and stabilized samples, before and after UV exposure. The presented SEM images were taken for samples before exposure, and for samples after the longest exposure (2500h for LLDPE and 2000h for LDPE-A). Moreover, the samples were examined before and after tensile testing (TT). The aim of this procedure is to visualize the

effect of tensile forces on the cracks formed during degradation under UV exposure. A magnification of 100x was used for all the neat samples, and magnifications of 500-1000x were used for the UV stabilized samples in order to observe the possible formation of small cracks on the surface (Figures 4.5 to 4.10, where we show the 250x magnification images).

The UV exposure caused significant degradation of the unstabilized polymers, with significant cracking visible in Figure 4.5(c,d) and Figure 4.8(c,d). The neat versions of LLDPE and LDPE-A samples had many cracks, which further increased in size after tensile testing. However, the change in crack size on LDPE-A was more significant than that in LLDPE. The cracks shown on the surface of LLDPE are discrete, defined and long, while the cracks formed on LDPE-A are many, smaller in length and more random. It also seems as if the cracks on LLDPE were initiated and propagated mainly through the axial direction (i.e. with the direction of the pulling). One fact to refer to is the higher stability of LLDPE due to its linear nature, that provides it with better mechanical properties than LDPE-A. This could explain the larger amount of cracks observed on LDPE-A after 2000 h of exposure, compared to the cracks observed on LLDPE after 2500 h of exposure.

On the other hand, a significant improvement was observed in all the stabilized samples. The stabilized forms of both polymers showed better surface integrity than the neat versions. Firstly, the LLDPE/UV1 aged sample showed a smooth intact surface with no significant scratches nor crack initiations before the TT. However, after conducting the TT on the exposed samples, it seems as if some cracks started developing (Figure 4.6(d)). It clearly shows that this formulation protected LLDPE from UV-initiated degradation. This crack formation after TT on the 2500 h exposed samples was more obvious on the LLDPE/UV2 sample (Figure 4.7(d)).

The surfaces of both the aged LDEP-A/UV1 and LDPE-A/UV2 samples do not show any indication of crack formation, even after long UV-exposure and TT (Figure 4.9(c,d) and Figure 4.10(c,d)). In general, the presented results prove that the additives were capable of protecting the samples, and that the neat version of the polymers cannot withstand the harsh environmental conditions. The only compounds that showed minor cracks after aging were the two treated LLDPE samples. In the discussion of the thermal and mechanical results we shall refer back to these observations.

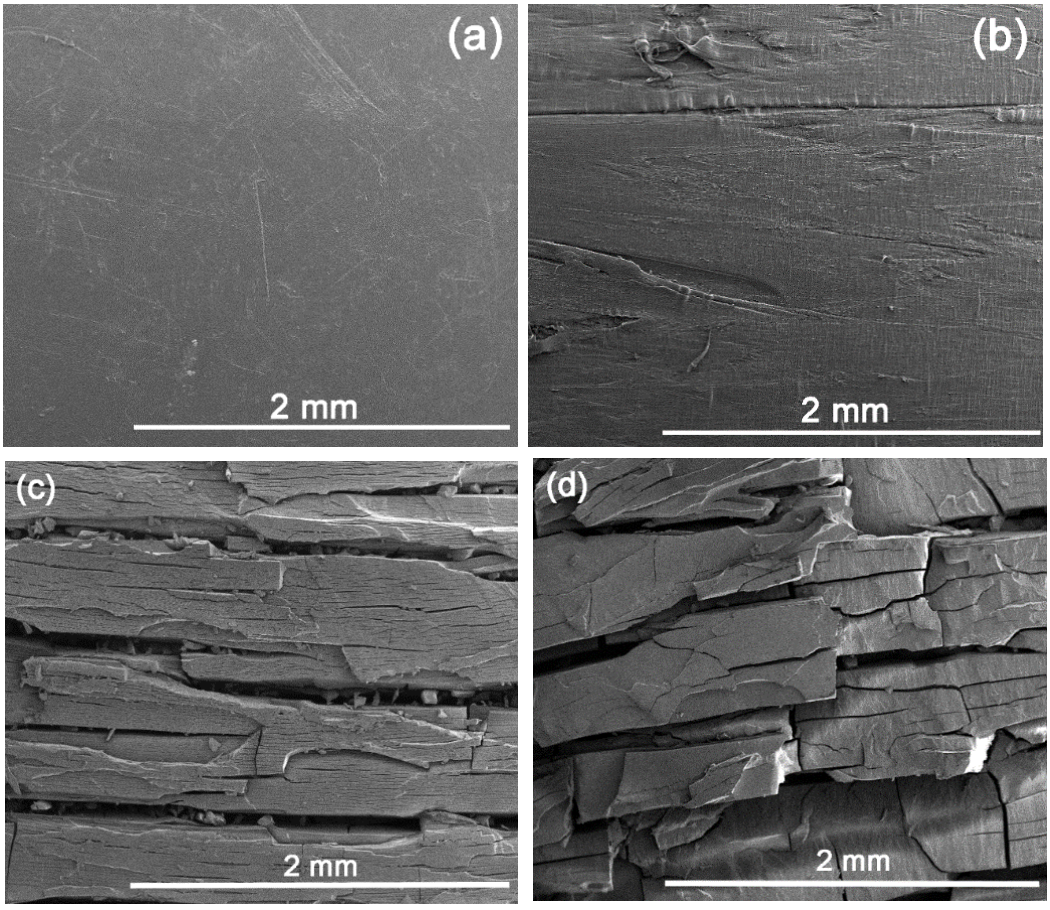

Figure 4.5 Neat LLDPE (a) unexposed – before TT, (b) unexposed – after TT, (c) 2500 h UV exposed – before TT, (d) 2500 h UV exposed – after TT.

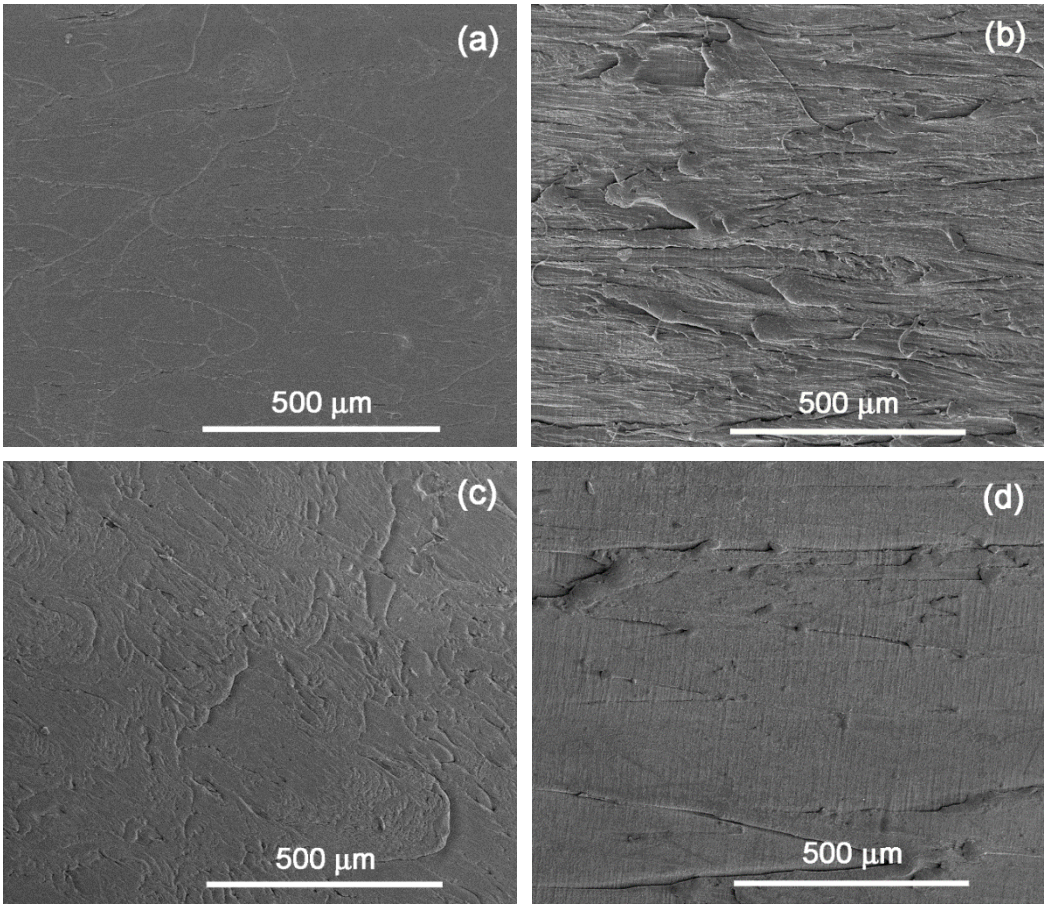

Figure 4.6 LLDPE/UV1 (a) unexposed – before TT, (b) unexposed – after TT, (c) 2500 h UV exposed – before TT, (d) 2500 h UV exposed – after TT.

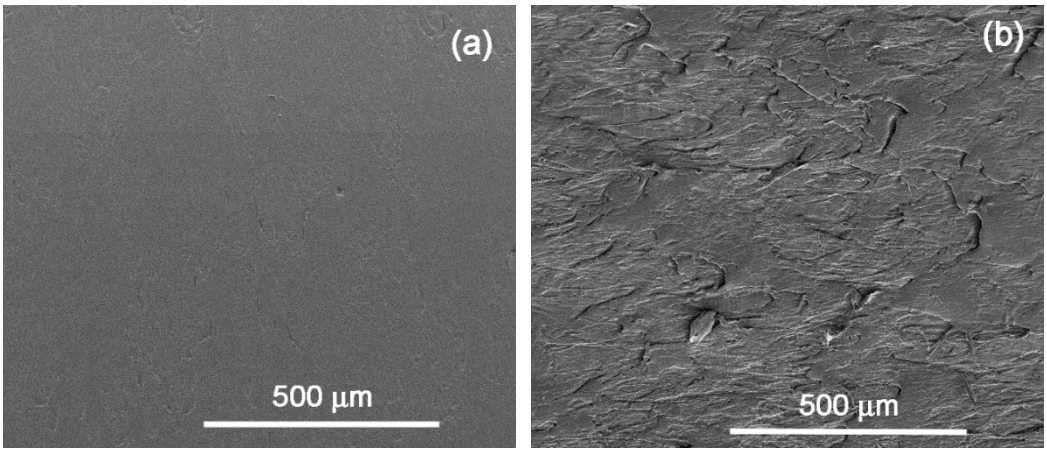

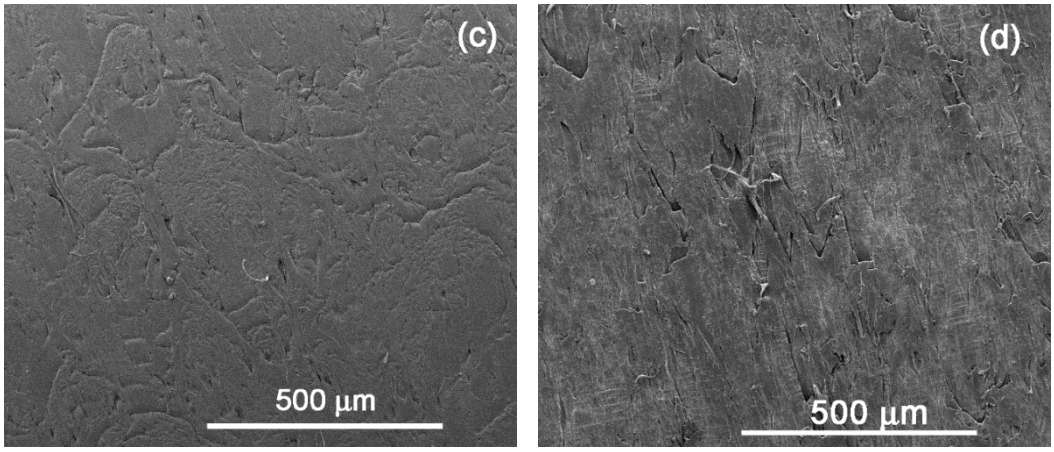

Figure 4.7 LLDPE/UV2 (a) unexposed – before TT, (b) unexposed – after TT, (c) 2500 h UV exposed – before TT, (d) 2500 h UV exposed – after TT.

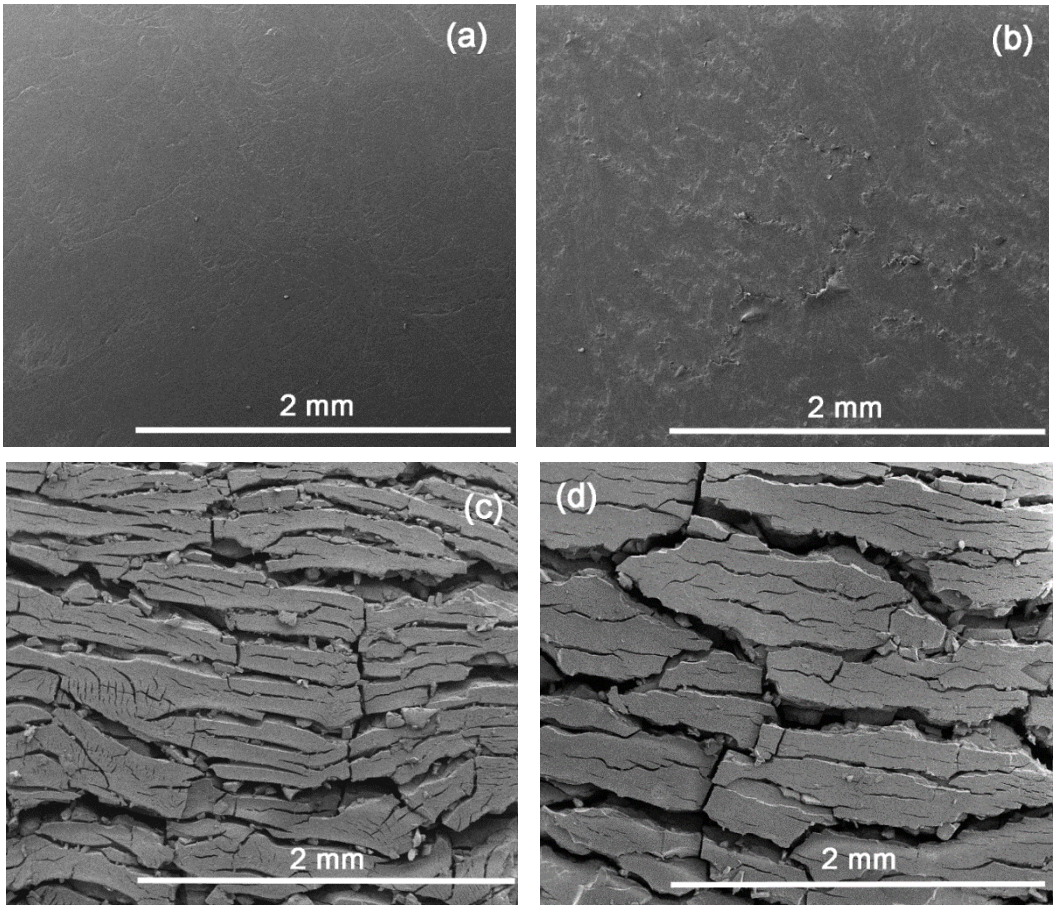

Figure 4.8 Neat LDPE-A (a) unexposed – before TT, (b) unexposed – after TT, (c) 2000 h UV exposed – before TT, (d) 2000 h UV exposed – after TT.

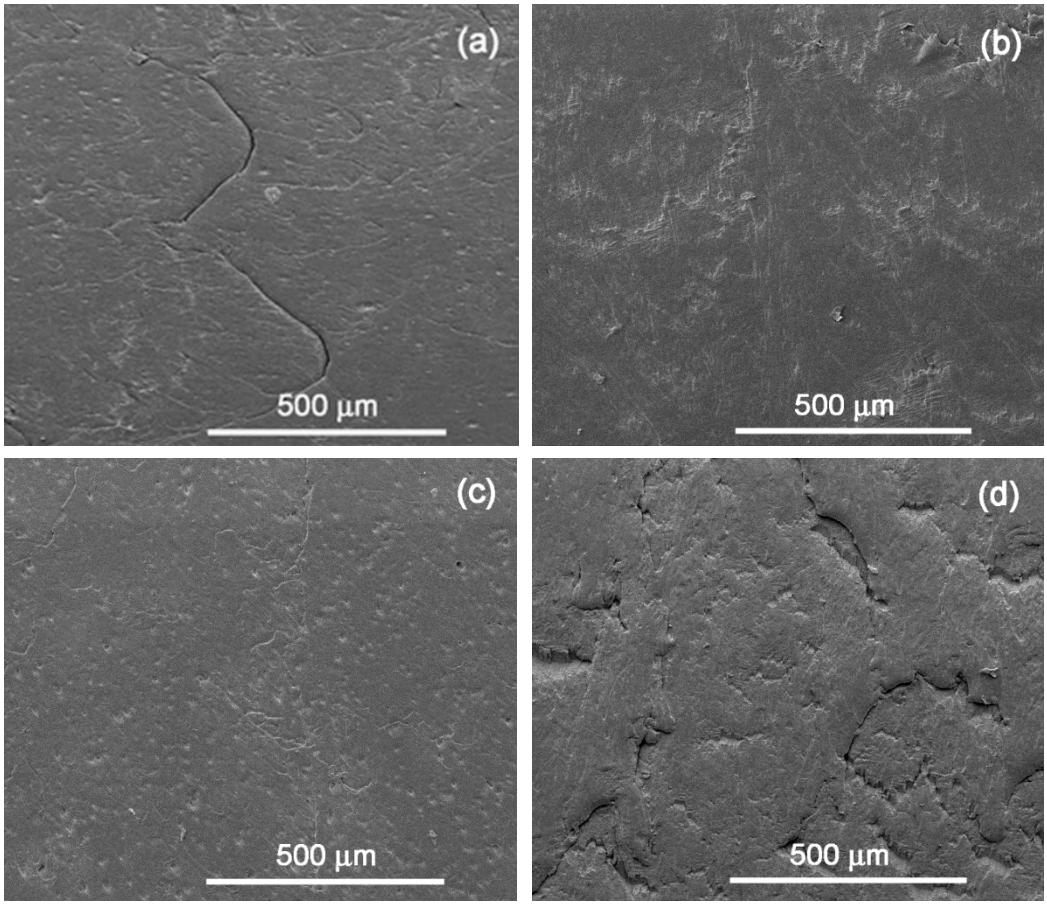

Figure 4.9 LDPE-A/UV1 (a) unexposed – before TT, (b) unexposed – after TT, (c) 2000 h UV exposed – before TT, (d) 2000 h UV exposed – after TT.

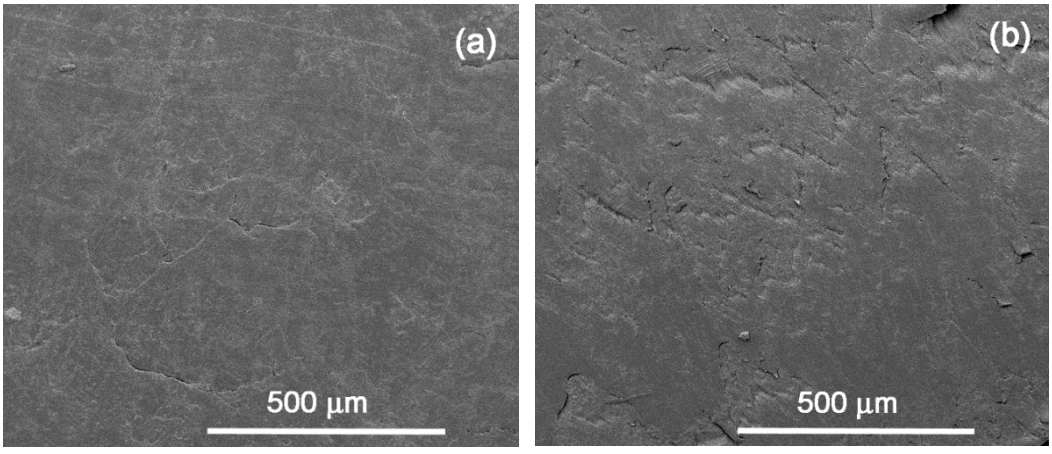

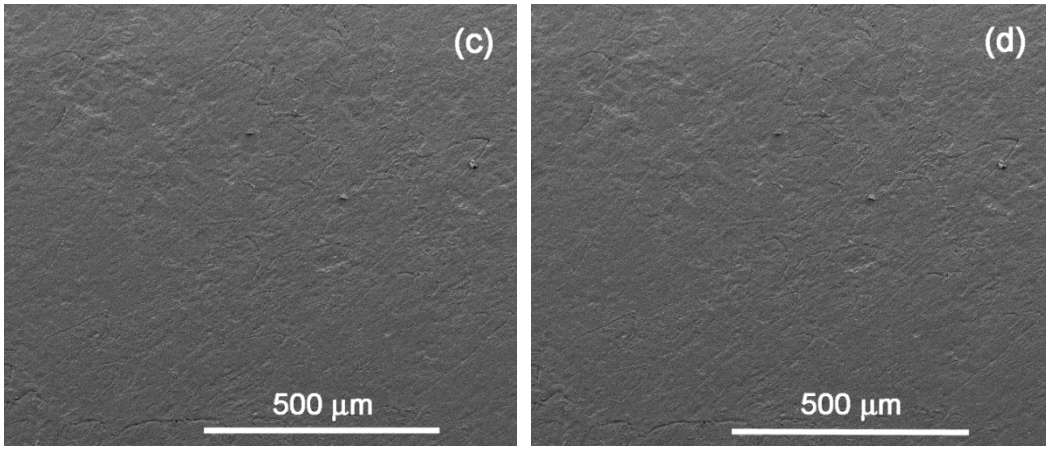

Figure 4.10 LDPE-A/UV2 (a) unexposed – before TT, (b) unexposed – after TT, (c) 2000 h UV exposed – before TT, (d) 2000 h UV exposed – after TT

4.3 Mechanical Characterization

The mechanical characterization of the examined UV-aged compounds was conducted through tensile testing and Izod impact testing. The aim of this characterization was to investigate to what extent UV-aging impacted on the mechanical properties of neat and UV/heat stabilized LLDPE and LDPE-A. A deterioration in some mechanical properties at any stage of the UV-aging gives an indication of the polymer's stability and resistance to aging at that stage. Mechanical properties such as tensile strength, Young's modulus, stress and stain at break, and impact toughness were measured for all the neat and UV stabilized compounds, after different UV aging periods.

4.3.1 Tensile testing

The tensile properties of the UV stabilized compounds after increasing UV exposure periods were investigated. These properties are reported in Tables 4.1 and 4.2 for LLDPE and LDPE-A, respectively. All the stress-stain curves are shown in Appendix A.

Table 4.1 Summary of LLDPE Tensile Testing Results

Samples	Young's modulus (MPa)	Tensile strength (MPa)	Strain at break (%)	Stress at break (MPa)
Neat LLDPE				
Neat [0 h]	154 ± 10	13.2 ± 0.3	424 ± 27	12.8 ± 0.3
Neat [500 h]	343 ± 46	11.0 ± 0.1	22.0 ± 3.0	10.6 ± 0.2
Neat [1500 h]	411 ± 98	7.1 ± 0.8	34.0 ± 11.0	6.6 ± 0.9
Neat [2500 h]	536 ± 80	5.0 ± 0.5	19.0 ± 6.4	4.7 ± 0.3
LLDPE/UV1				
UV1 [0 h]	72.3 ± 4.8	13.8 ± 0.1	980 ± 40	13.4 ± 0.2
UV1 [500 h]	85.3 ± 4.7	13.3 ± 0.5	978 ± 67	13.0 ± 0.5
UV1 [1500 h]	90.2 ± 4.6	13.0 ± 0.6	926 ± 68	12.9 ± 0.7
UV1 [2500 h]	105 ± 3	13.1 ± 0.3	878 ± 31	12.8 ± 0.3
LLDPE/UV2				
UV2 [0 h]	94.7 ± 0.8	16.4 ± 0.6	492 ± 191	15.7 ± 0.6
UV2 [500 h]	95.2 ± 1.2	16.9 ± 0.3	804 ± 23	16.5 ± 0.3
UV2 [1500 h]	102 ± 9	13.4 ± 1.1	235 ± 105	12.5 ± 1.3
UV2 [2500 h]	109 ± 7	16.1 ± 1.0	645 ± 127	15.6 ± 1.0

It is clear from both tables that the tensile properties of the neat polymers decayed significantly, which is in line with the previously presented SEM results, and the results in literature [11,31]. Both the neat polymers experienced a reduction in tensile strength by 60%, accompanied with a reduction in both strain and stress at break, as a result of the UV-exposure. The reduction in strain at break was ascribed to embrittlement as a result of increased cross-linking of the polymer [11,31], but

weakening of the polymer due to UV-initiated chain scission probably played a more predominant role in this case. Both the neat polymers experienced a gradual increase in Young's modulus with increasing UV exposure time, which was also reported in the literature [31]. The values increased by 70% for LLDPE and 55% for LDPE-A. The higher Young's modulus values are characteristic of brittle materials and can be explained by an increased crystallinity caused by the re-crystallization of the shorter chains that resulted from chain scission. In this case UV-initiated crosslinking is also a possibility, and this will also contribute to the higher modulus values. That is, the apparent increase in Young's modulus with aging is considered as a form of degradation, and obviously not an improvement as it is at the expense of ductility [30–32,49]. Also, the recrystallized chains are short and unattached, which leaves a space for a crack to form within the detached chains. Further, LLDPE is easier to crystallize than LDPE-A, due to its linear nature [82]. The linear grades of polyethylene are also more susceptible to cross-linking reactions as a result of weathering [38].

On the other hand, the tensile values of the stabilized samples were significantly different from those of the neat ones. Firstly, the tensile strength and the stress at break remained almost constant with aging, for both LLDPE and LDPE-A. This supports the microscopic findings presented earlier, in which no significant cracks were observed on the surface of the stabilized compounds. Moreover, the Young's modulus values slightly increased with aging in the stabilized compounds of both polymers, which is an expected result of aging and is probably due to some extent of UV-initiated crosslinking. These results prove that the additives did protect the samples during photo-degradation and conserved most of their mechanical properties.

Table 4.2 Summary of LDPE-A Tensile Testing Results

Samples	Young's modulus (MPa)	Tensile Strength (MPa)	Strain at Break (%)	Stress at Break (MPa)
Neat LDPE-A				
Neat [0 h]	122 ± 12	17.3 ± 0.4	135 ± 8	17.0 ± 0.3
Neat [1000 h]	297 ± 24	9.6 ± 0.3	37.0 ± 9.1	9.5 ± 0.4
Neat [1500 h]	336 ± 49	8.5 ± 0.3	24.0 ± 1.3	8.4 ± 0.3
Neat [2000 h]	289 ± 37	6.6 ± 0.6	21.0 ± 2.0	6.3 ± 0.6
LDPE-A/UV1				
UV1 [0 h]	143 ± 10	19.5 ± 0.2	134 ± 3	19.4 ± 0.2
UV1 [1000 h]	146 ± 5	20.7 ± 0.4	143 ± 7	20.6 ± 0.4
UV1 [1500 h]	142 ± 5	20.2 ± 0.2	140 ± 3	20.0 ± 0.2
UV1 [2000 h]	155 ± 12	20.7 ± 0.6	151 ± 6	20.5 ± 0.5
LDPE-A/UV2				
UV2 [0 h]	133 ± 6	18.1 ± 0.2	145 ± 6	18.0 ± 0.2
UV2 [1000 h]	139 ± 4	18.9 ± 0.8	140 ± 2	18.8 ± 0.9
UV2 [1500 h]	129 ± 6	18.5 ± 0.5	139 ± 7	18.4 ± 0.6
UV2 [2000 h]	132 ± 12	17.7 ± 0.6	140 ± 4	17.6 ± 0.4

The Young's modulus values of the stabilized samples were lower than those of the neat polymer. In other words, the addition of the UV stabilizers reduced the increase in stiffness with aging of stabilized compounds but maintained their tensile strength and stress at break. This can be ascribed to the ability of the UV stabilizers to reduce or prevent chain scissions during UV-aging. For instance, chain scissions lead to

formation of shorter chains that can fold and form crystalline regions, and this leads to an increase in the stiffness [30,32]. Generally, the increase in stiffness of the stabilized compounds was negligible, which indicates that little or no chain scissions have occurred. In the case of LLDPE, a slight increase in stiffness with aging was observed, which was not noted in LDPE-A compounds. LDPE-A/UV2 samples had the most stable stiffness at all exposure periods. This can be used as an indication to this compound having the least amount of chain scissions during UV aging, compared to the others. In the case of LDPE-A, the Young's modulus values were found to be slightly higher in the stabilized compounds, compared to the neat sample. Additionally, the tensile strength and stress at break values in both stabilized compounds of LDPE-A were almost similar, and higher than those of the LLDPE stabilized compounds. The improved tensile results of all the stabilized compounds indicate that the employed UV absorbers were effective and have absorber some of the UV radiation and dissipated it as explained earlier in section 2.2.3.3.

It is important to note that both the LLDPE/UV1 and LLDPE/UV2 results showed higher standard deviation values compared to the other samples. The neat LDPE-A aged samples also showed a higher variation in Young's modulus values. Inhomogeneity of the samples could be one explanation of such results. Inhomogeneity could arise from a lack of proper dispersion of the additives in the polymer matrix during the extrusion process. This is because the added amounts of UV additives were very small compared to the mass of polymer (0.1 wt%), which may lead to inconsistency of dispersion during bag mixing or extrusion. Another reason behind the scattering and inconsistency in some of the tensile test results is the thickness of the samples with respect to the period of exposure. It is noted that the tensile samples (3 mm) was too thick for the UV light to penetrate deep enough

into the samples. In other words, it is possible that some of the samples degraded or started to degrade at the surface, keeping the core of the sample intact. The dimensions of the intact core could have varied between the samples. These variations could significantly affect the tensile results, as the characterization is not performed on a fully-UV degraded sample.

4.3.2 Impact testing

Izod impact testing was conducted to measure the impact strength of the samples, which gives more information about the toughness of the sample. Measurements were performed on the neat and stabilized samples, for all the UV aging periods. The impact test results are summarized in Tables 4.3 and 4.4.

Both neat polymers experienced about 50% reduction in Izod impact strength after UV exposure, while the stabilized compounds showed little or no reduction. LLDPE/UV1, LDPE-A/UV1 and LDPE-A/UV2 compounds showed almost no change in Izod impact strength with increasing UV aging. This indicates that the employed stabilizers have maintained the toughness of the samples with UV-aging.

Table 4.3 Summary of LLDPE Impact Testing Results

Sample	Izod impact strength (kJ/m^2)
Neat LLDPE	
Neat [0h]	23.4 ± 2.1
Neat [500h]	19.6 ± 2.3
Neat [1500h]	16.2 ± 1.7
Neat [2500h]	9.8 ± 2.5
LLDPE/ UV1	
UV1 [0h]	18.5 ± 1.3
UV1 [500h]	18.0 ± 1.0
UV1 [1500h]	18.9 ± 3.2
UV1 [2500h]	19.2 ± 1.1
LLDPE/ UV2	
UV2 [0h]	21.2 ± 4.4
UV2 [500h]	20.4 ± 2.2
UV2 [1500h]	20.7 ± 1.0
UV2 [2500h]	12.9 ± 5.8

On the other hand, the impact strength of LLDPE/UV2 remained constant up to 1500 h of exposure, but then decreased significantly at 2500h of exposure. This is in line with the crack development observed in the SEM image of this sample and indicates that the UV2 formulation may not be so effective in protecting LLDPE. This again can be attributed to the chain scissions that took place in this compound during UV-aging. For instance, chain scissions have led to recrystallized chains that were short and unattached, which left a place for cracks to form easily within any of

the detached chains. The mechanical properties of the compounds can be an indication to the severity of chain scissions that have taken place in each compound. In this case, it can be shown that LDPE-A compounds had better properties, and therefore better UV resistance, and this was also supported by the previously discussed SEM images.

Table 4.4 Summary of LDPE-A Impact Test Results

Sample	**Izod impact strength [kJ/m^2]**
Neat LDPE-A	
Neat [0h]	19.1 ± 4.9
Neat [1000h]	21.29 ± 2.1
Neat [1500h]	16.48 ± 1.4
Neat [2000h]	10.29 ± 1.6
LDPE-A/ UV1	
UV1 [0h]	15.94 ± 0.6
UV1 [1000h]	17.62 ± 2.5
UV1 [1500h]	18.79 ± 1.9
UV1 [2000h]	17.11 ± 1.5
LDPE-A/ UV2	
UV2 [0h]	18.00 ± 2.4
UV2 [1000h]	18.94 ± 2.1
UV2 [1500h]	18.43 ± 3.2
UV2 [2000h]	19.74 ± 4.1

4.4 Thermal Analysis

4.4.1 Thermogravimetric analysis (TGA)

The thermal decomposition behavior of UV aged samples was studied through thermogravimetric TGA to examine the thermal stability of the samples. The thermogravimetric curves were obtained for all the samples (Figures 4.11 to 4.19), and the degradation temperature (T_d) was determined at the maximum rate of weight loss and reported in Tables 4.5 and 4.6 for LLDPE and LDPE-A, respectively. The thermal decomposition profiles of the pure polymers and the UV stabilized compounds were examined at a heating rate of 10 °C min^{-1} under nitrogen atmosphere.

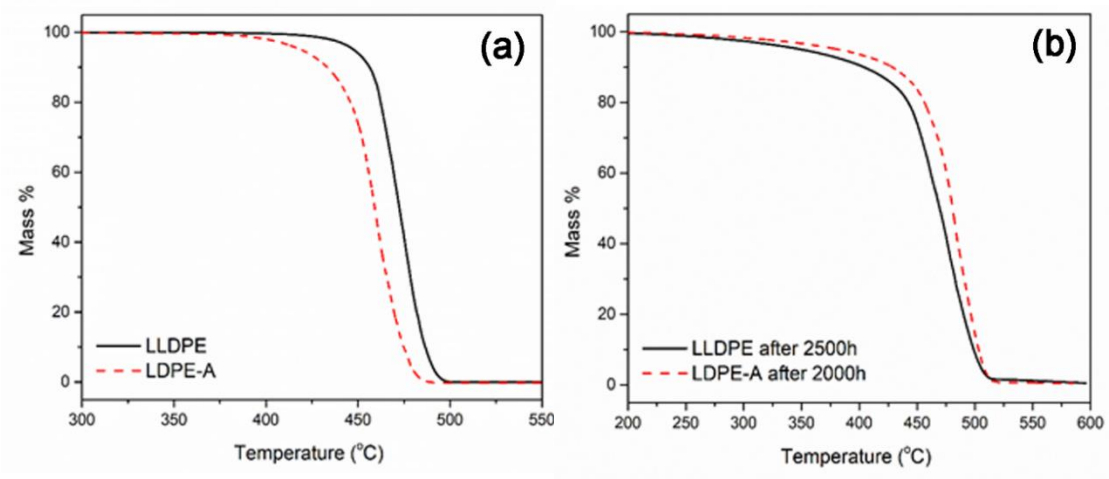

Figure 4.11 Thermal decomposition of neat LLDPE and LDPE-A (a) before UV aging and (b) after UV aging.

Both unexposed polymers showed a one-step decomposition (Figure 4.11). The maximum rate of weight loss was observed at 476 °C and 460 °C for unaged LLDPE and LDPE-A, respectively, which confirms the higher thermal stability of LLDPE. The higher thermal stability of LLDPE is in agreement with literature [83,

[84], and this ranking can be correlated with the branching degree and the number of the tertiary carbons that are the most reactive parts of the polymer molecule. LLDPE presented minimal branching when compared to LDPE-A, and thus a higher thermal stability. However, the UV aged neat polymers showed different thermal behavior (Figure 4.11(b)). The thermal decomposition of the aged LLDPE started at a lower temperature than the aged LDPE-A (Tables 4.5 and 4.6). The degradation temperature at the longest exposure periods was 477 °C and 487 °C for aged LLDPE and LDPE-A, respectively. It seems as if the UV-aging reduced the thermal stability of LLDPE more than that of LDPE-A, probably because LLDPE does not have long branches that could protect the main chain against UV-initiated chain scission.

The thermal decomposition behavior of the neat LLDPE and LDPE-A was clearly affected by the UV-exposure, as shown in Figures 4.12 and 4.13. The thermal decomposition of the UV aged samples started at lower temperatures in both polymers. The onset degradation temperatures of the samples with the longest exposure periods (2500h for LLDPE and 2000h for LDPE-A) were significantly lower than those of the unexposed samples, especially in the case of LLDPE. The UV exposure of LLDPE clearly reduced its thermal stability, while the thermal stability of LDPE-A increased after UV exposure. The most probable reason for this is the long branches in LDPE-A that probably crosslink during UV-exposure, making the polymer more thermally stable. This can also be seen in the increasing degradation temperature values (temperatures of maximum weight loss rate) with increasing aging times for both polymers. In LLDPE, T_d increased up to 1500 h of exposure, and then decreased significantly at 2500 h (Table 4.5), whereas in LDPE-A, T_d was observed to continuously increase with increasing UV exposure time (Table 4.6). The increase of T_d with aging was reported by [82], in which the

degradation temperature of thermally aged LLDPE pipes increased with aging up to 7200 h. This was explained by the effect of thermal oxidation that leads to crosslinking, and that the increased crosslink density increased the thermal stability of the sample. However, the conducted analysis showed an increase in T_d just up to 1500 h of exposure in LLDPE, and then a decrease for longer exposure periods. This indicates that the effect of UV aging on polyethylene differs from the effect of thermal aging as reported in the literature. Polyethylenes are susceptible to both chain scissions and cross-linking during photo-oxidation. Chain scission happens when the chains become weak and consequently cut at their reactive points, where the free radicals are. The chain scissions lead to an increased melt flow index and reduced molecular weight [36]. In other words, the temporary increase in T_d observed in LLDPE could be attributed to the increased density of cross-linking. However, the longer UV exposure periods has led to more chain scissions which accordingly led to a weaker structure and reduced thermal stability. This was also supported by the decreasing degradation onset temperature values with longer exposure. (Table 4.5).

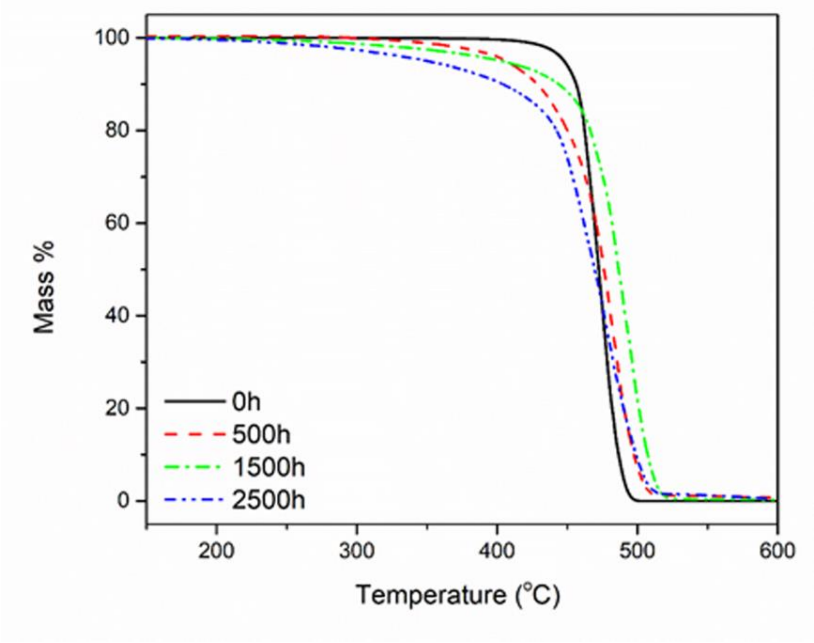

Figure 4.12 Thermal decomposition of UV-aged neat LLDPE

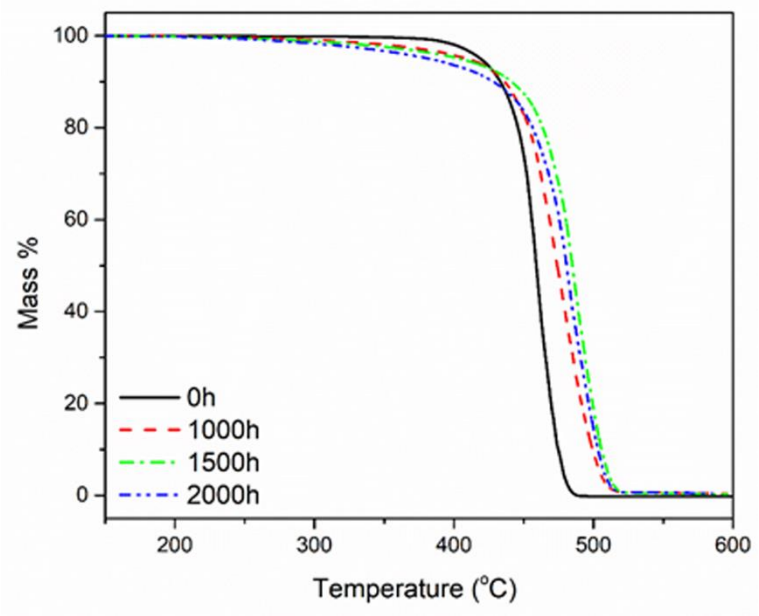

Figure 4.13 Thermal decomposition of UV-aged neat LDPE-A

The addition of the UV stabilizers resulted in significant changes in the thermal decomposition of the polymers (Figures 4.14 to 4.19). The effect of UV stabilizers was apparent in both unaged and aged samples. The degradation temperatures of

both unaged LLDPE and LDPE-A increased by more than 20 °C as a result to the addition of UV stabilizers (Tables 4.5 and 4.6). Similarly, the aged UV stabilized samples all showed an increase in thermal stability compared to the neat polymers. However, the UV-exposure influenced the thermal degradation behavior of LLDPE and LDPE-A in different ways. The UV1 and UV2 formulations showed very similar degradation behavior for both polymers, but this behavior is different from that of the two neat polymers. In the case of LLDPE/UV1, the degradation temperature followed a similar trend to that observed in neat LLDPE, in which it continued to increase up to 1500 h of exposure. After that, T_d decreased to 485.7 °C, which was about 12 °C less than the T_d of the unaged compound. The behavior of LLDPE/UV2 was different, as the degradation temperature decreased at all exposure periods, and decreased significantly after 2500 h of exposure to reach 479 °C, which is about 20 °C lower than that of the unaged compound. This indicates that LLDPE/UV1 is thermally more stable after UV aging than LLDPE/UV2.

In the case of LDPE-A, the difference in T_d between the unaged and aged formulations was found to be less than that of the LLDPE formulations. LDPE-A/UV1 showed a slight increase in T_d after 1000 h of exposure, and then decreased to reach 471.4 °C after 2000 h, which was 9 °C less than that of the unaged formulation. LDPE-A/UV2 showed the highest thermal stability of the four formulations.

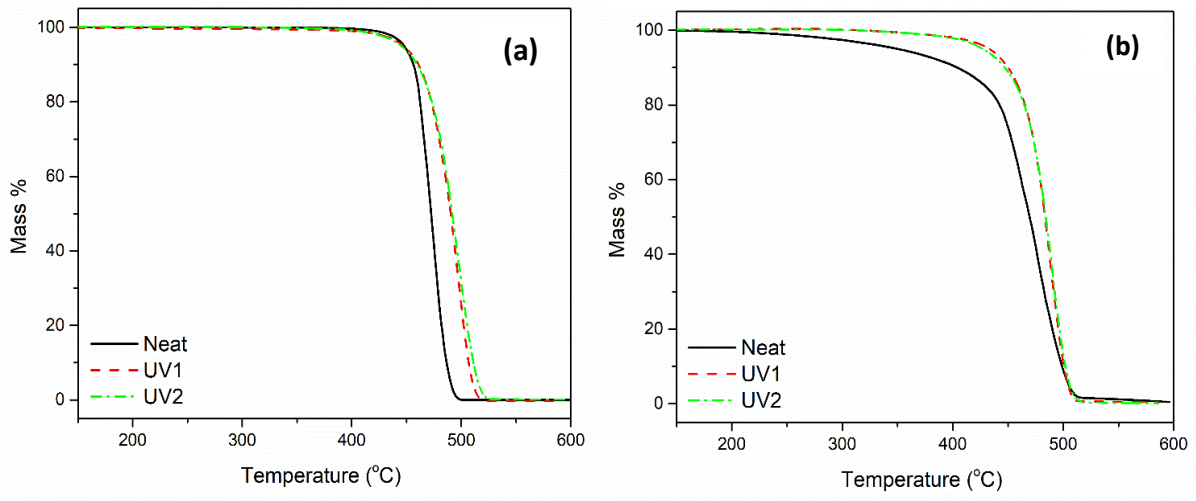

Figure 4.14 Effect of UV stabilizers on the thermal decomposition of (a) unaged LLDPE, and (b) LLDPE aged for 2500 h.

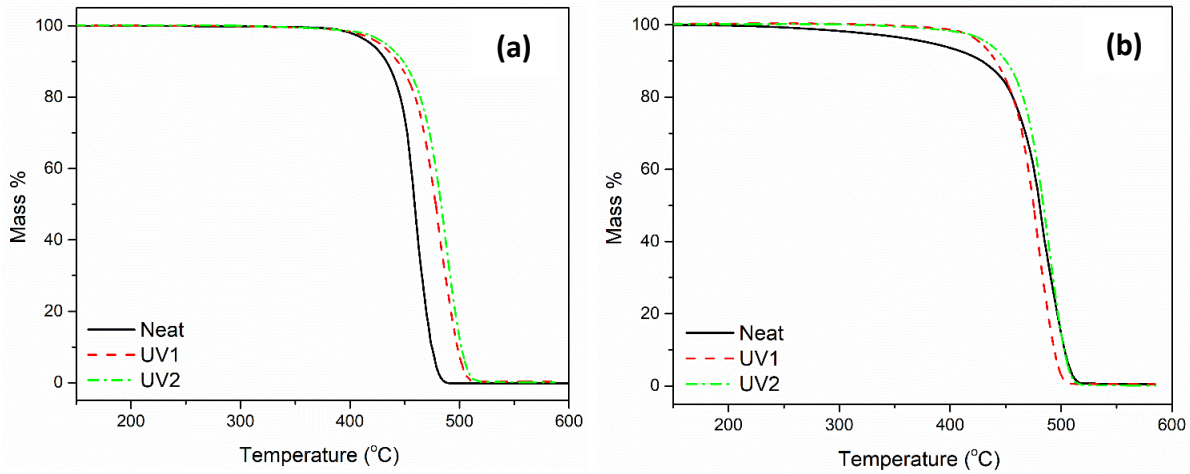

Figure 4.15 Effect of UV stabilizers on the thermal decomposition of (a) unaged LDPE-A, and (b) LDPE-A aged for 2000 h.

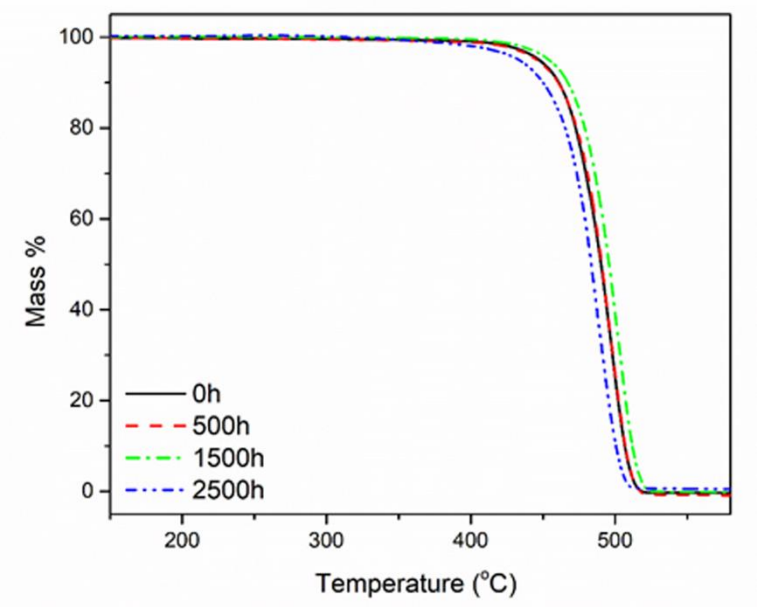

Figure 4.16 Thermal decomposition of UV-aged LLDPE/UV1 samples.

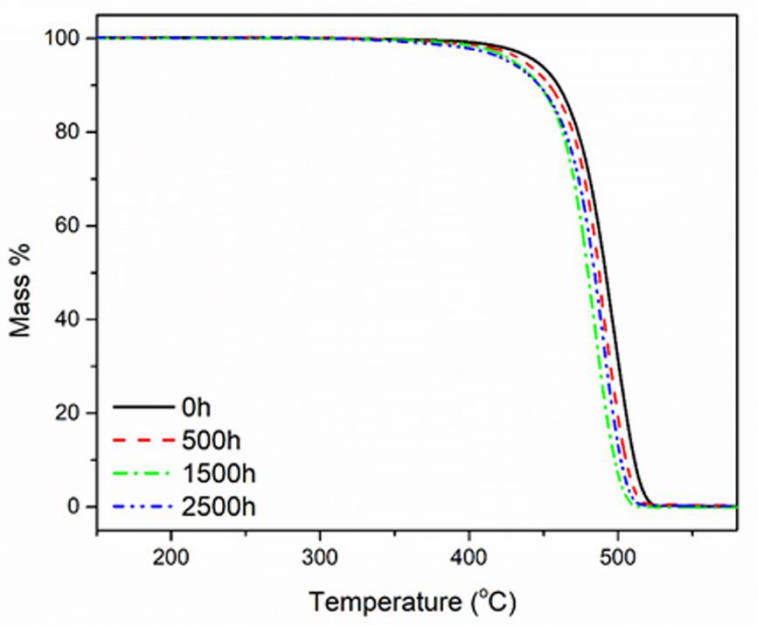

Figure 4.17 Thermal decomposition of UV-aged LLDPE/UV2 samples.

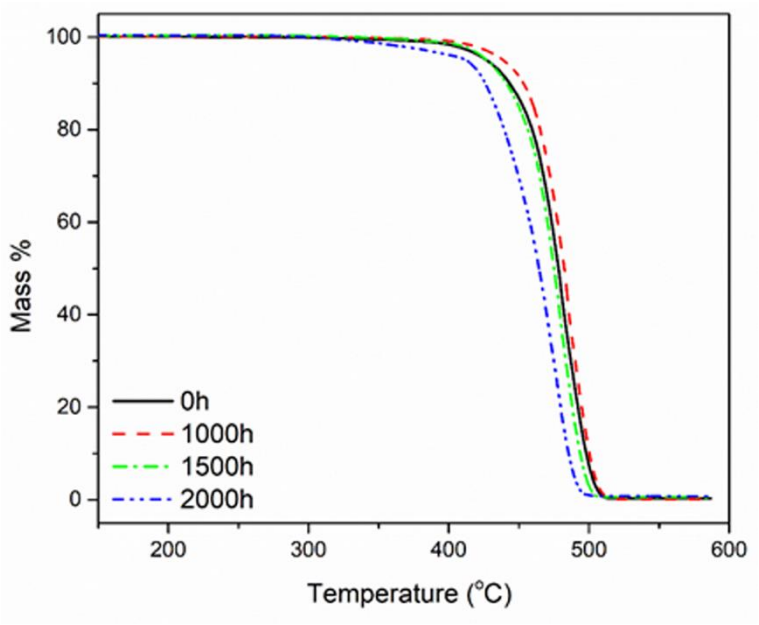

Figure 4.18 Thermal decomposition of UV-aged LDPE-A/UV1 samples.

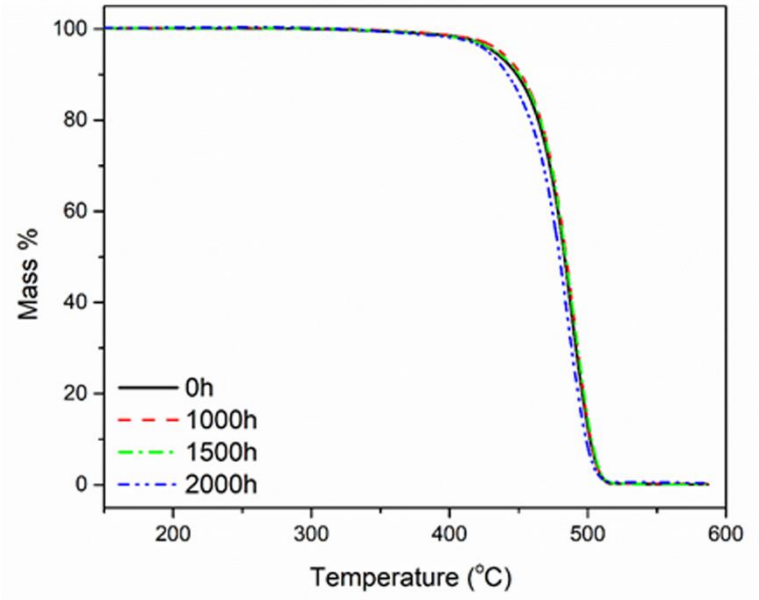

Figure 4.19 Thermal decomposition of UV-aged LDPE-A/UV2 samples.

Table 4.5 TGA Results for LLDPE

Sample	Onset temperature, $T_{d,5\%}$ (°C)	Degradation temperature, T_d (°C)
Neat LLDPE		
Neat [0h]	447.7	476.2
Neat [500h]	406	485.8
Neat [1500h]	370.3	497.3
Neat [2500h]	354.6	477.0
LLDPE/UV1		
UV1 [0h]	447.1	497.8
UV1 [500h]	445.8	498.5
UV1 [1500h]	454.2	502.1
UV1 [2500h]	433.1	485.7
LLDPE/UV2		
UV2 [0h]	445.4	498.9
UV2 [500h]	437.3	489.2
UV2 [1500h]	430.5	482.6
UV2 [2500h]	426.1	479.4

Table 4.6 TGA Results for LDPE-A

Sample	Onset temperature, $T_{d,5\%}$ (°C)	Degradation temperature, T_d (°C)
Neat LDPE-A		
Neat [0h]	419.0	460.2
Neat [1000h]	409.3	478.6
Neat [1500h]	403.6	481.7
Neat [2000h]	385.1	486.8
LDPE-A/ UV1		
UV1 [0h]	431.0	480.1
UV1 [1000h]	438.9	484.7
UV1 [1500h]	412.3	478.5
UV1 [2000h]	408.6	471.4
LDPE-A/ UV2		
UV2 [0h]	433.4	487.0
UV2 [1000h]	436.2	488.5
UV2 [1500h]	434.8	487.1
UV2 [2000h]	433.7	486.7

4.4.2 Differential scanning calorimetry (DSC)

In this analysis, a greater emphasis was placed on the first heating stage, as it represented the history of the samples (i.e. effect of exposure). The aim of this analysis was to understand the changes in melting points and crystallinity of the neat and stabilized samples, as a result of UV exposure. The melting temperature (T_m) and enthalpy (ΔH_m) were obtained from the DSC first heating cycle. The crystallization temperature (T_c) and enthalpy (ΔH_c) were obtained from the DSC

cooling cycle (Figures 4.20 – 4.23). The melting enthalpy (or heat of fusion) is an indicator of total crystallinity, as it is directly proportional to the mass fraction crystallinity in a polymer [9,82].

For the pure unaged polymers, the melting enthalpies ΔH_m were found to be 68.4 and 73.3 J/g for LLDPE and LDPE-A, respectively. The melting temperatures T_m were 125.0 °C and 115.5 °C for LLDPE and LDPE-A, respectively. Although the melting enthalpies of both polymers were almost similar, which implies a similar total crystallinity, the melting temperature of LLDPE was significantly higher. This is attributed to the fact that the crystals in LLDPE, which exhibit a higher density fraction with minimal branching, are thicker than those in LDPE [22,85]. LLDPE formed larger crystals through chain folding and lamellar growth as a result of its more linear morphology. In LDPE-A the high long branching content restricts the chains from folding and forming bigger crystals [1,38]. Therefore, a higher temperature is required to melt the bigger crystals, and that explains the higher melting temperature of LLDPE. For the aged samples of the neat polymers, a reduction in the melting temperature of LLDPE by 12 °C was observed after 2500 h of exposure, while for LDPE-A the melting temperature did not change significantly and remained almost constant after 2000 h of UV exposure. Both neat polymers experienced a significant increase in the melting enthalpy, which refers to the increase in crystallinity, which is the result of chain scission which gives rise to shorter chains that can crystallize easier. It has been reported that the chain scissions that are photochemically induced at an exposure temperature of 60 °C allow restructuring of the chains and lead to a higher crystallinity. At longer exposure periods, the higher crystallinity initiates cracks on the surface, which in return promote stress concentration. The stress concertation at the cracks along with the

scission of inter-crystalline bonds result in crack propagation [9]. Moreover, the long branches in LDPE-A that probably crosslink during UV-exposure, make the polymer more thermally stable. This was also seen in the presented TGA results, where the degradation temperature values increased with increasing aging times for LDPE-A, but decreased significantly after 1500h of exposure in LLDPE. The thermal analysis proves that LLDPE becomes more susceptible to chain sections, than LDPE-A, as a result of UV-exposure. Finally, the crystallization temperature and enthalpy values in the cooling cycle for both neat polymers did not change significantly with aging and remained similar.

For the stabilized compounds, LLDPE/UV1 showed higher melting temperatures after UV-aging than those of the neat polymer after similar periods of UV-aging, and these temperatures did not change as a result of UV-aging. This indicates that the addition of these stabilizers has conserved most of the properties of the polymer and improved its resistance against UV weathering. Moreover, the increase in enthalpy after aging was generally less than what observed in the neat versions. This indicates that less or no chain scissions took place during UV-aging as explained earlier in section 4.3.1. In LLDPE/UV2, a small decrease in T_m was observed after 1500h and 2500h of exposure, and the enthalpy increased by 30 J/g after 2500 h of exposure, which was the highest among the four compounds. This can indicate that this compound experienced more chain scissions than the other compounds, as stated earlier. These results support the previously presented TGA results, where LLDPE/UV2 samples experienced a significant reduction in the onset degradation temperature. It can be seen that the UV2 formulation was not as effective as UV1 in LLDPE.

The LDPE-A compounds showed a similar behavior to that of the neat version.

Minor fluctuations in the melting temperature were observed, which can be considered negligible, and an increase in ΔH_m by 10 J/g was observed in both LDPE-A compounds after 2000h of UV-aging. This again indicates that little or no chain scissions took place in LDPE-A during aging, by the act of UV absorbers and HALS. However, the increase in enthalpy probably refers to the crosslinking of long branches in LDPE-A that happened during UV-exposure.

All the stabilized compounds showed an increase in the crystallization temperature (T_c) at all exposure periods.

Another interesting observation was the higher values of enthalpy ΔH_m of all the stabilized compounds, than the neat version of the polymers. This observation was reported in the literature and attributed to the fact that UV absorbers act as nucleating agents. That is, those inorganic particles act as seeding points that attract the polymer chains and help them to crystallize around them (i.e. forming a crystalline part). Therefore, the presence of UV absorbers in the polymer matrix allows it to form more crystals or crystalline folds during thermal decomposition [9]. In addition, the crystallization temperature (T_c) values of all the stabilized compounds were higher than those of the neat versions, at all exposure periods. This supports the nucleating theory, as if there is a nucleation, the polymer will begin to crystallize at a higher temperature than when there is no nucleation [9].

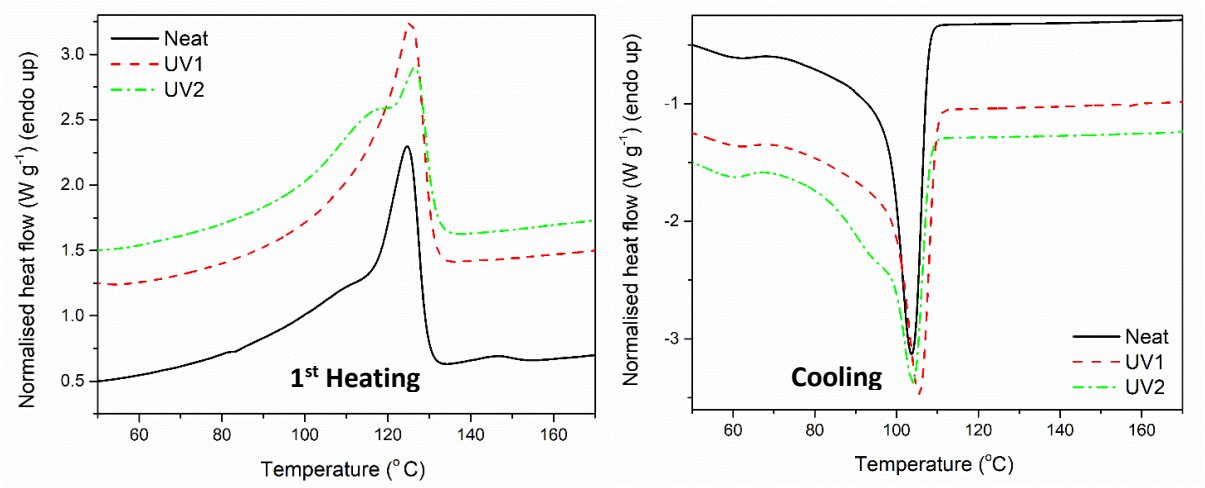

Figure 4.20 DSC cooling and heating (1st heating) curves of unaged LLDPE compounds

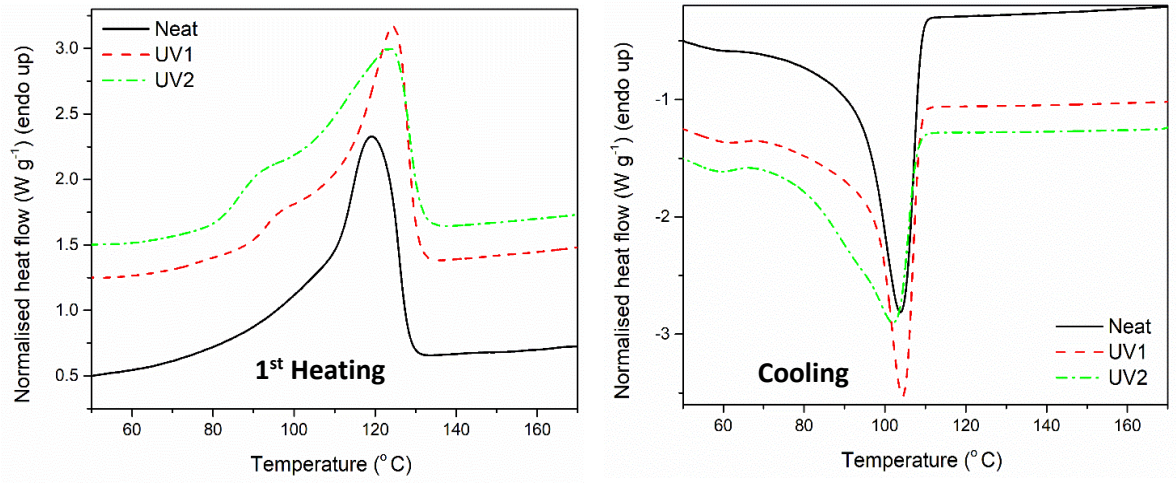

Figure 4.21 DSC cooling and heating (1st heating) curves of aged LLDPE compounds for 2500h

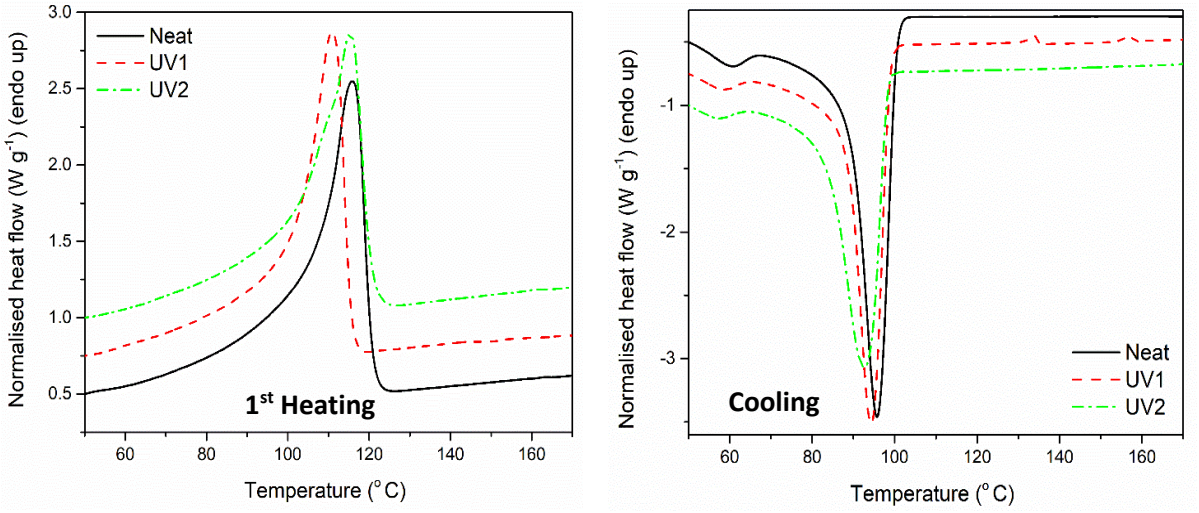

Figure 4.22 DSC cooling and heating (1st heating) curves of unaged LDPE-A compounds

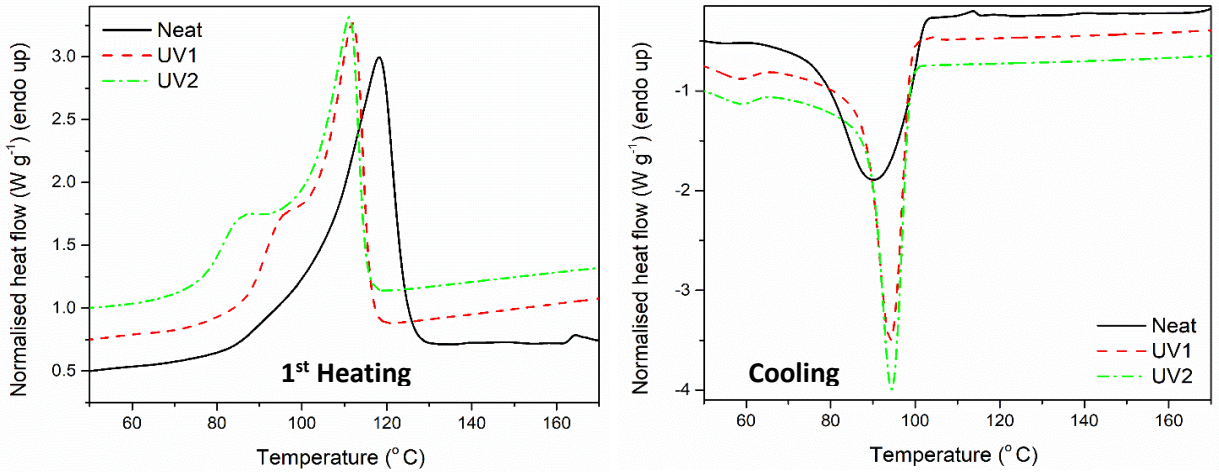

Figure 4.23 DSC cooling and heating (1st heating) curves of aged LDPE-A compounds for 2000h

Table 4.7 DSC Results for LLDPE

Sample	**Melting temperature, T_m (°C)**	**Melting enthalpy, ΔH_m (J/g)**	**Crystallization temperature, T_c (°C)**	**Crystallization enthalpy, ΔH_c (J/g)**
Neat LLDPE				
Neat [0h]	125.0	68.4	103.9	70.2
Neat [500h]	117.7	110.8	91.6	66.3
Neat [1500]	116.8	113.4	92.0	75.6
Neat [2500h]	113.4	112.7	104.1	73.6
LLDPE/ UV1				
UV1 [0h]	125.5	89.3	105.7	64.5
UV1 [500h]	127.7	96.1	105.6	63.2
UV1 [1500h]	125.5	96.3	106.2	63.5
UV1 [2500h]	124.5	105.5	108.7	67.4
LLDPE/ UV2				
UV2 [0h]	126.7	89.8	104.1	69.8
UV2 [500h]	126.4	90.2	105.5	66.9
UV2 [1500h]	124.4	112.3	102.1	72.7
UV2 [2500h]	122.5	119.2	103.6	71.68

Table 4.8 DSC Results for LDPE-A

Sample	**Melting temperature, T_m (°C)**	**Melting enthalpy, ΔH_m (J/g)**	**Crystallization temperature, T_c (°C)**	**Crystallization enthalpy, ΔH_c (J/g)**
Neat LDPE-A				
Neat [0h]	115.5	73.3	94.4	74.4
Neat [1000h]	114.7	89.6	90.2	68.6
Neat [1500]	114.3	105.6	89.8	69.3
Neat [2000h]	116.1	106.3	90.4	72.2
LDPE-A/ UV1				
UV1 [0h]	111.0	92.5	94.4	67.8
UV1 [1000h]	115.2	94.0	93.0	69.8
UV1 [1500h]	116.8	94.8	93.0	68.2
UV1 [2000h]	112.1	101.3	94.4	69.0
LDPE-A/ UV2				
UV2 [0h]	115.6	89.5	96.1	69.7
UV2 [1000h]	114.4	99.0	93.7	68.7
UV2 [1500h]	114.6	101.2	93.4	70.1
UV2 [2000h]	113.3	99.2	94.8	69.2

In conclusion, the thermal analysis results were in agreement with the presented mechanical characterization and microscopic analysis. To sum up, the analyzed PE grades reacted differently to oxidative-photo-degradation. It was also found that although LLDPE is thermally more stable than LDPE grades, it has shown a lower resistance against UV-aging. The two formulations that were both based on a

synergistic combination of HALS and UV absorbers have significantly enhanced the stability of PE grades against UV-weathering. The mechanical and thermal analyses have shown that the introduction of both formulations has decreased or prevented chain scissions, which was apparent in the Young's modulus and melting enthalpy values.

However, the selection of one optimal solution is not a direct decision. For instance, the first conclusion that have been approved by all the presented results is the higher stability of LDPE-A compounds against UV-aging, than LLDPE compounds. Although the same formulations were employed in both polymers, LDPE-A compounds showed better mechanical and thermal properties than LLDPE compounds. This can be attributed to the structure of LDPE-A that employs long branches, which protected the main chain against UV-initiated chain scission [5, 32]. Moreover, a study conducted by [5] reported that the structure of LDPE grades that comprises more amorphous regions and branches plays a significant role in controlling the effectiveness of UV stabilizers. The study showed that LDPE films were more stable and protected against UV aging than LLDPE films, as the generated free radicals from HALS have a diffusion ability to interact with amorphous zones of PE structures. In other words, HALS become more effective in PE structures that have more amorphous zones, than the ones with more crystalline regions.

Furthermore, another significant observation was the lower stability of LLDPE/UV2 compounds (compared to LLDPE/UV1). This formulation was based on a combination of Sabostab 119 (HALS) and Tinuvin 1577 (UV absorbers). Although this formulation was very effective in LDPE-A, an opposite performance was observed in the case of LLDPE. This can be ascribed to the nature of the polymer as

explained, and also can be related to the mechanism of action of the additives. In fact, the selection of an optimal HALS cannot be achieved directly, as the mechanism of action of HALS is generally circumstances-dependent as explained in section 2.2.3.2. Also, the chemical structure of HALS does not change during photooxidation, and therefore the reduced performance of a certain HALS cannot be attributed to a chemical reason, but rather to other physical factors [86]. Two important parameters that can be further investigated to assess the performance of a HALS in a certain polymer are compatibility and solubility. Several studies reported reduced performance of different types of HALS that vary in structure and molecular weight, when their compatibility was poor [86]. It can be concluded that either compatibility or solubility, or both may have influenced the effectiveness of one or more of the additives. Time constraints and lack of sophisticated apparatus did not allow performing such analysis to specifically identify the reasons behind the reduced performance of UV2 in LLDPE.

4.5 Fourier-Transform Infrared (FTIR) Spectroscopy

Fourier-transform infrared spectroscopy (FTIR) is a technique used to obtain information about the changes in a polymer's chemical composition after UV-aging. This analysis was performed to evaluate the degree of degradation by measuring the amount of one of the major photo-degradation products, the carbonyl groups. The carbonyl index (CI) was calculated by the integral of the carbonyl peak (1650-1800 cm^{-1}) and the C-H peak (1420 - 1480 cm^{-1}).

$$CI = \frac{Absorption\ of\ carbonyl\ species_{1650-1800\ cm^{-1}}}{Absorption\ of\ C-H\ peak_{1420-1480\ cm^{-1}}}$$

Both neat LLDPE and LDPE-A showed increased CI with UV aging. The CI for neat the LLDPE samples was 0.67 after 500 h of exposure, while for neat LDPE-A it was 0.87 after 1000 h of exposure. The CI continued to increase in the neat versions to reach 1.50 and 1.15 in LLDPE and LDPE-A, after 2500 h and 2000 h of UV aging, respectively. These values indicate that the amount of carbonyl groups on the LLDPE surface was higher, compared to LDPE-A, after the longest periods of exposure.

On the other hand, all the stabilized compounds had zero CI, due to the absence of any peaks at 1650-1800 cm^{-1} (Figures 4.24 and 4.25). This refers to a lack of degradation products in these samples. This indicates that the UV stabilizers have sufficiently protected the samples from photo-degradation.

However, according to a study conducted by [31], the carbonyl index is not a reliable indication of photo-degradation. This is because the oxidation process begins on the surface and free radicals propagate towards the center of the sample leading to further degradation. This technique can measure a depth of 1-2 µm only from the sample surface. which limits the total oxidative products measured and consequently may not represent the bulk sample that was 50 µm thick or thicker. Therefore, the formation of some degradation products in some of the stabilized samples is possible, even though it was not observed in the conducted FT-IR analysis. However, the previously presented results have given us an indication to the most promising stabilized compounds.

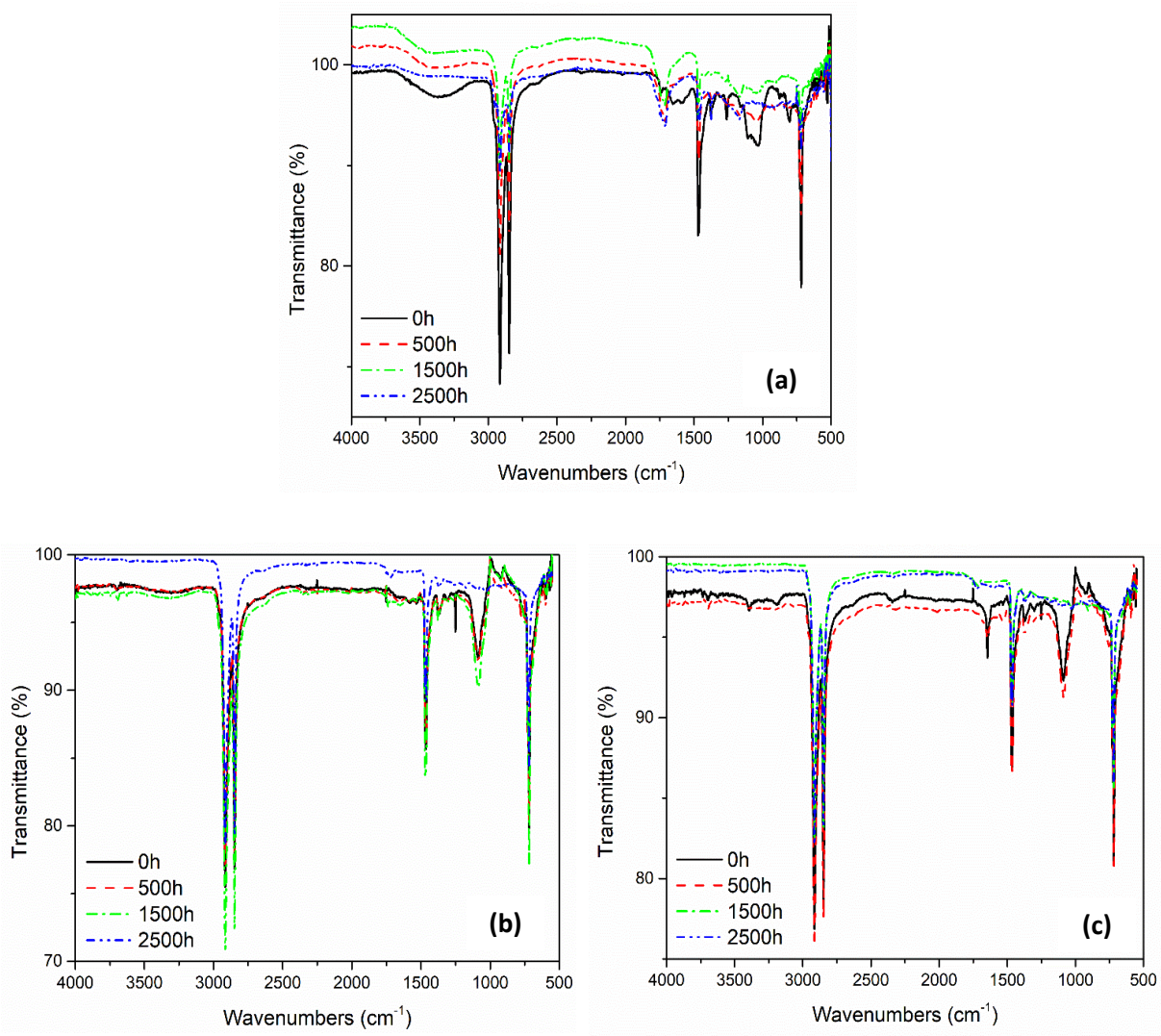

Figure 4.24 FT-IR spectra of (a) neat LLDPE, (b) LLDPE/UV1 compounds, and (c) LLDPE/UV2 compounds at different UV-exposure periods

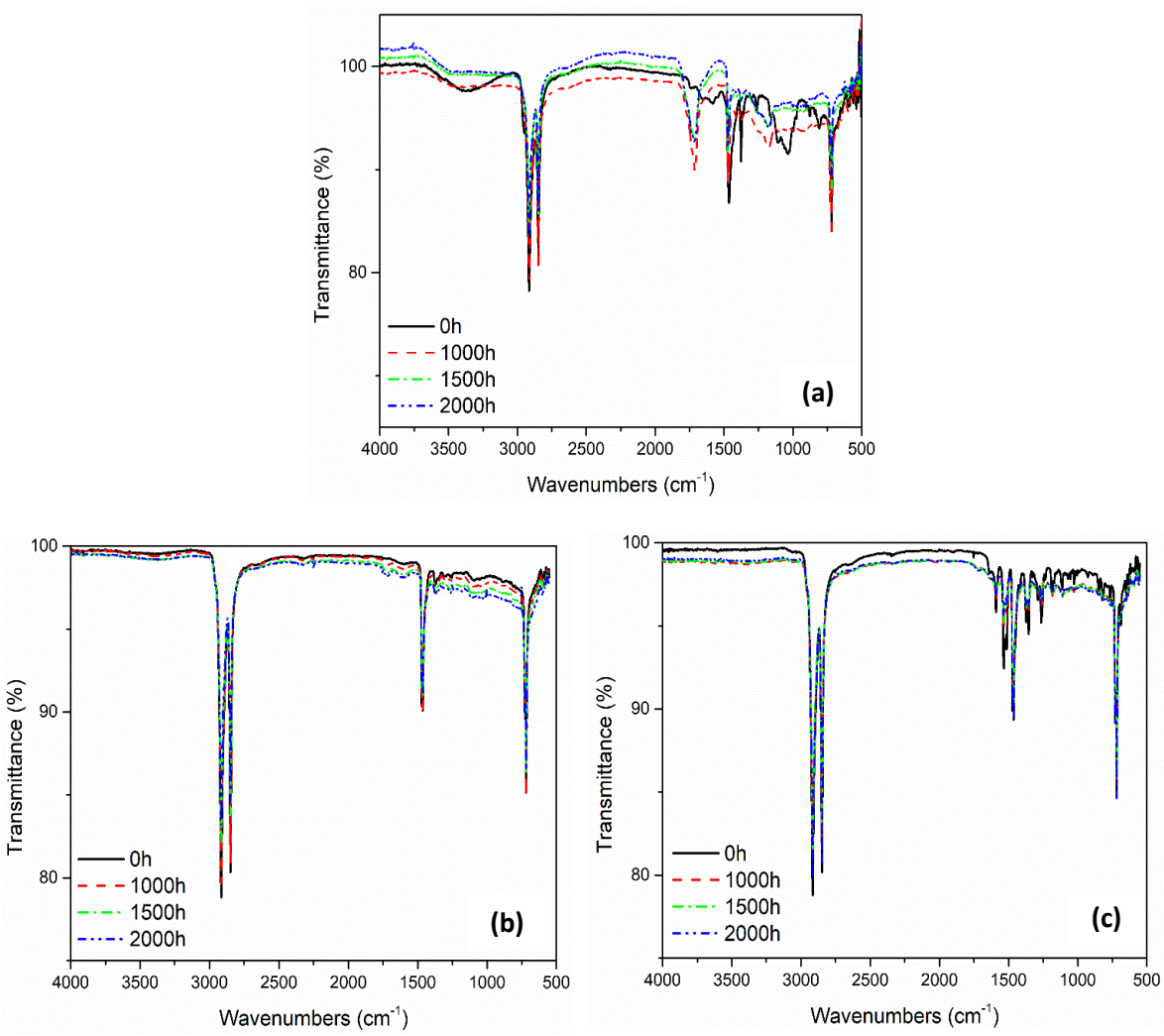

Figure 4.25 FT-IR spectra of (a) neat LDPE-A, (b) LDPE-A/UV1 compounds, and (c) LDPE-A/UV2 compounds at different UV-exposure periods

Chapter 5: Comparison Between Flame Retardancy of LLDPE and LDPE-A

5.1 Thermal Decomposition of FR-Containing Compounds

A thorough thermal analysis was conducted on the FR compounds prior conducting the flammability test. The aim of this analysis was to obtain an initial understanding and assessment of the role of the FR additives and their effect on the thermal decomposition of the polymers.

The onset of decomposition temperature refers to the temperature where it is assumed that a significant amount of fuel consumption has begun, or in other words the beginning of decomposition. The onset of decomposition temperature in this analysis was defined as the temperature at 5% weight loss ($T_{d,5\%}$). The degradation temperature (T_d) was determined at the maximum rate of weight loss, and the char yield as the % residue at 600 °C and 800 °C. The thermal decomposition profiles of the pure components (additives, pure polymers) and of the FR-containing compounds were examined at a heating rate of 10 °C min^{-1} under nitrogen atmosphere.

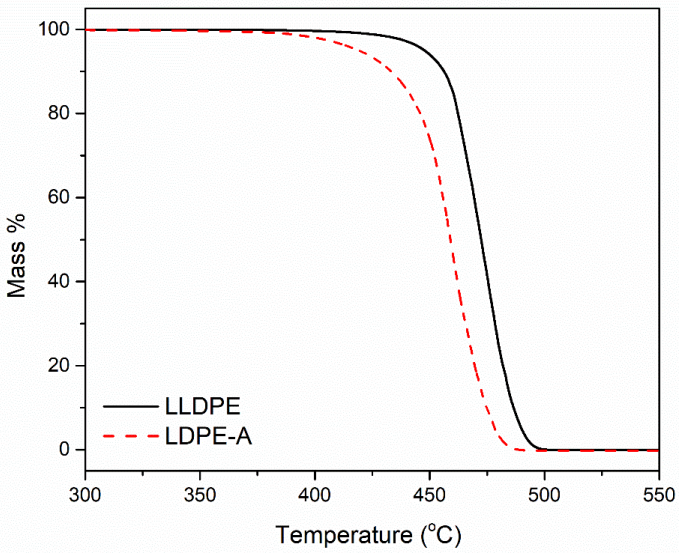

Figure 5.1 TGA curves of pure LLDPE and LDPE-A under nitrogen

Starting with the pure polymers, both polymers exhibited a one-step decomposition under nitrogen (Figure 5.1), as presented earlier in section 4.4.1, with the onset of LDPE-A and LLDPE backbone degradation ($T_{d,5\%}$) in the range of 419 – 448 °C respectively. The maximum rate of weight loss was observed at 476 °C and 460 °C for LLDPE and LDPE-A respectively. Both neat polymers had negligible residue values, verifying the little char formation which characterizes polyolefins. When comparing the PE grades, LLDPE presented a higher thermal stability under nitrogen than LDPE-A. The higher thermal stability of LLDPE is in agreement with literature [83,84], and this ranking can be correlated with the branching degree and the number of the tertiary carbons that are the most reactive parts of the polymer molecule. LLDPE presents minimal branching when compared to the LDPE grades, and thus higher thermal stability.

Turning to the pure FR additives, TGA analysis revealed that the $T_{d,5\%}$ varied between 243 and 380 °C, which is significantly lower than those of the pure polyethylene grades (Figure 5.2). The onset decomposition temperature, degradation temperature and residue at 800 °C for the FR additives are reported in Table 5.1. More specifically, the degradation of the alkoxy amine (triazine derivative, Flamestab NOR116), which is a nitrogen-based FR, was found to be a two-step process with maximum rates of weight loss at 290 and 437 °C, and with a residue of 4%, implying a low charring ability. PPM Triazine HF is also a nitrogen-based additive, but it presented a higher residue (17.3% under N_2), showing its role as a charring source. The commercial mixture of the Triazine HF with ammonium polyphosphate (PPM Triazine 765) exhibited negligible char, with more than two steps of thermal decomposition. The two-step decomposition can be attributed to the used ratio of the CFA:APP in the commercial system. When the CFA content is

high, the corresponding system has an excessive, unnecessary amount of charring source and a lack of acid source. Therefore, a part of the CFA cannot be dehydrated into char and decomposes into gas products [79].

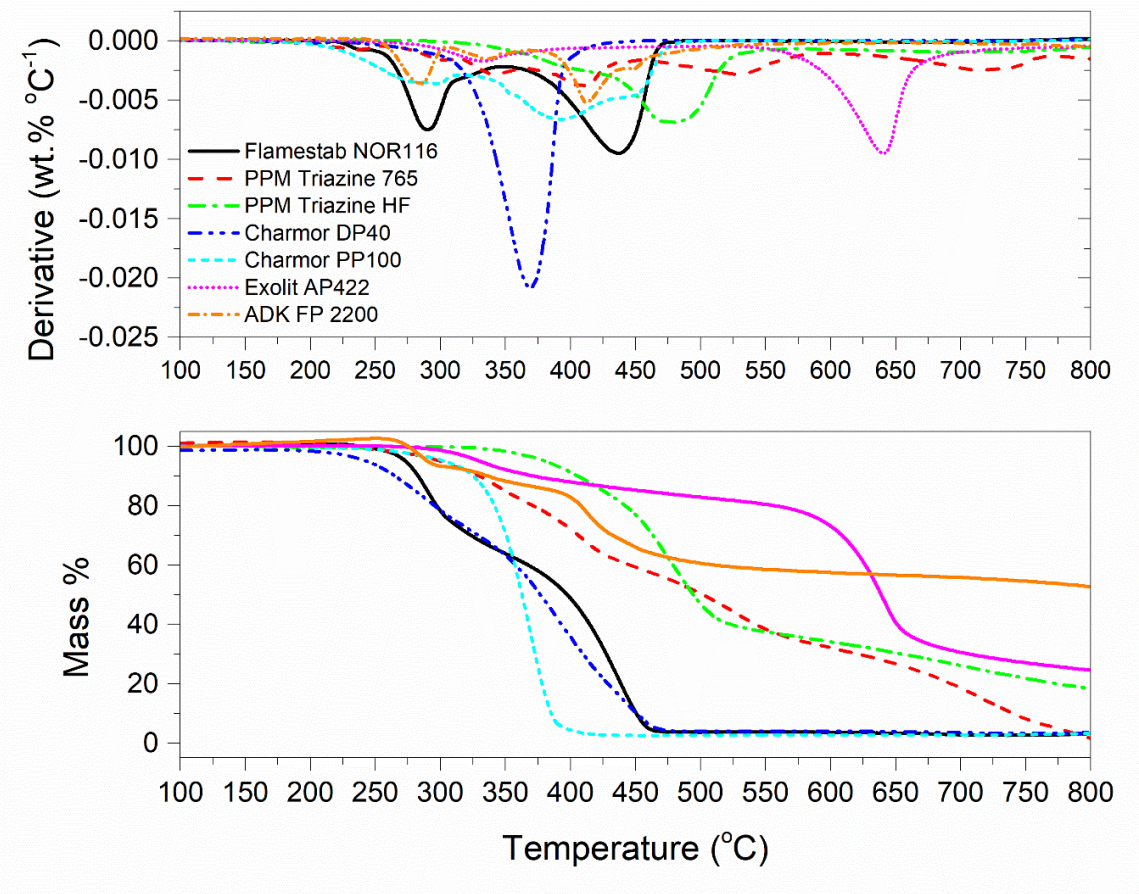

Figure 5.2 TGA curves of pure FR additives under nitrogen atmosphere.

Similarly, the two pentaerythritol derivatives [Charmor PP100 (polypentaerythritol) and Charmor DP40 (dipentaerythritol)] did not yield a significant amount of char (3.6%, 3.9%), and they presented mainly one step of thermal decomposition with respective onsets of degradation at 243.1 °C and 303.8 °C. The pentaerythritol derivatives obviously decompose into gas phase products in the absence of an acid source. As far as ammonium polyphosphate (Exolit AP422) is concerned, its decomposition profile presented a first weight loss peak at 330 °C under N_2,

attributed to the elimination of NH_3 and H_2O during the thermal decomposition of the polyphosphate. The second peak appearing at 641 °C is attributed to the release of phosphoric acid, polyphosphoric acid and metaphosphoric acid with the decomposition of APP [79]. Moreover, Exolit AP422 produced a high char residue of 23.5%. This can be explained by the polyphosphoric acid itself that was reverted to phosphoric acid and volatile gases during the decomposition, such as NH_3, N_2, which cause the char to swell. NH_3 reacts with phosphoric acid, gathering in the swollen char layer to produce the corresponding salt, and this salt constitutes a block protecting the underlying material [65].

ADK Stab FP 2200 exhibited the most promising TGA curve in terms of intumescence. It is a blend of phosphorus-nitrogen compounds and the thermal degradation occurs in two main steps, with the first T_d at 292 °C and the second at 412 °C, corresponding potentially to the loss of water and small molecules such as NH_3, further carbonization and the thermal degradation of char residue. The TGA curve is similar to the one of the alkoxy amine (Flamestab NOR116), but the char residue at 800 °C was found much higher, i.e. 51%. This char yield was in fact the highest value among all the examined FRs, implying that this FR system combines a carbon source, an acid source and a blowing agent, and presents high charring ability under the synergism of phosphorus and nitrogen compounds.

Table 5.1 TGA Results for the Flame Retardants

Flame retardant additive	**Onset temperature, $T_{d,5\%}$ (°C)**	**Degradation temperature, T_d (°C)**	**Residue at 800 °C (%)**
Flamestab NOR116	273.4	290, 437.2	4%
PPM Triazine 765	299.8	--	0.6%
PPM Triazine HF	380.2	478.1	17.3%
Charmor DP40	303.8	369.2	3.9%
Charmor PP100	243.1	388.7	3.6%
Exolit AP422	330.5	330, 641.4	23.5%
ADK FP 2200	290.2	292, 412.2	51.2%

The presence of the FRs in the polymer matrix resulted in changes in the TGA curves compared to the neat version of the polymers. As can be seen in Figures 5.3 and 5.4, the thermal decomposition of the FR-containing compounds involved more than one degradation step, with lower onset temperature values compared to the neat versions (Tables 5.2 and 5.3). This is obviously due to the earlier degradation of the additives. the $T_{d,5\%}$ value was decreased in the range of 330-422 °C under nitrogen, which was found in other polyethylene FR systems and was attributed to the lower stability of the bonds in the FR molecules (such as P-O and C-N) compared to the uniform C-C bonds in polyethylene [21,87]. The lowest $T_{d,5\%}$ values were observed in the cases of FR5 and FR6, i.e. when the pentaerythritol derivatives and APP were used, and can be attributed to the formation of thermally unstable ester mixtures between the -P-OH group in the APP molecules and the -OH group in the CFA [64].

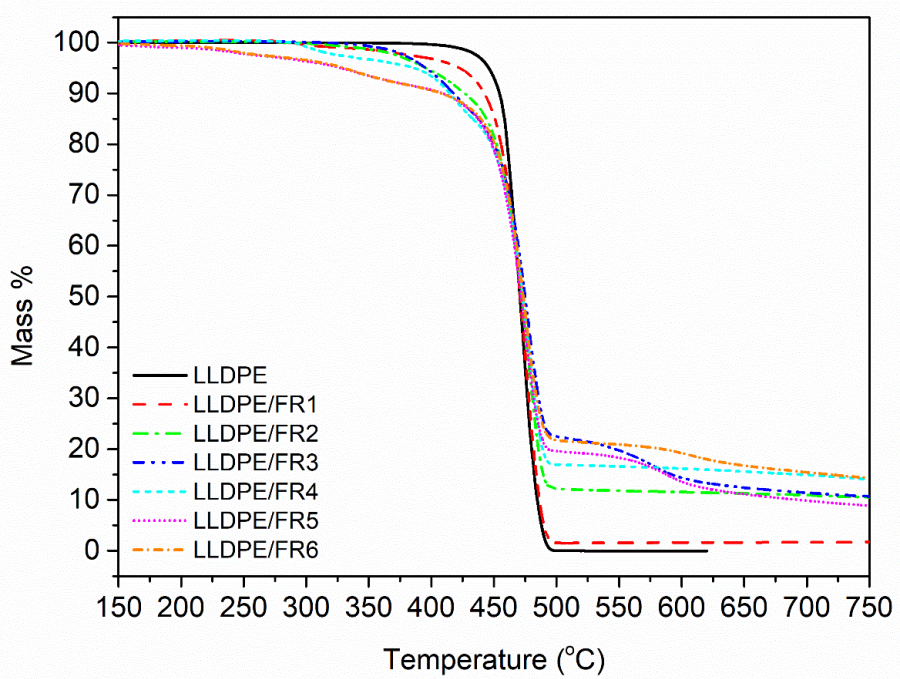

Figure 5.3 TGA curves of LLDPE FR-containing compounds

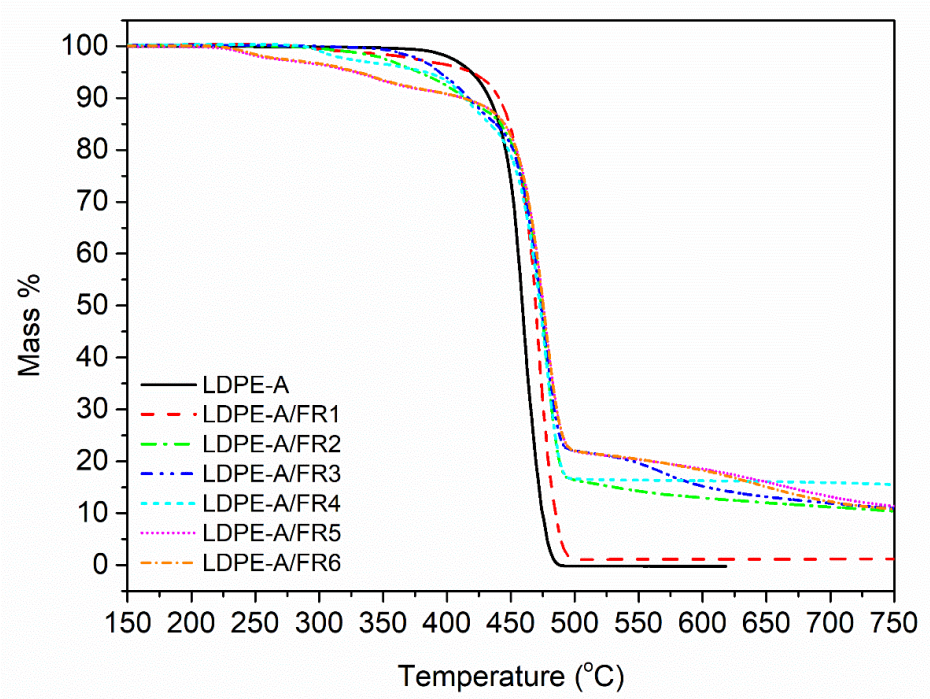

Figure 5.4 TGA curves of LDPE-A FR-containing compounds

Table 5.2 TGA Results for LLDPE FR- Containing Compounds

FR Formulations	**Onset temperature, $T_{d,5\%}$ (°C)**	**Degradation temperature, T_d (°C)**	**Residue at 600 °C (%)**	**Residue at 800 °C (%)**
Neat LLDPE	447.7	476	0	0
LLDPE – FR1	421.9	475.3	1.8	1.6
LLDPE - FR2	395.2	478	11.45	9.8
LLDPE – FR3	394.9	477.2	13.3	9.9
LLDPE – FR4	385.7	477.7	16	12.6
LLDPE – FR5	327	474.9	12.25	7.9
LLDPE – FR6	330	475.4	18	13.1

When comparing the degradation temperatures at the maximum weight loss (T_d), the addition of FRs resulted in an increase in T_d (Tables 5.2 and 5.3), proving the formation of a protective char layer and improving the thermal stability of polyethylene. In the work of Makhlouf et al. [87], an increase in the T_d by 30 °C was observed in the case of the effective LLDPE FR formulation. In the work of Xie and Qu [88], the flame retarding mechanism of the expandable graphite/halogen-free FR system for LLDPE also gave rise to such an increase in the thermo-oxidative degradation temperature. It can be seen in Tables 5.2 and 5.3 that T_d has increased for all the LDPE-A FR-containing compounds, compared to the neat version, by about 15 °C. In LLDPE compounds, the increase was almost insignificant (up to 2 °C).

Table 5.3 TGA Results for LDPE-A FR- Containing Compounds

FR Formulations	**Onset temperature, $T_{d,5\%}$ (°C)**	**Degradation temperature, T_d (°C)**	**Residue at 600 °C (%)**	**Residue at 800 °C (%)**
Neat LDPE-A	419	460.2	0	0.2
LDPE-A – FR1	419	471.5	1.4	1.1
LDPE-A - FR2	378	477.3	12.57	9.3
LDPE-A – FR3	394	476.5	14.2	9.5
LDPE-A – FR4	383.5	477.7	16.2	14.2
LDPE-A – FR5	327.7	477.9	17.6	9.8
LDPE-A – FR6	330.4	477.6	17.08	9.5

The residue in the TGA can also be correlated with the formation of a protective char layer during the polymer combustion [62–64,79,87,89]. FR1, which contained a nitrogen-based additive, failed to increase the char yield, so it is anticipated that the relevant formulation will not be efficient due to a lack of the acid source. On the other hand, the addition of the other FRs dramatically increased the residue, with the highest value observed for FR4 (16.2%) in the case of LDPE-A and FR6 (18%) for LLDPE at 600 °C. It is important to emphasize that the low residue of the pure pentaerythritol derivatives (Charmor DP40 and PP100) was not observed in the FR5 and FR6 formulations, since along with the acid source, they can result in an effective intumescent system. However, it should be pointed out that in the literature, there is no direct correlation between the char residue and the UL94 V ranking; when the compound presents higher residue, it presents potentially better flammability properties, but it is not necessary that the highest amount of char gives

V0 in UL94 ranking. This also has to do with the proper ratio of charring agent to acid source, so as to produce the optimum char layer morphology, e.g. tiny bubbles embedded on the surface of each large bubble, and a compact and continuous intumescent char [62].

5.2 Flammability Test

UL 94 tests are widely used to evaluate the flame resistance of polymers. The results fall into three categories with burning ratings V0, V1, and V2, with V0 corresponding to the highest level of flame resistance. The results of the FR-containing polyethylene grades are given in Figures 5.5 and 5.6 for LLDPE and LDPE-A respectively. In both polyethylene grades, FR1 presented a low flame resistance since the total burning time was the longest and the samples failed in the UL 94 testing (NC: not classified). It is in agreement with the TGA results where the char yield was low (up to 2 %), and this proves that nitrogen-based compounds alone cannot achieve a V0 rating for polyethylene [79]. In fact, the relevant nitrogen-based radical generator is mentioned to perform well when combined with triazine derivatives for polyolefin foams and films [90].

In the case of LLDPE (Figure 5.5), FR3 and FR5 presented the lowest burning times in LLDPE compounds; 356 and 235 s respectively, but they failed to obtain a safe UL 94 ranking. The other formulations (FR2, FR4, FR6) presented poorer results and failed in presenting a safe UL 94 ranking. In the case of LDPE-A (Figure 5.6), FR3 was proved significantly efficient reaching a UL 94 V0 rating and a low total burning time (1.4 s). FR3 is the mixture of the triazine derivative and APP in a 1:3 ratio of the charring agent to APP with a total loading of 35 wt.%; the mechanism of phosphorus-nitrogen synergism is considered to be provided by the ultimate formation of phosphorous oxynitride, which is a high-temperature resistant

material [90]. FR3 performance can be correlated with the TGA results, where it presented the highest onset of thermal degradation for the LDPE-A FR-containing compounds, with an increase in T_d by 16 °C and a char yield of almost 10% at 800 °C under nitrogen. FR4 presented the next lower burning time (43.3 s), a performance which can again be correlated with the high char yield in the TGA (14% at 800 °C) and an increase in T_d by almost 18 °C. The other formulations (FR2, FR5, FR6) presented poorer results in terms of UL 94 ranking; especially for FR2 it can be said that the commercial mixture of the triazine derivative with APP (PPM Triazine 765) was not as efficient as the FR3-containing grade, where the same mixture was prepared in a ratio CFA:APP = 1:3. The low FR efficiency of FR2 can also be correlated to the zero char yield of the additive alone in the TGA test.

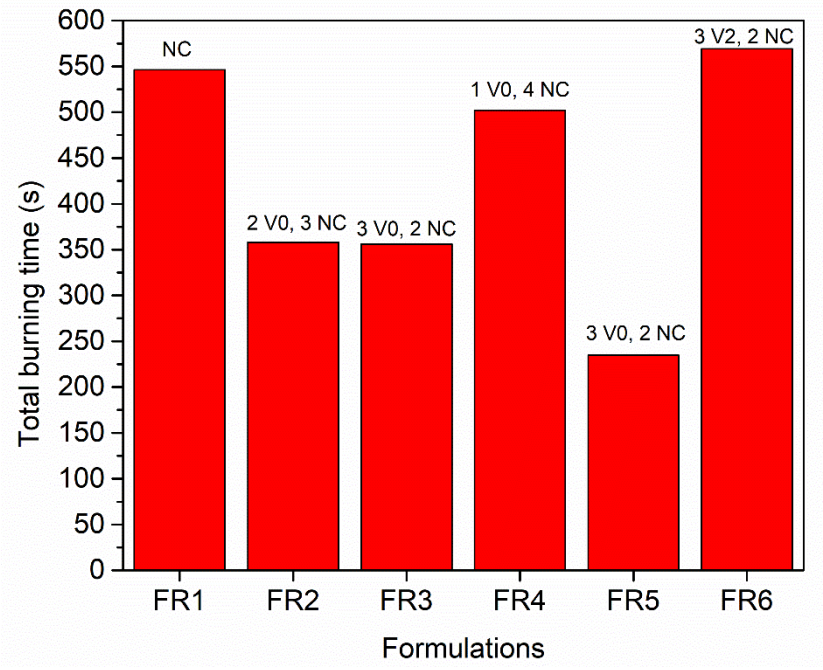

Figure 5.5 UL 94 V results for LLDPE FR-containing compounds

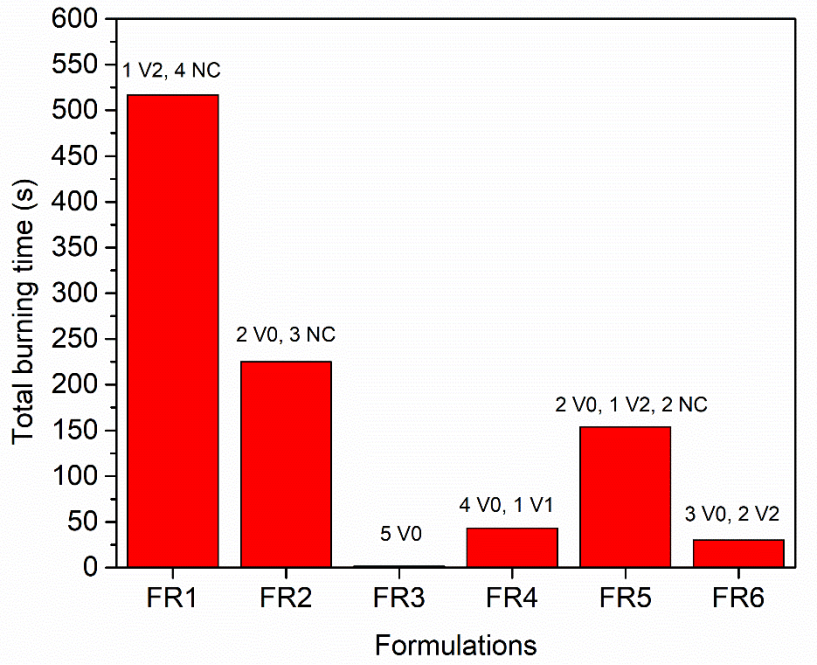

Figure 5.6 UL 94 V results for LDPE-A FR-containing compounds

When comparing the two polyethylene grades, it is interesting to note that in general, all the FRs presented smaller burning times and higher reproducibility in LDPE-A compounds compared to LLDPE. Inherently, LDPE-A is thermally less stable than LLDPE (Figure 5.1) but was found to be more effectively flame retarded through the examined formulations. A possible reason for the poorer performance of the flame retardants in LLDPE can be the less homogenous dispersion of the additives in the polymer matrix and/or the premature decomposition of the additives, e.g. of APP, due to internal shear during the extrusion and/or the injection step. Therefore, to further investigate the poor performance of LLDPE formulations, SEM analysis was performed on the two formulations that achieved promising results in LDPE-A (FR3 and FR4) to compare the dispersion of the relevant additives in both polymers. SEM images were taken for the relevant additives, as well as FR3 and FR4 compounds on the fractured cross section surfaces of the UL 94 bars prior to and after the testing, as shown in the next section (Figures 5.7 and 5.8).

5.3 Microscopic Analysis

Starting with LDPE-A/FR3 compound, which gave the safest V0 ranking result, it can be seen that the additives APP and Triazine (Figure 5.7 (a-b)) were well dispersed in the polymer matrix with a small number of aggregates (Figure 5.7 (c)). The smooth surface of the commercial APP [89] and the shape of Triazine HF can be distinguished in consistence with similar SEM images for APP systems in polyolefins [91]. However, the additives incorporation induced some gaps/voids and cavitation, that are a sign of incompatibility and can have a negative impact on the mechanical properties [89]. The gaps/voids can especially be attributed to the premature decomposition of the APP due to internal shear and the release of NH_3.

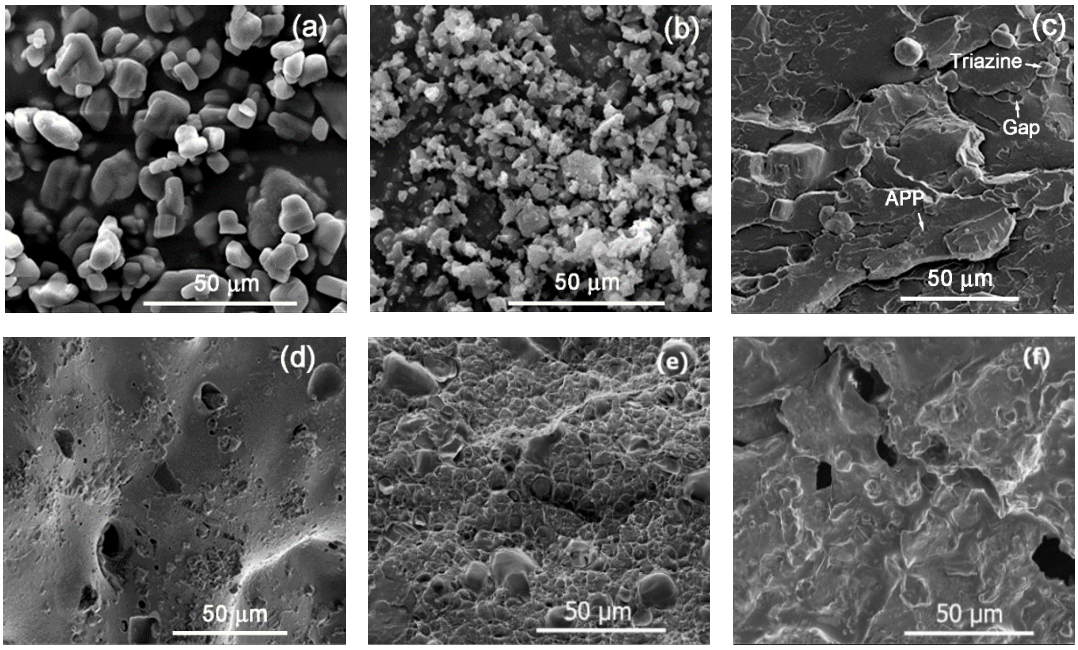

Figure 5.7 Comparison between FR3-containing fractured surfaces of UL94 bars: (a) neat APP, (b) neat Triazine, (c) LDPE-A/FR3 prior to UL 94, (d) LDPE-A/FR3 char after UL 94, (e) LLDPE/FR3 prior UL 94, and (f) LLDPE/FR3 char after UL 94.

The char (Figure 5.7(d)) for LDPE-A/FR3 looks dense and coherent with an intense foamed structure. Despite the formation of some small holes, a nicely formed intumescent layer is observed which successfully prevented oxygen and heat exchange to penetrate deeper into the material, thus showing the best herein flame retardance performance [87].

In LLDPE/FR3 (Figure 5.7(e)), the additives can also be seen in the polymer matrix, but the surface is less continuous and presents a higher extent of voids, potentially implying a more intense decomposition of APP which will physically impede the formation of a dense and compact protective layer during the burning test, resulting in formulation failure [62]. The intense decomposition of APP can be correlated to the different melt viscosities and thus to internal shear with respect to the branching type and degree. The processing behavior of LDPE-A will be different due to the long-chain branching [92,93], as LDPE-A spherical molecules are less entangled and have a lower viscosity than LLDPE. On the other hand, LLDPE has more voids and its molecules are strongly entangled, which can be attributed to the high internal shear. At the shear rates commonly applied during extrusion, the broad molecular weight distribution and the long-chain branching in LDPE-A cause it to have more compact and “spherical” molecules and a greater response to shear compared to the linear, entangled LLDPE molecules. As a result of the increased shear thinning compared to that of LLDPE, the melt viscosity of LDPE-A at higher shear rates is significantly lower than that of the linear resins [85,92,93]. Furthermore, the char of LLDPE/FR3 compound (Figure 5.7(f)) presented a different morphology than that observed in the case of LDPE-A/FR3.

Although the char showed some foaming, big gaps and holes were created which allowed oxygen to penetrate deeper into the material and therefore resulted in poor

flame retardancy [87]. This can be the consequence of poor or inhomogeneous dispersion of the additives.

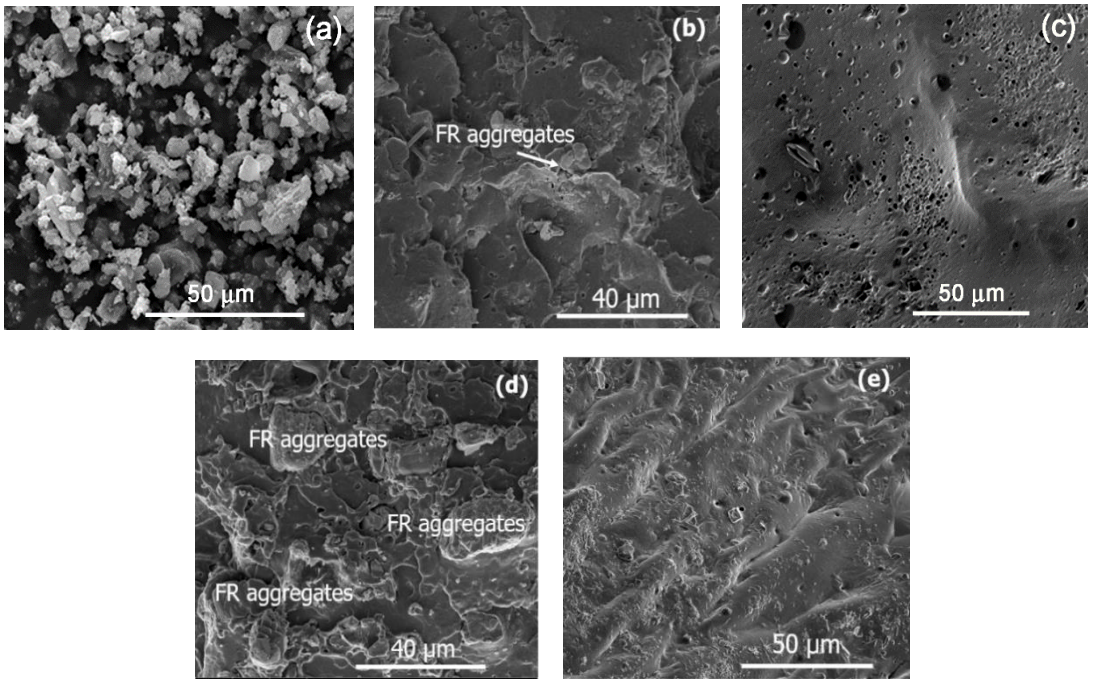

Figure 5.8 Comparison between FR4-containing fractured surfaces of UL 94 bars: (a) neat ADK Stab additive, (b) LDPE-A/FR4 prior UL 94, (c) LDPE-A/FR4 after UL 94, (d) LLDPE/FR4 prior UL 94, and (e) LLDPE/FR4 after UL 94.

On the other hand, the FR4-containing compounds presented significantly less voids. However, agglomeration of additive particles was apparent in all cases, which seems to be the main reason for the inconsistency in the FR results for both polymers. However, the dispersion problems are more obvious in the case of LLDPE, probably due to the higher melt viscosity. The char quality for the FR4 samples was also investigated by SEM. Accordingly, LDPE-A/FR4 (Figure 5.8(c)) showed a surface similar to that of LDPE-A/FR3, but the swelling of the surface was weaker with numerous tiny holes. This resulted in a lower UL94 classification, nevertheless still four V0 classifications were achieved. On the contrary, in the case

of LLDPE/FR4 (Figure 5.8(e)), the char morphology was totally different; almost no swelling of the surface and a discontinuous char, resembling the initial morphology of the surfaces prior to the burn test.

5.4 Mechanical and rheological characterization

The mechanical and rheological properties of the most promising FR formulations (FR3 and FR4 compounds) were measured. Tensile and impact tests were carried out to explore the effect of the FRs on the mechanical performance of the selected compounds. Melt flow rate (MFR) was measured to investigate the effect of relevant FRs on the viscosity and processability of the selected compounds.

Table 5.4 summarizes the rheological and mechanical properties of the pure polyethylenes and of the most promising FR formulations (FR3 and FR4 compounds). The processability of the FR-containing grades can be roughly assessed based on the MFR values. In the case of LLDPE, both formulations (FR3 and FR4) resulted in MFR decrease by more than 40%. In the case of LDPE-A, FR3 formulation did not greatly influence the MFR of the pure polymers, while FR4 caused a reduction by more than 50%, indicating higher melt viscosities.

Regarding the mechanical properties, the neat version of LLDPE had higher values of strain at break than LDPE-A, due to the higher ductility of LLDPE because of the difference in branching [1,22,84]. When adding the FRs, it can be generally said that the tensile and the impact strength were not dramatically affected despite the high loadings (FR3: 35 wt.%, FR4 30 wt.%). More specifically, in LLDPE, the tensile strength deceased by 15% and 20% in both FR3 and FR4, and the Young's modulus did not fluctuate significantly. A reduction of 7% was observed in impact strength in both FR3 and FR4, and the strain at break also decreased by 26% and 48% in FR3 and FR4 respectively. In LDPE-A, the tensile strength decreased by 16.5% (FR3)

and 23% (FR4), along with an increase in Young's modulus by 25-30%. The impact strength remained constant, and the strain at break was reduced by 27-28% for FR3 and FR4. The relevant decreases can be considered low compared to the values mentioned in literature (>25 % change for tensile strength) [62,88] for similar loadings of halogen-free flame retardants. Having in mind that LDPE-A/FR3 is the most promising formulation in terms of safe UL94 V0 ranking, it is concluded that it can also satisfy the requirements in terms of good mechanical properties.

The significant changes in the tensile and impact properties of LLDPE formulations compared to the pure version can be correlated to the poorer distribution and dispersion of the additives in the polymer matrix, as discussed above based on the SEM analysis.

Table 5.4 Rheological (MFR) and Mechanical Properties of Neat Polyethylenes and Selective FR Polyethylene Formulations.

Formulation	**MFR (g/10 min)**	**Tensile strength (MPa)**	**Strain at break (%)**	**Young's Modulus (MPa)**	**Izod Impact strength (kJ/m^2)**
			LLDPE		
Neat	1.01 ± 0.01	13.2 ± 0.3	424 ± 27	154 ± 10	23.4 ± 2.1
FR3	0.56 ± 0.04	11.2 ± 0.7	315.6 ± 59.7	140.7 ± 6.3	21.9 ± 2.2
FR4	0.58 ± 0.05	10.5 ± 0.2	219.7 ± 42.0	157.5 ± 14.4	21.8 ± 2.0
			LDPE-A		
Neat	0.28 ± 0.01	17.3 ± 0.4	135 ± 8	122 ± 12	19.1 ± 4.9
FR3	0.22 ± 0.01	14.4 ± 0.7	96.7 ± 2.7	169.1 ± 13.8	20.5 ± 2.5
FR4	0.11 ± 0.01	13.3 ± 0.2	95.0 ± 6.0	152.6 ± 12.5	21.5 ± 0.7

5.5 Melting Behavior

The melting behavior of the most promising FR formulations (FR3 and FR4 compounds) was examined in order to identify the effect of the flame retardants on the melting point and the crystallinity of the polymers (Table 5.5).

In general, the incorporation of the flame retardants (FR3, FR4) at the specific loadings (30 and 35 % wt) did not significantly change the thermal properties of the polyethylene grades (Figures 5.9 and 5.10). A slight increase in the melting point by almost 2 °C was found for both PE grades, while for the case of FR3, an increase in the melting enthalpy- which is directly proportional to the crystallinity, was also observed. The relevant additives are infusible in the pertinent temperature range, and

potentially retard the melting process of the pure polyethylene macromolecules. In the case of LLDPE, the melt crystallization upon cooling occurred earlier, i.e. at a noticeable higher T_c.

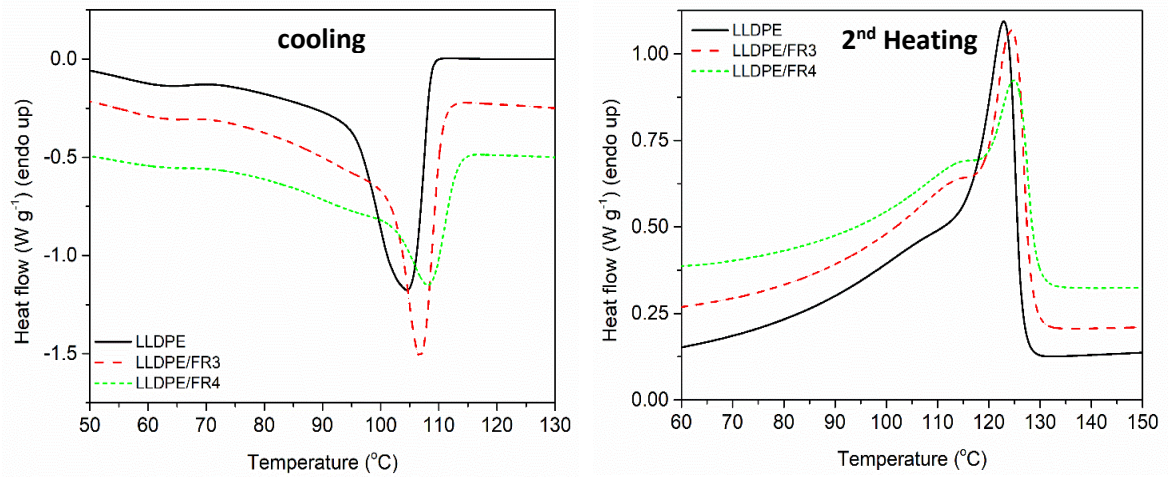

Figure 5.9 DSC cooling and heating (2nd heating) curves of LLDPE/ FR3 and FR4 compounds

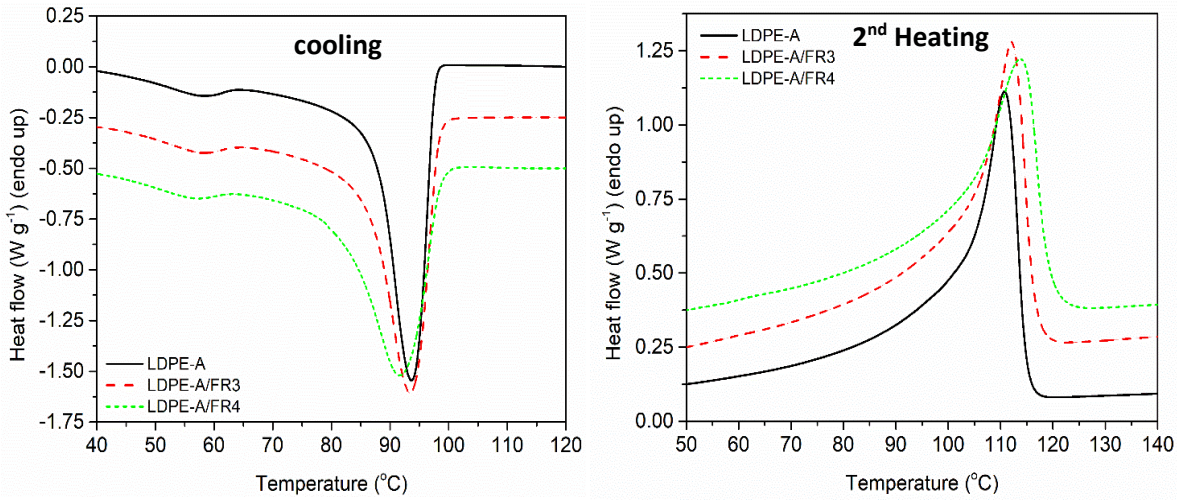

Figure 5.10 DSC cooling and heating (2nd heating) curves of LDPE-A/ FR3 and FR4 compounds

Table 5.5 DSC Results of Neat Polyethylenes and Selective FR Polyethylene Formulations.

Sample	**Crystallization temperature, T_c (°C)**	**Crystallization enthalpy, ΔH_c (J/g)**	**Melting temperature, T_m (°C)**	**Melting enthalpy, ΔH_m (J/g)**
		LLDPE		
Neat	103.9	70.2	122.0	94.1
FR3	107.1	99.4	124.0	101.9
FR4	108.6	86.4	124.4	87.9
		LDPE-A		
Neat	94.4	74.4	110.1	91.3
FR3	93.2	108.5	112.6	102.9
FR4	91.7	93.1	114.0	93.7

Chapter 6: Conclusion and Recommendations

6.1 Conclusion

The preceding work presented an investigation of the UV stability and flame retardancy of two polyethylene grades for an irrigation pipelines application. The useful lifetime of polyethylene pipes in Qatar is reduced significantly by that act of UV radiation, humidity and heat, and the process of storing the new pipes in warehouses gives rise to flammability concerns. Hence, the main aim of this work was to propose optimized solutions for each of the two concerns, by analyzing two grades of polyethylene; LLDPE and LDPE, compounded in new formulations with a variety of additives that were reported to provide promising results. Based on the conducted experimental analyses and presented discussion, the following can be concluded:

- Although LLDPE is known to have a higher thermal stability than LDPE grades, it has shown a weaker resistance against UV aging than LDPE-A. Which gives LDPE-A a plus when it comes to outdoor applications. This was attributed to the long branches in LDPE-A that protected the main chain against UV-initiated chain scission.
- All the performed characterization techniques proved the effectives of the employed UV formulations in enhancing the useful lifetime of both polymers and improving their resistance to weathering.
- UV absorbers acted as nucleating agents in both polymers, as shown in the DSC results. This has led to an increase in the melting enthalpy for all the samples, and to a higher crystallization temperature.
- The thermal analysis has clearly shown the higher stability of LDPE-A compounds, which was attributed to the structure of the polymer. LDPE-A has more amorphous regions, compared to LLDPE, which allows the

additives to diffuse easily into the matrix, compared to LLDPE.

- All the presented characterization showed that both formulations were effective in LDPE-A, as LDPE-A/UV1 and LDPE-A/UV2 compounds had very similar results. In other words, both UV absorber classes; benzophenones and benzotriazoles were able to absorb the harmful UV radiation. And, the employed HALS were able to trap the radicals and slow any initiated photodegradation or terminate it.
- The flammability results of LLDPE compounds showed poorer results than LDPE-A compounds, which was unexpected. These findings have firstly highlighted the high thermal stability of LDPE-A. Secondly, the poor results were partially attributed to dispersion issues as shown by the microscopic and mechanical analyses.
- An FR formulation (FR3) of a triazine derivative and ammonium polyphosphate at a ratio of 1:3 (Char forming agent, CFA: Acid source, APP) and a total loading of 35 wt.% was found to be the most efficient for LDPE-A, achieving a UL 94 V0 ranking and upgrading the thermal stability of the polymer. The thermal, rheological (MFR) and mechanical properties did not significantly change for this most promising LDPE-A/FR3 formulation.
- The use of FR3 in LDPE-A has led to an increase in the thermal degradation temperature by more than 15 °C, along with a char residue which reached 10% at 800 °C.
- The SEM images of LLDPE/FR3 samples presented a less continuous surface with a higher extent of voids., which indicated a more intense decomposition of APP, which can physically impede the formation of a

dense and compact protective layer. The intense decomposition of APP was correlated to the different melt viscosities and thus to internal shear with respect to the branching type and degree. Moreover, the additives incorporation induced some voids and cavitation, which was a sign of incompatibility, and could be another reason behind the poorer performance.

6.2 Recommendations for Future Work

The following recommendations can be proposed for future work:

- Investigating the effect of thermal aging on the analyzed UV formulations, and comparing the resistance of PE grades against UV and thermal aging.
- Evaluation of the mechanism of action of HALS in the examined UV formulations, to fully understand the obtained results.
- Extending the analysis of promising FR formulations by designing new formulations with lower loadings but based on the same employed additives.
- Development of flame-retarded and UV stabilized PE compounds, and assess the possible interactions between the different FR structures and the UV stabilization additives.

References

[1] S. Ronca, “Polyethylene,” in *Brydson’s Plastics Materials*, 8th ed., M. Gilbert, Ed. Elsevier Ltd, 2017, pp. 247–278.

[2] DALLAS, “Polyolefins Market Consumption worth 169,892.4 Kilotons by 2018,” 2013. [Online]. Available: http://www.prnewswire.com/news-releases/polyolefins-market-consumption-worth-1698924-kilotons-by-2018-222655431.html. [Accessed: 25-Dec-2018].

[3] R. M. Patel, “Polyethylene,” *Multilayer Flex. Packag.*, pp. 17–34, 2016.

[4] G. Wypych, “LLDPE linear low density polyethylene,” *Handb. Polym.*, pp. 185–189, 2016.

[5] A. A. Basfar and K. M. Idriss Ali, “Natural weathering test for films of various formulations of low density polyethylene (LDPE) and linear low density polyethylene (LLDPE),” *Polym. Degrad. Stab.*, vol. 91, no. 3, pp. 437–443, 2006.

[6] A. Dehbi, A. H. I. Mourad, and A. Bouaza, “Ageing effect on the properties of tri-layer polyethylene film used as greenhouse roof,” *Procedia Eng.*, vol. 10, pp. 466–471, 2011.

[7] J. V. Gulmine, P. R. Janissek, H. M. Heise, and L. Akcelrud, “Degradation profile of polyethylene after artificial accelerated weathering,” *Polym. Degrad. Stab.*, vol. 79, no. 3, pp. 385–397, 2003.

[8] Y. C. Hsu *et al.*, “The effect of comonomer concentration and distribution on the photo-oxidative degradation of linear low density polyethylene films,” *Polymer (Guildf).*, vol. 119, pp. 66–75, 2017.

[9] M. Liu and A. R. Horrocks, “Effect of carbon black on UV stability of LLDPE films under artificial weathering conditions,” *Polym. Degrad. Stab.*, vol. 75, no.

3, pp. 485–499, 2002.

[10] S. M. Al-Salem, G. Abraham, O. A. Al-Qabandi, and A. M. Dashti, “Investigating the effect of accelerated weathering on the mechanical and physical properties of high content plastic solid waste (PSW) blends with virgin linear low density polyethylene (LLDPE),” *Polym. Test.*, vol. 46, pp. 116–121, 2015.

[11] H. J. Jeon and M. N. Kim, “Degradation of linear low density polyethylene (LLDPE) exposed to UV-irradiation,” *Eur. Polym. J.*, vol. 52, no. 1, pp. 146–153, 2014.

[12] D. Rasouli, N. T. Dintcheva, M. Faezipour, F. P. La Mantia, M. R. Mastri Farahani, and M. Tajvidi, “Effect of nano zinc oxide as UV stabilizer on the weathering performance of wood-polyethylene composite,” *Polym. Degrad. Stab.*, vol. 133, pp. 85–91, 2016.

[13] G. Wypych, “LDPE low density polyethylene,” *Handb. Polym.*, pp. 178–184, 2016.

[14] C. DeArmitt and R. Rothon, *Applied Plastics Engineering Handbook*, 2nd ed. 2016.

[15] L. Walker, “Some 400 tons of waste added to Qatar’s landfills daily,” *Doha News*, 2014. [Online]. Available: http://dohanews.co/qatar-dumps-400-tons-waste-daily-landfill.

[16] M. R. Kamal and R. Saxon, “Weatherability of thermoplastic piping,” 1973.

[17] M. Aubert *et al.*, “Versatile bis(1-alkoxy-2,2,6,6-tetramethylpiperidin-4-yl)-diazenes (AZONORs) and related structures and their utilization as flame retardants in polypropylene, low density polyethylene and high-impact polystyrene,” *Polym. Degrad. Stab.*, vol. 97, no. 8, pp. 1438–1446, 2012.

[18] R. Pfaendner, “Flame retardants for polyethylene,” in *Handbook of Industrial Polyethylene and Technology*, M. Spalding and A. Chatterjee, Eds. Wiley, 2016, pp. 921–934.

[19] P. Kiliaris and C. D. Papaspyrides, *Polymers on Fire*. Elsevier B.V., 2014.

[20] M. Lewin and E. D. Weil, *Mechanisms and modes of action in flame retardancy of polymers*. Woodhead Publishing Ltd, 2011.

[21] B. Liang, X. Hong, M. Zhu, C. Gao, C. Wang, and N. Tsubaki, “Synthesis of novel intumescent flame retardant containing phosphorus, nitrogen and boron and its application in polyethylene,” *Polym. Bull.*, vol. 72, no. 11, pp. 2967–2978, 2015.

[22] A. Peacock, *Handbook of Polyethylene: Structures, Properties and Application*. Marcel Dekker, Inc., 2000.

[23] J. R. Collier, “Polymer Structure,” *Ind. Eng. Chem.*, vol. 61, no. 9, pp. 50–65, 1969.

[24] andrew j. Peacok and A. Calhoun, “polymer Chemistry.pdf.” p. 2006.

[25] L. W. McKeen, “Introduction to Plastics and Polymers Compositions,” *Eff. UV Light Weather Plast. Elastomers*, pp. 1–16, 2013.

[26] S. Rajaram, “Global Markets for Plastics Additives,” *BCC Research*, 2018. [Online]. Available: https://www.bccresearch.com/market-research/plastics/global-markets-for-plastics-additives-report-pls022f.html.

[27] “Plastics Europe Association of Plastics Manufacturers,” 2015. .

[28] “Polyolefins Market Consumption worth 169,892.4 Kilotons by 2018,” 2013. [Online]. Available: http://www.prnewswire.com/news-releases/polyolefins-market-consumption-worth-1698924-kilotons-by-2018-222655431.html.

[29] P. A. Dilara and D. Briassoulis, “Degradation and stabilization of low-density

polyethylene films used as greenhouse covering materials," *J. Agric. Eng. Res.*, vol. 76, no. 4, pp. 309–321, 2000.

[30] S. M. Al-Salem, "Influence of natural and accelerated weathering on various formulations of linear low density polyethylene (LLDPE) films," *Mater. Des.*, vol. 30, no. 5, pp. 1729–1736, 2009.

[31] Y. C. Hsu, M. P. Weir, R. W. Truss, C. J. Garvey, T. M. Nicholson, and P. J. Halley, "A fundamental study on photo-oxidative degradation of linear low density polyethylene films at embrittlement," *Polymer (Guildf).*, vol. 53, no. 12, pp. 2385–2393, 2012.

[32] F. P. La Mantia, N. T. Dintcheva, V. Malatesta, and F. Pagani, "Improvement of photo-stability of LLDPE-based nanocomposites," *Polym. Degrad. Stab.*, vol. 91, no. 12, pp. 3208–3213, 2006.

[33] G. Pritchard, *Plastics Additives: An A-Z reference*. POLYMER SCIENCE AND TECHNOLOGY SERIES, 1998.

[34] D. Feldman, "Polymer weathering: Photo-oxidation," *J. Polym. Environ.*, vol. 10, no. 4, pp. 163–173, 2002.

[35] L. W. McKeen, "Introduction to the Weathering of Plastics," *Eff. UV Light Weather Plast. Elastomers*, pp. 17–41, 2013.

[36] D. Price and R. Horrocks, "Polymer Degradation and the Matching of FR Chemistry to Degradation," in *Fire Retardancy of Polymeric Materials*, 2nd ed., C. Wilkie and A. Morgan, Eds. CRCPress, 2010, pp. 15–42.

[37] M. Tolinski, *Antioxidants and Heat Stabilization*. Elsevier Inc., 2012.

[38] M. Tolinski, "Ultraviolet Light Protection and Stabilization," in *Additives for Polyolefins*, Elsevier Inc., 2012, pp. 45–60.

[39] B. Y. Zhao, X. W. Yi, R. Y. Li, P. F. Zhu, and K. A. Hu, "Characterization to

the weathering extent of LLDPE/LDPE thin film," *J. Appl. Polym. Sci.*, vol. 88, no. 1, pp. 12–16, 2003.

[40] A. R. Kakroodi and D. Rodrigue, "Degradation behavior of maleated polyethylene / ground tire rubber thermoplastic elastomers with and without stabilizers," *Polym. Degrad. Stab.*, vol. 98, no. 11, pp. 2184–2192, 2013.

[41] V. Dobrescu, G. Andrei, and C. Andrei, "The Antioxidizing Effect of Sterically Hindered Amines in Thermal Oxidation of Low Density Polyethylene," *Eur. Polym. J.*, vol. 24, no. 3, pp. 289–294, 2000.

[42] F. Gugumus, "Possibilities and limits of synergism with light stabilizers in polyolefins 2. UV absorbers in polyolefins," *Polym. Degrad. Stab.*, vol. 75, no. 2, pp. 309–320, 2002.

[43] M. Scoponi, S. Cimmino, and M. Kaci, "Photo-stabilisation mechanism under natural weathering and accelerated photo-oxidative conditions of LDPE films for agricultural applications," *Polymer (Guildf).*, vol. 41, no. 22, pp. 7969–7980, 2000.

[44] Z. J. Shen, D. Okada, F. Lin, A. Tintikakis, and S. Anderson, "Breaking the scaling barrier of large area lateral power devices: An 1m flip-chip power MOSFET with ultra low gate charge," *Proc. 16th Int. Symp. Power Semicond. Devices ICs (ISPSD'04), May 24, 2004 - May 27, 2004*, vol. 16, no. DECEMBER, pp. 387–390, 2004.

[45] I. Grigoriadou, K. M. Paraskevopoulos, K. Chrissafis, E. Pavlidou, T. G. Stamkopoulos, and D. Bikiaris, "Effect of different nanoparticles on HDPE UV stability," *Polym. Degrad. Stab.*, vol. 96, no. 1, pp. 151–163, 2011.

[46] T. Tang *et al.*, "Combination of fumed silica with carbon black for simultaneously improving the thermal stability, flame retardancy and

mechanical properties of polyethylene," *Polymer (Guildf).*, vol. 55, no. 13, pp. 2998–3007, 2014.

[47] M. Gilbert, "Relation of Structure to Chemical Properties," in *Brydson's Plastics Materials*, Elsevier Ltd, 2017, pp. 75–102.

[48] Y. Lv *et al.*, "Outdoor and accelerated laboratory weathering of polypropylene: A comparison and correlation study," *Polym. Degrad. Stab.*, vol. 112, pp. 145–159, 2015.

[49] E. Dalmolin *et al.*, "Degradability of linear polyolefins under natural weathering," *Polym. Degrad. Stab.*, vol. 96, no. 4, pp. 703–707, 2010.

[50] V. Ambrogi, C. Carfagna, P. Cerruti, and V. Marturano, "Additives in Polymers," in *Modification of Polymer Properties*, C. Jasso-Gastinel and J. Kenny, Eds. Elsevier Inc., 2017, pp. 87–108.

[51] G. Wypych, *Handbook of UV Degradation and Stabilization*. 2015.

[52] P. Gijsman, "A review on the mechanism of action and applicability of Hindered Amine Stabilizers," *Polym. Degrad. Stab.*, vol. 145, pp. 2–10, 2017.

[53] M. Edge, J. M. Peña, C. M. Liauw, B. Valange, and N. S. Allen, "Studies of synergism between carbon black and stabilisers in LDPE photodegradation," *Polym. Degrad. Stab.*, vol. 72, no. 2, pp. 259–270, 2002.

[54] W. Focke, P. Mashele, and N. Nhlapo, "Stabilization of Low-Density Polyethylene Films Containing Metal Stearates as Photodegradants," *J. VINYL Addit. Technol.*, vol. 21, pp. 129–133, 2011.

[55] M. Zeni, "Photostabilized LDPE Films with UV Absorber and HALS as Protection against the Light for Rosé Sparkling Wine," *J. Food Process. Technol.*, vol. 03, no. 07, 2012.

[56] P. N. S. Poveda, H. M. Viana, and L. G. D. A. Silva, "Behavior of linear low

density polyethylene films under UV ageing for agricultural application," in *Characterization of Minerals, Metals, and Materials 2015*, 2015, no. 2, pp. 253–258.

[57] N. Brushlinsky, M. Ahrens, S. . Sokolov, and P. Wagner, "World Fire Statistics," 2018.

[58] D. Price, G. Anthony, and P. Carty, *Introduction: polymer combustion, condensed phase pyrolysis and smoke formation*. Woodhead Publishing Ltd.

[59] A. Morgan and C. Wilkie, "An Introduction to Polymeric Flame Retardancy, Its Role in Materials Science, and the Current State of the Field," in *Materials, Fire Retardancy of Polymeric*, 2nd ed., C. Wilkie and A. Morgan, Eds. CRCPress, 2010, pp. 1–15.

[60] Pinfa., "Pinfa. Phosphorus, Inorganic & Nitrogen Flame Retardants Association." [Online]. Available: www.pinfa.org.

[61] P. David, *Toxicity of fire retardants in relation to life safety and environmental hazards*. Woodhead Publishing Ltd.

[62] M. Ba, B. Liang, and C. Wang, "Synthesis and Characterization of a Novel Charring Agent and Its Application in Intumescent Flame Retardant Polyethylene System," *Fibers Polym.*, vol. 18, no. 5, pp. 907–914, 2017.

[63] S. Nie *et al.*, "Thermal and flame retardant properties of novel intumescent flame retardant low-density polyethylene (LDPE) composites," pp. 999–1004, 2012.

[64] S. Nie, Y. Hu, L. Song, Q. He, D. Yang, and H. Chen, "Synergistic effect between a char forming agent (CFA) and microencapsulated ammonium polyphosphate on the thermal and flame retardant properties of polypropylene," no. April, pp. 1077–1083, 2008.

[65] X. Hu, Y. Li, and Y. Wang, “Synergistic Effect of the Charring Agent on the Thermal and Flame Retardant Properties of Polyethylene,” *Macromol. Mater. Eng.*, pp. 208–212, 2003.

[66] Z. Shao, C. Deng, Y. Tan, M. Chen, L. Chen, and Y. Wang, “Flame retardation of polypropylene via a novel intumescent fl ame retardant : Ethylenediamine-modi fi ed ammonium polyphosphate,” *Polym. Degrad. Stab.*, vol. 106, pp. 88–96, 2014.

[67] “Information, Technical Additives, Plastic: Chimassorb ® 81,” no. November. pp. 1–3, 2010.

[68] “Information, Technical Additives, Plastic: Tinuvin ® 1577,” no. August, pp. 1–3, 2010.

[69] “Information, Technical Additives, Plastic: Chimassorb ® 944,” no. November. pp. 3–5, 2010.

[70] “SABO ® stab UV 119 SABO ® stab UV 119 Properties.” pp. 1–2, 2017.

[71] “Information, Technical Additives, Plastic: Flamestab ® NOR 116,” no. August. pp. 1–2, 2016.

[72] “MCA ® PPM Triazine 765 Physical Properties : Safety and Handling.” pp. 1–2.

[73] “MCA ® PPM Triazine HF Chemical Formula.” .

[74] “Information, Technical Additives, Plastic: Exolit AP422.” .

[75] “Information, Technical Additives, Plastic: ADK STAB FP-2200.” pp. 1–7, 2009.

[76] “Information, Technical Additives, Plastic: Charmor ™ DP40.” 2012.

[77] “Information, Technical Additives, Plastic: Charmor ™ PP100.” 2012.

[78] “TECHNICAL DATA STRUKTOL ® CALCIUM STEARATE Struktol

Company of America TECHNICAL DATA," no. 330, pp. 13–14.

[79] S. Liao, C. Deng, S. Huang, J. Cao, and Y. Wang, "An Efficient Halogen-free Flame Retardant for Polyethylene : Piperazine- modified Ammonium Polyphosphates with Different Structures *," *Chinese J. Polym. Sci.*, vol. 34, no. 11, pp. 1339–1353, 2016.

[80] N. Billingham, "Degradation," *Encyclopedia of Polymer Science and Technology*. pp. 1–49.

[81] Al-Malaika, "Stabilization," *Encyclopedia of Polymer Science and Technology*. pp. 179–229.

[82] J. Weon, "Effects of thermal ageing on mechanical and thermal behaviors of linear low density polyethylene pipe," *Polym. Degrad. Stab.*, vol. 95, no. 1, pp. 14–20, 2010.

[83] J. A. Molefi, A. S. Luyt, and I. Krupa, "Thermochimica Acta Comparison of LDPE , LLDPE and HDPE as matrices for phase change materials based on a soft Fischer – Tropsch paraffin wax," *Thermochim. Acta*, vol. 500, no. 1–2, pp. 88–92, 2010.

[84] A. S. Luyt, J. A. Molefi, and H. Krump, "Thermal , mechanical and electrical properties of copper powder filled low-density and linear low-density polyethylene composites," vol. 91, pp. 1629–1636, 2006.

[85] D. Simpson and G. Vaughan, "Ethylene polymers, LLDPE," *Encyclopedia of Polymer Science and Technology*. Wiley & Sons, pp. 441–482.

[86] F. Gugumus, "Aspects of the impact of stabilizer mass on performance in polymers 2 . Effect of increasing molecular mass of polymeric HALS in PP," *Polym. Degrad. Stab.*, vol. 67, pp. 299–311, 2000.

[87] G. Makhlouf, M. Hassan, M. Nour, Y. Abdel-Monem, and A. Abdelkhalik,

"Evaluation of fire performance of linear low-density polyethylene containing novel intumescent flame retardant," *J. Therm. Anal. Calorim.*, vol. 130, no. 2, pp. 1031–1041, 2017.

[88] R. Xie and B. Qu, "Synergistic effects of expandable graphite with some halogen-free flame retardants in polyolefin blends.," *Polym. Degrad. Stab.*, vol. 71, pp. 375–380, 2001.

[89] T. Yu, T. Tuerhongjiang, C. Sheng, and Y. Li, "Composites: Part A Phosphorus-containing diacid and its application in jute/poly (lactic acid) composites: Mechanical, thermal and flammability properties," *Compos. Part A*, vol. 97, pp. 60–66, 2017.

[90] B. Kaul, "PPM triazines lightweight organo-polymeric universal fire and flame retardant synergists," *Rubber Fiber Plast.*, vol. 11, pp. 190–196, 2016.

[91] Z. Shao, C. Deng, Y. Tan, M. Chen, L. Chen, and Y. Wang, "An efficient mono-component polymeric intumescent flame retardant for polypropylene: Preparation and application.," *ACS Appl. Mater. Interfaces*, vol. 6, pp. 7363–7370, 2014.

[92] N. Maraschin, "Ethylene polymers LDPE," *Encyclopedia of Polymer Science and Technology*. Wiley & Sons, pp. 412–441.

[93] R. Kuhn and H. Kromer, "Structures and properties of different low density polyethylenes," *Colloid Polym. Sci.*, vol. 1092, pp. 1083–1092, 1982.

Appendix A: Tensile Stress-Stain Curves

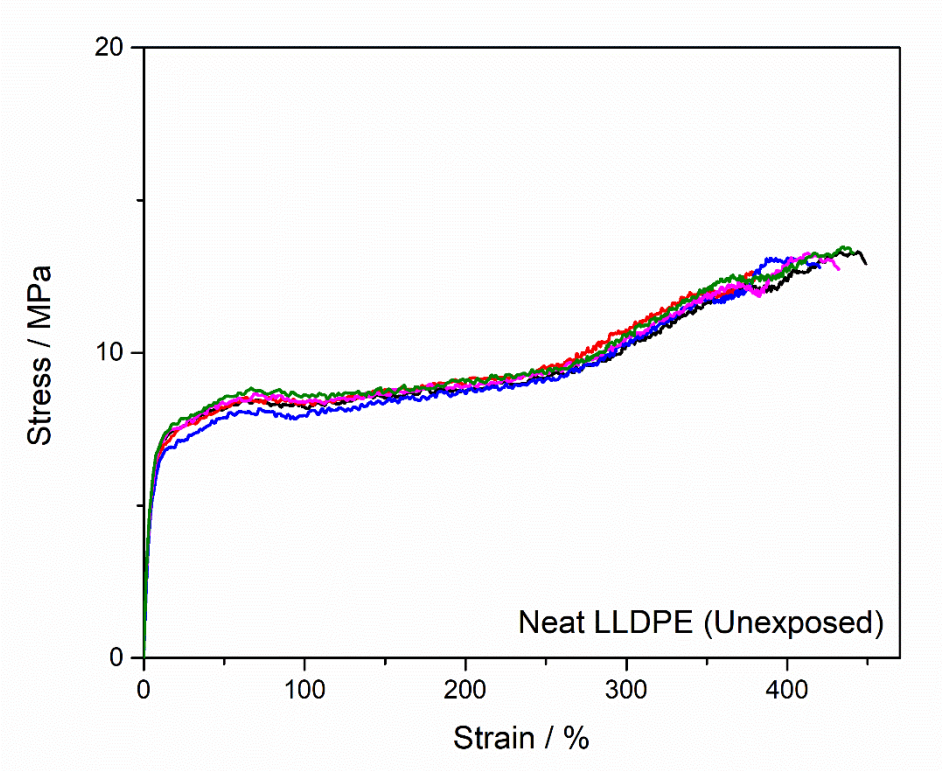

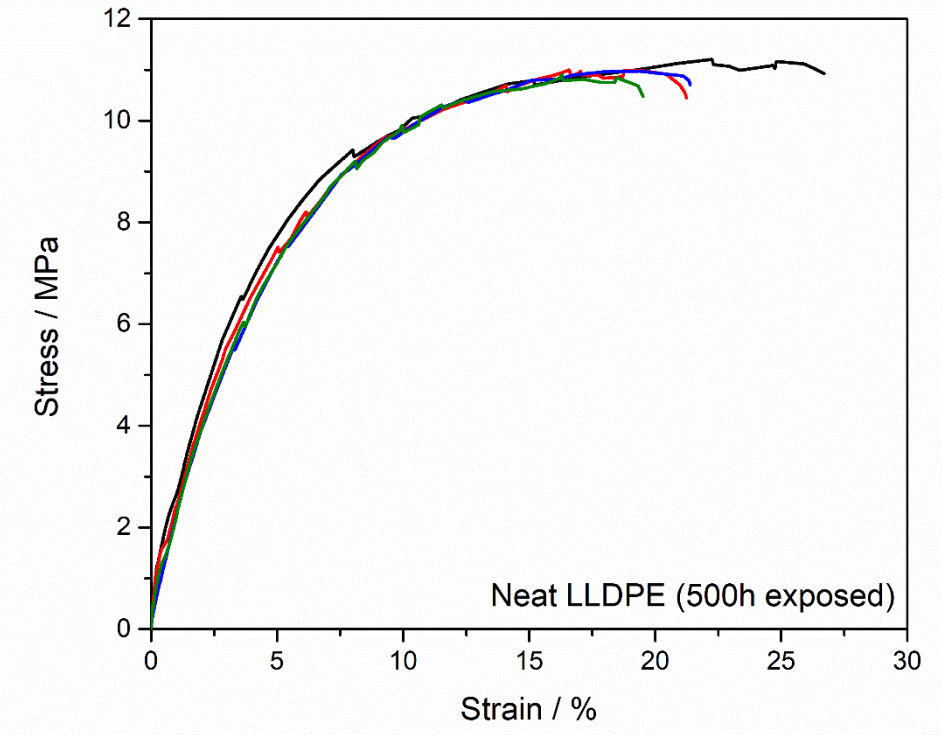

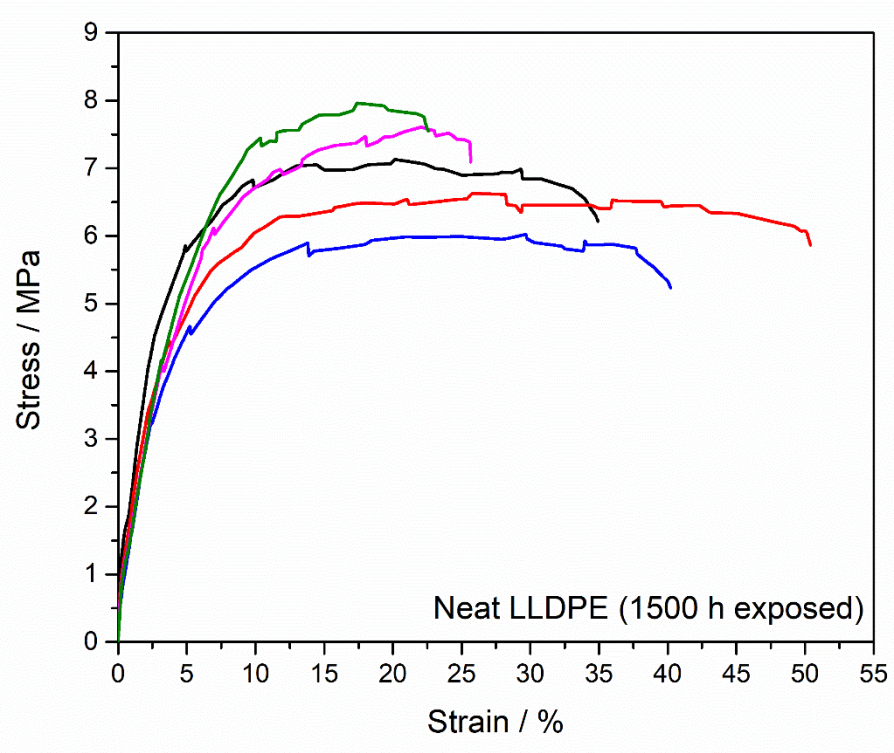
Stress / MPa
Strain / %
Neat LLDPE (1500 h exposed)
0
1
2
3
4
5
6
7
8
9
0
5
10
15
20
25
30
35
40
45
50
55

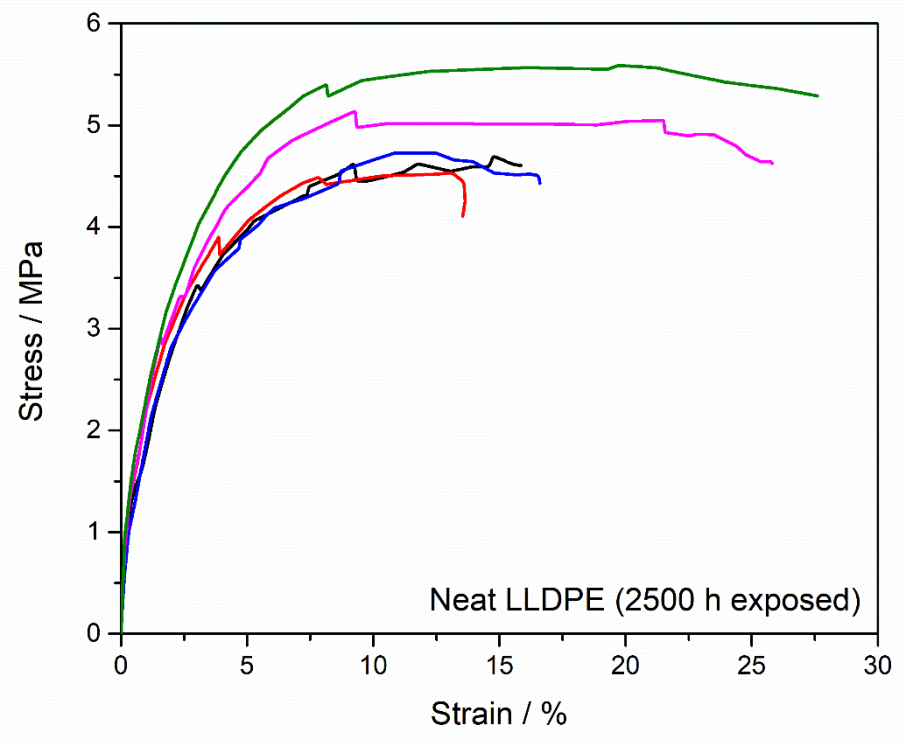
Stress / MPa
Strain / %
Neat LLDPE (2500 h exposed)
0
1
2
3
4
5
6
0
5
10
15
20
25
30

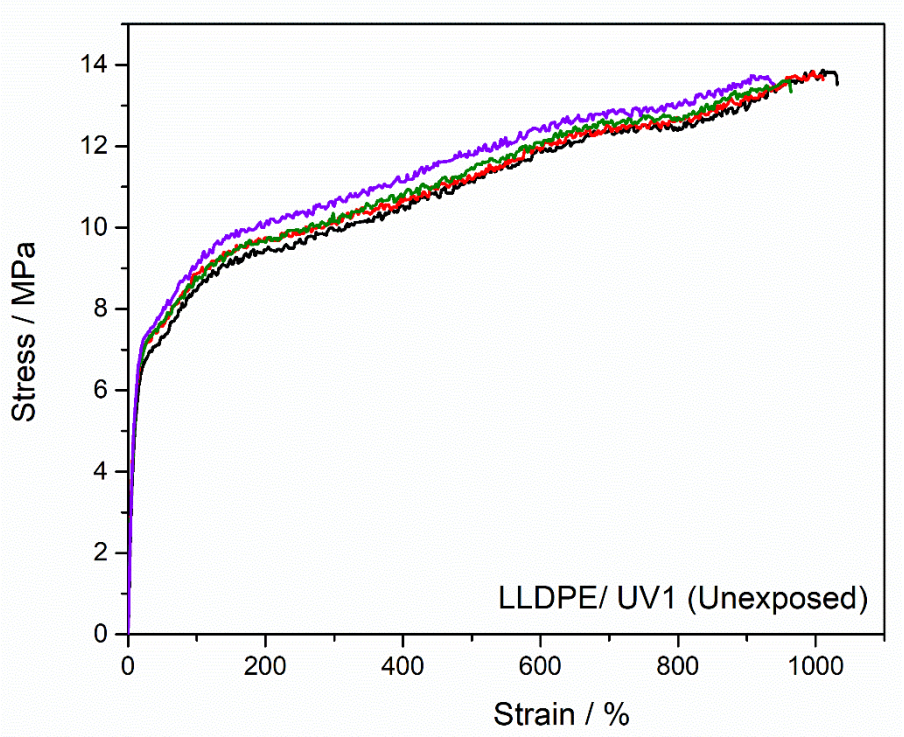
Stress / MPa
Strain / %
LLDPE/ UV1 (Unexposed)
0
2
4
6
8
10
12
14
0
200
400
600
800
1000

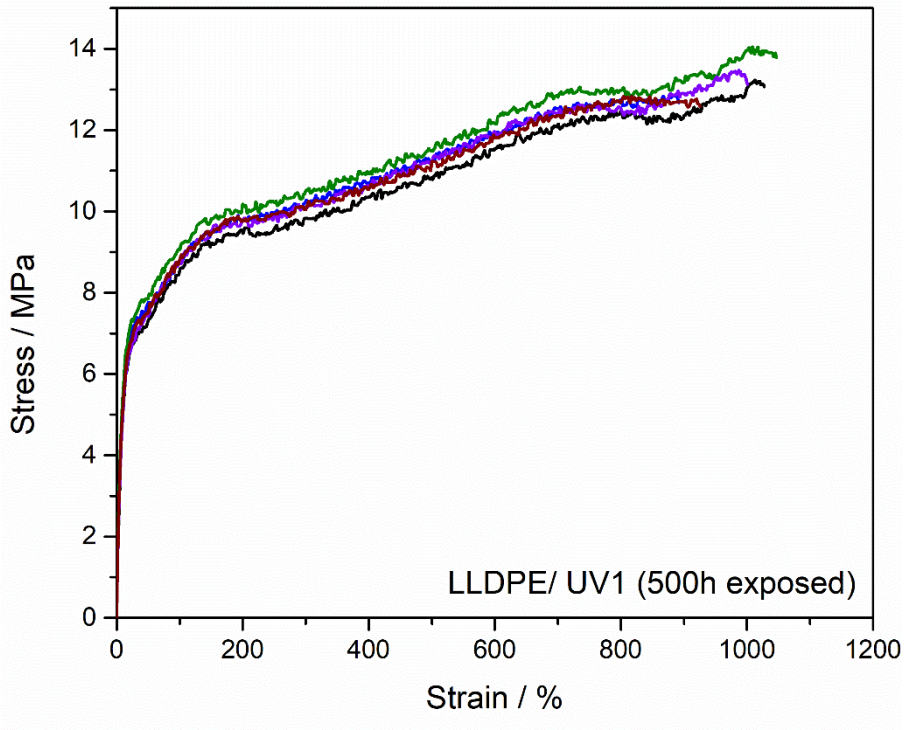
Stress / MPa
Strain / %
LLDPE/ UV1 (500h exposed)
0
2
4
6
8
10
12
14
0
200
400
600
800
1000
1200

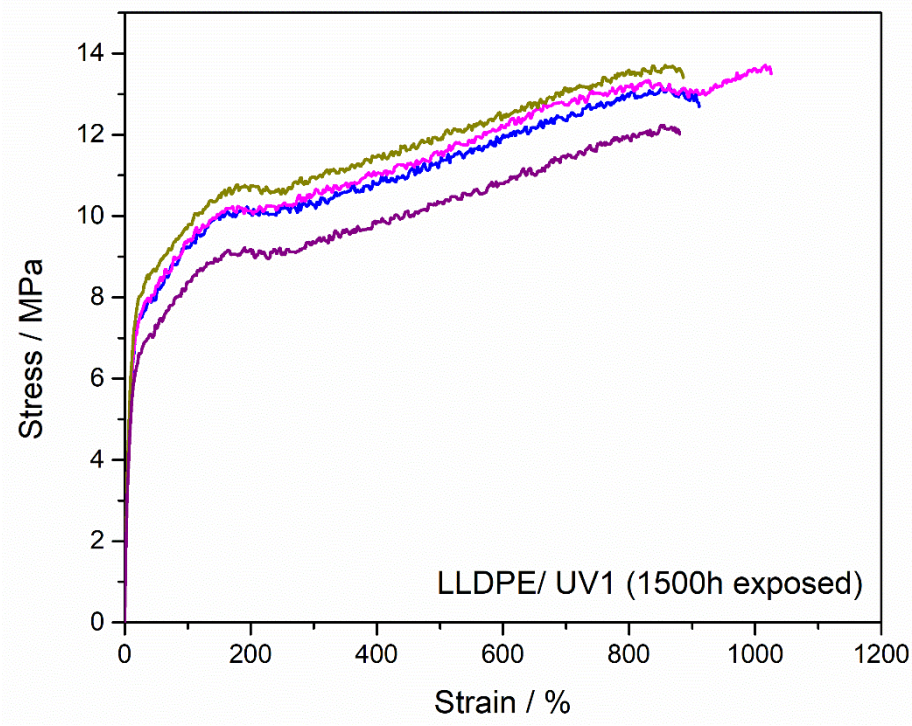
Stress / MPa
Strain / %
LLDPE/ UV1 (1500h exposed)
0
2
4
6
8
10
12
14
0
200
400
600
800
1000
1200

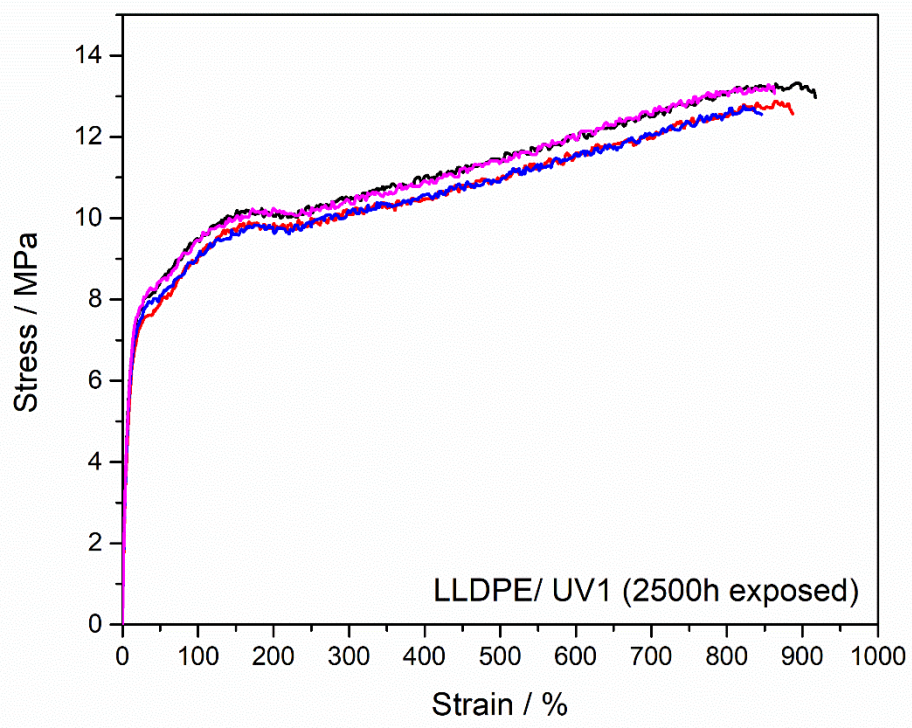
Stress / MPa
Strain / %
LLDPE/ UV1 (2500h exposed)
0
2
4
6
8
10
12
14
0
100
200
300
400
500
600
700
800
900
1000

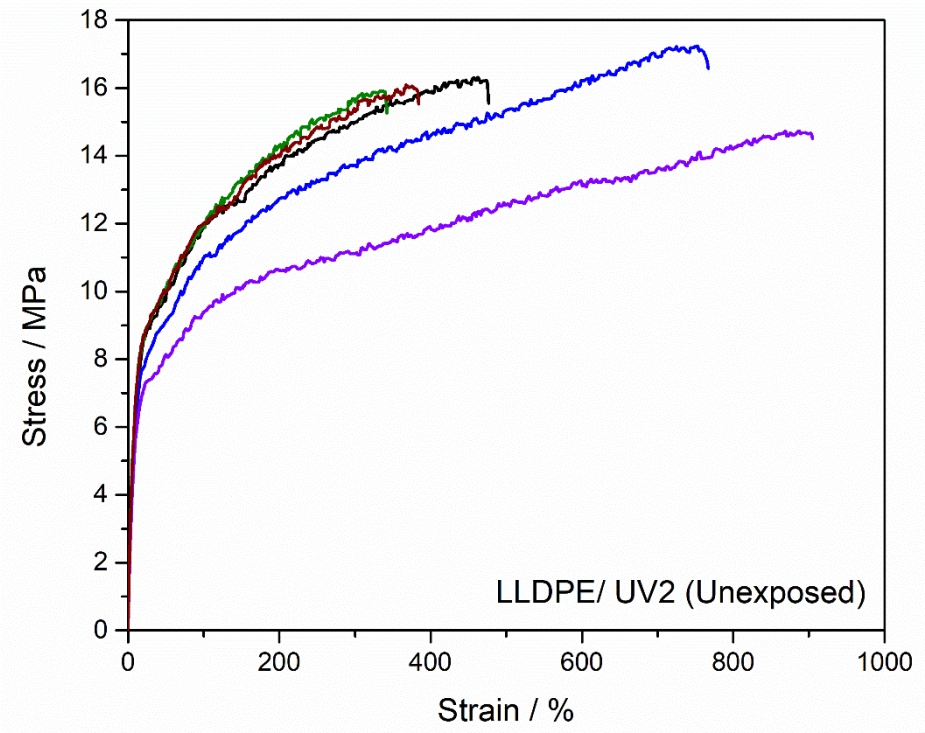
Stress / MPa
Strain / %
LLDPE/ UV2 (Unexposed)
0
2
4
6
8
10
12
14
16
18
0
200
400
600
800
1000

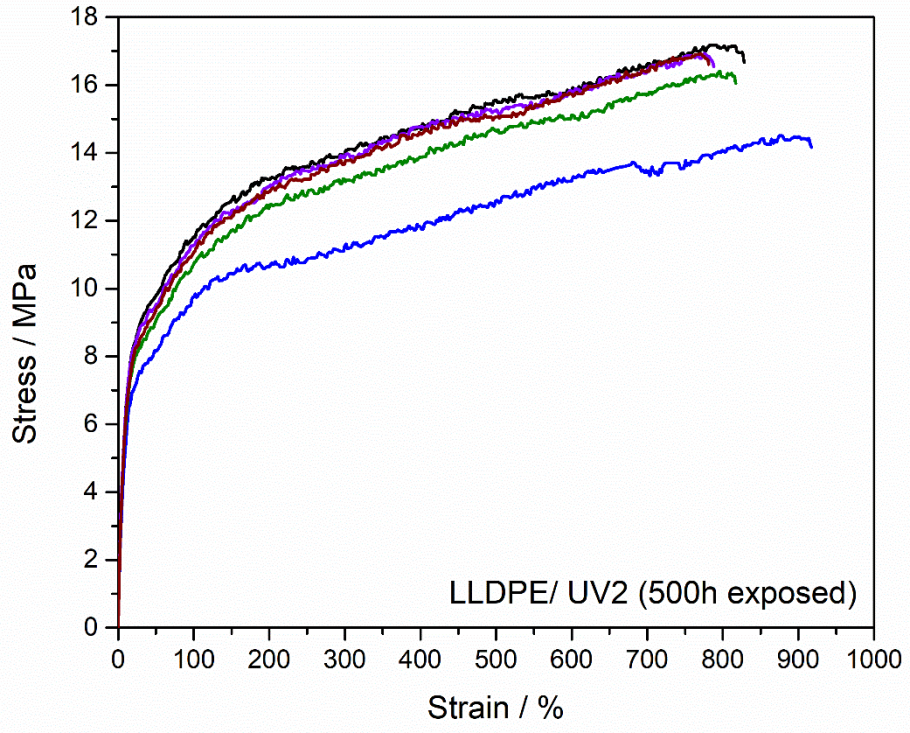
Stress / MPa
Strain / %
LLDPE/ UV2 (500h exposed)
0
2
4
6
8
10
12
14
16
18
0
100
200
300
400
500
600
700
800
900
1000

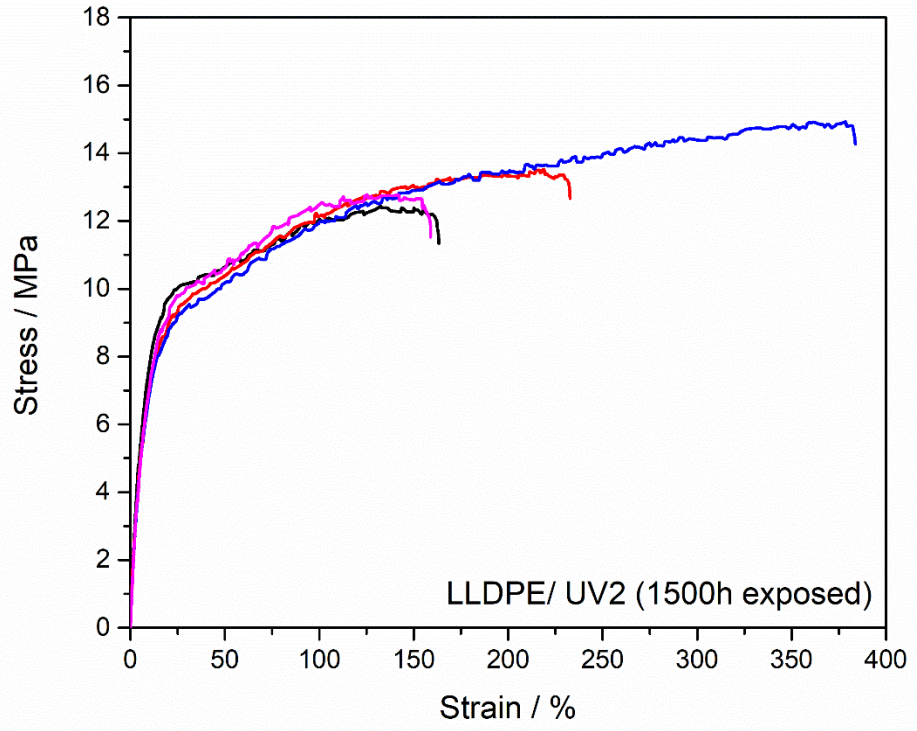
Stress / MPa
Strain / %
LLDPE/ UV2 (1500h exposed)
0
2
4
6
8
10
12
14
16
18
0
50
100
150
200
250
300
350
400

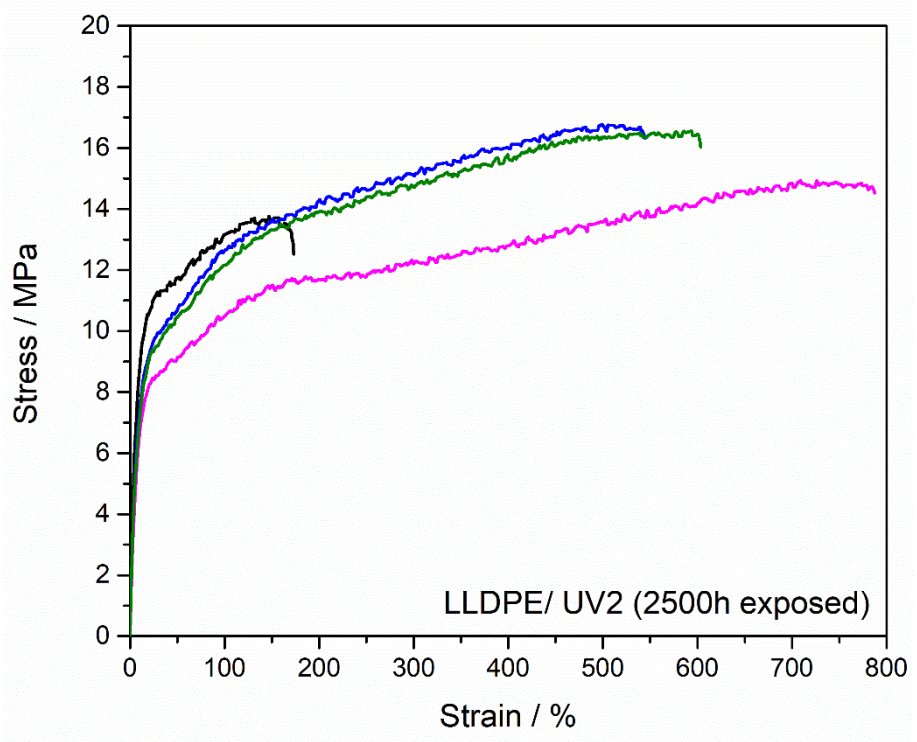
Stress / MPa
Strain / %
LLDPE/ UV2 (2500h exposed)
0
2
4
6
8
10
12
14
16
18
20
0
100
200
300
400
500
600
700
800

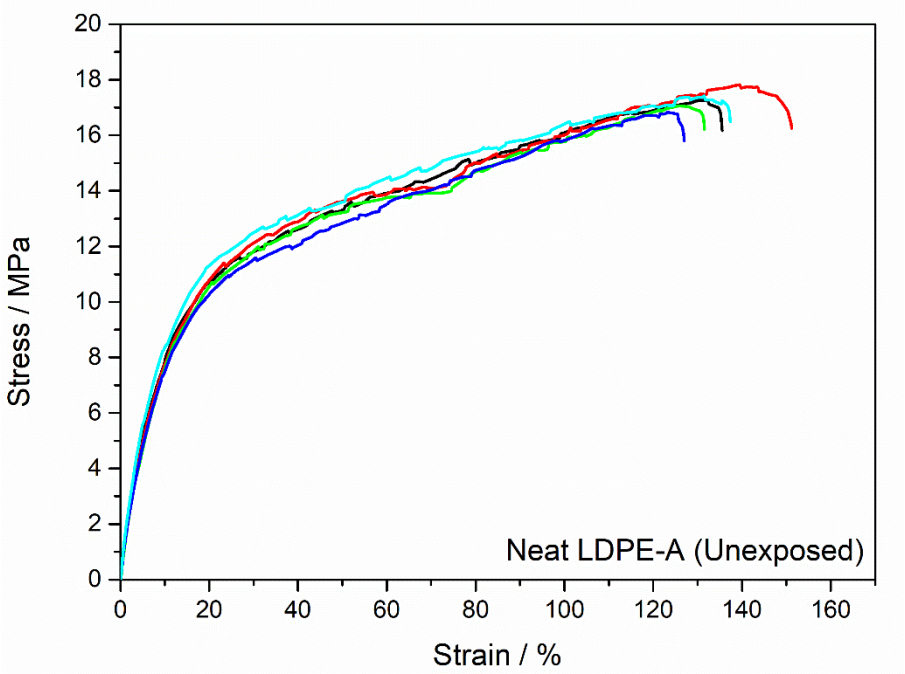
Stress / MPa
Strain / %
Neat LDPE-A (Unexposed)
0
2
4
6
8
10
12
14
16
18
20
0
20
40
60
80
100
120
140
160

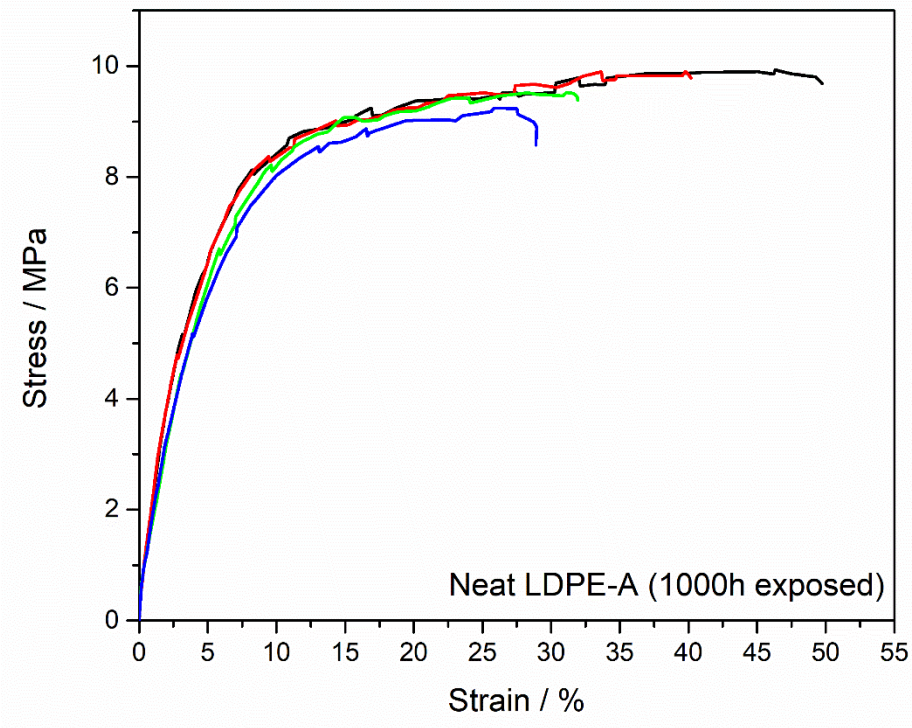
Stress / MPa
Strain / %
Neat LDPE-A (1000h exposed)
0
2
4
6
8
10
0
5
10
15
20
25
30
35
40
45
50
55

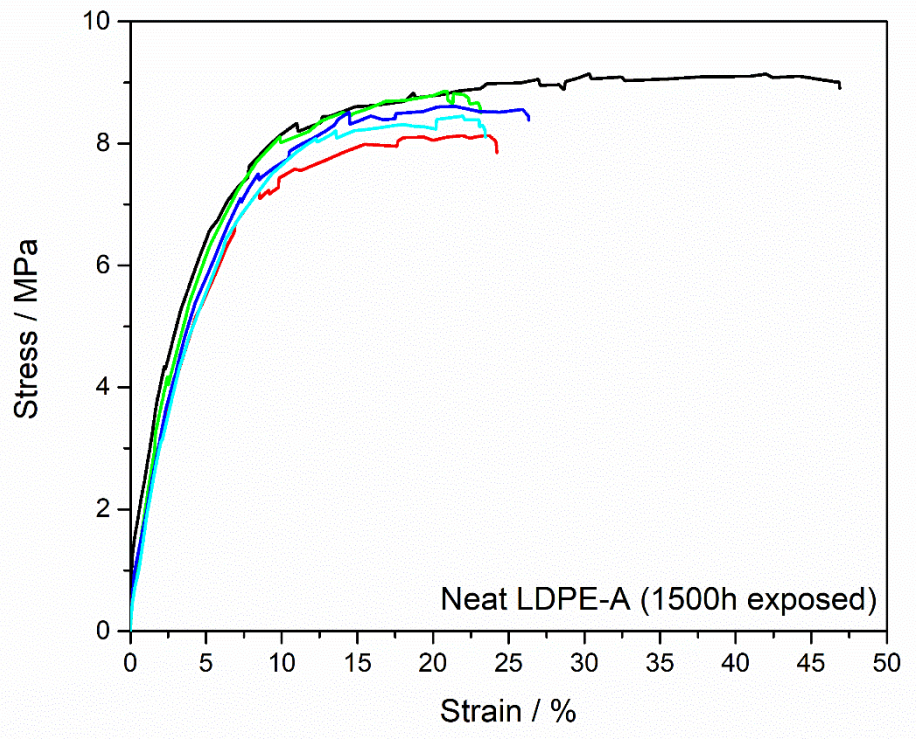
Stress / MPa
Strain / %
Neat LDPE-A (1500h exposed)
0
2
4
6
8
10
0
5
10
15
20
25
30
35
40
45
50

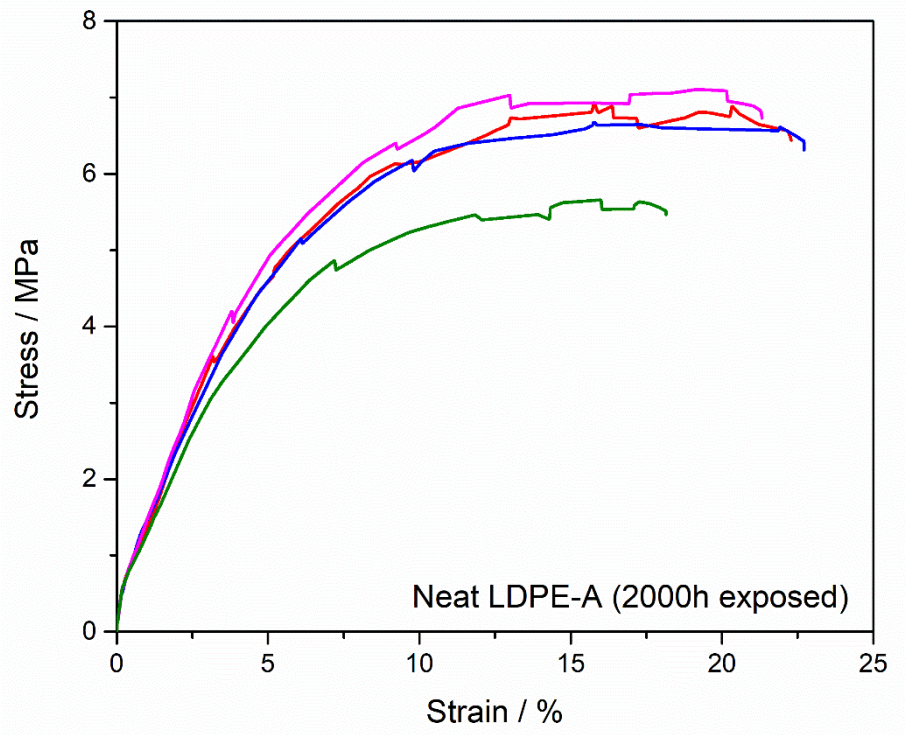
Stress / MPa
Strain / %
Neat LDPE-A (2000h exposed)
0
2
4
6
8
0
5
10
15
20
25

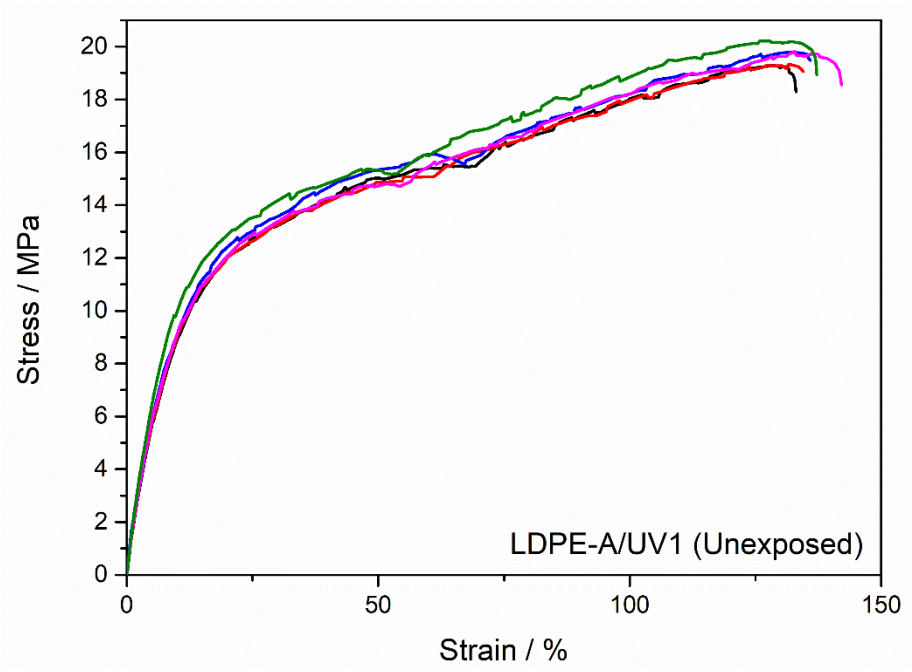
Stress / MPa
Strain / %
LDPE-A/UV1 (Unexposed)
0
2
4
6
8
10
12
14
16
18
20
0
50
100
150

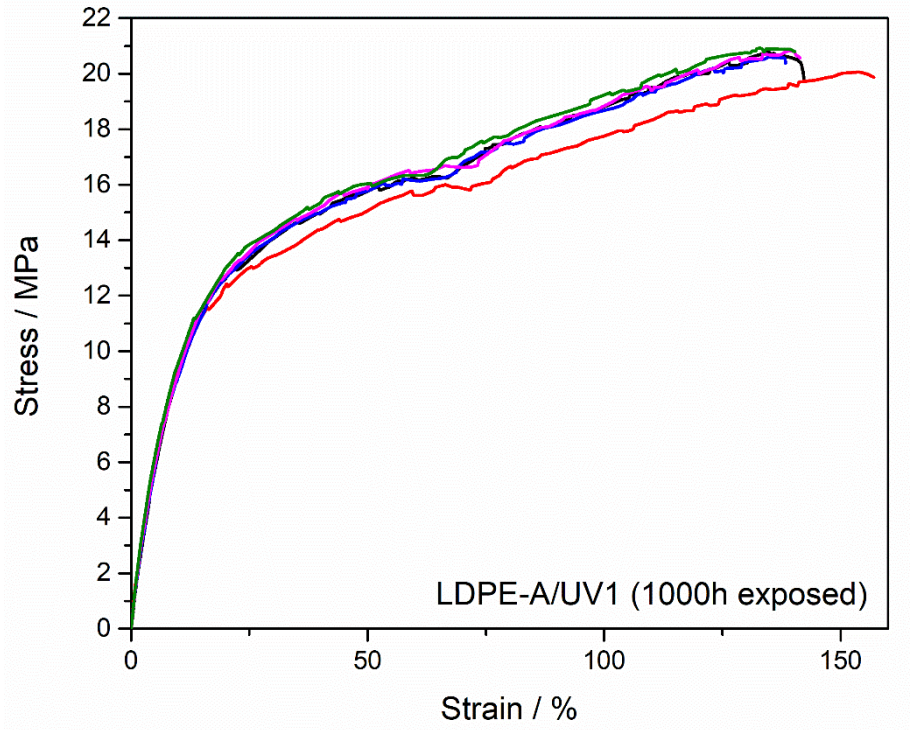
Stress / MPa
Strain / %
LDPE-A/UV1 (1000h exposed)
0
2
4
6
8
10
12
14
16
18
20
22
0
50
100
150

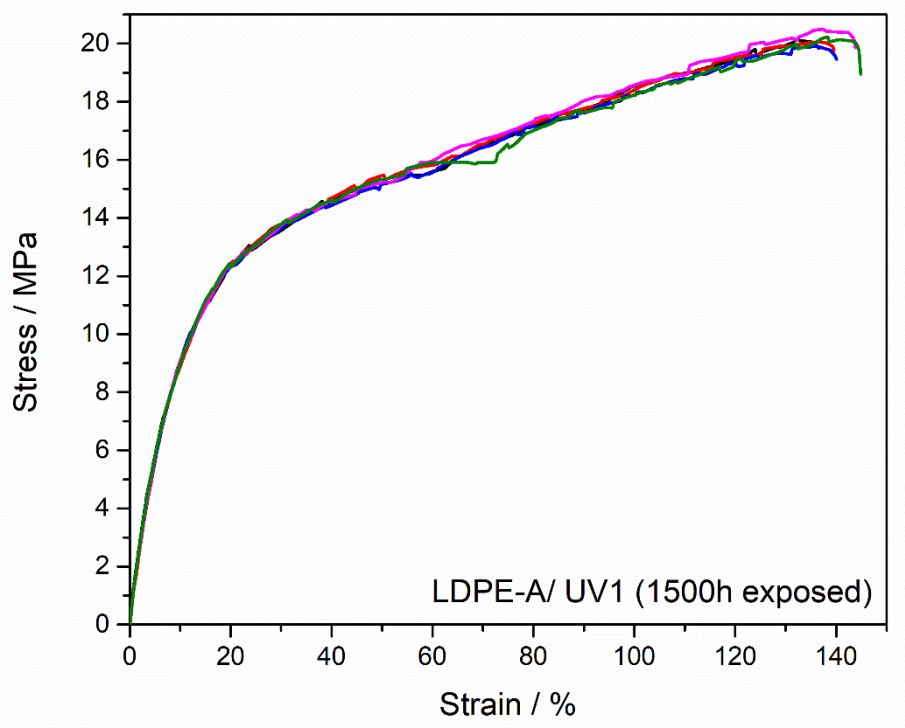
Stress / MPa
Strain / %
LDPE-A/ UV1 (1500h exposed)
0
2
4
6
8
10
12
14
16
18
20
0
20
40
60
80
100
120
140

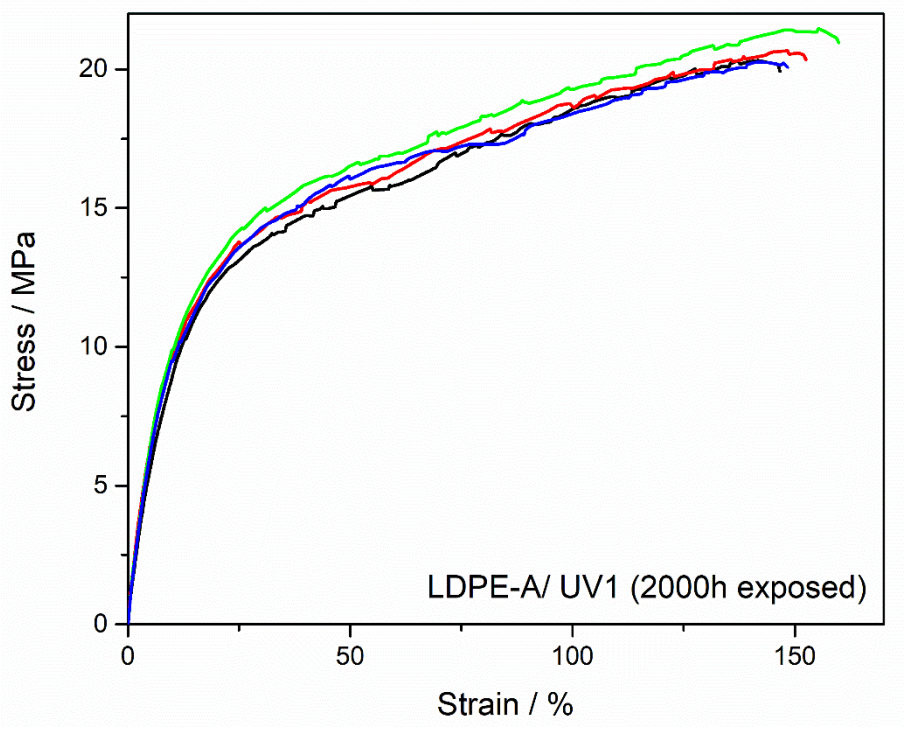
Stress / MPa
Strain / %
LDPE-A/ UV1 (2000h exposed)
0
5
10
15
20
0
50
100
150

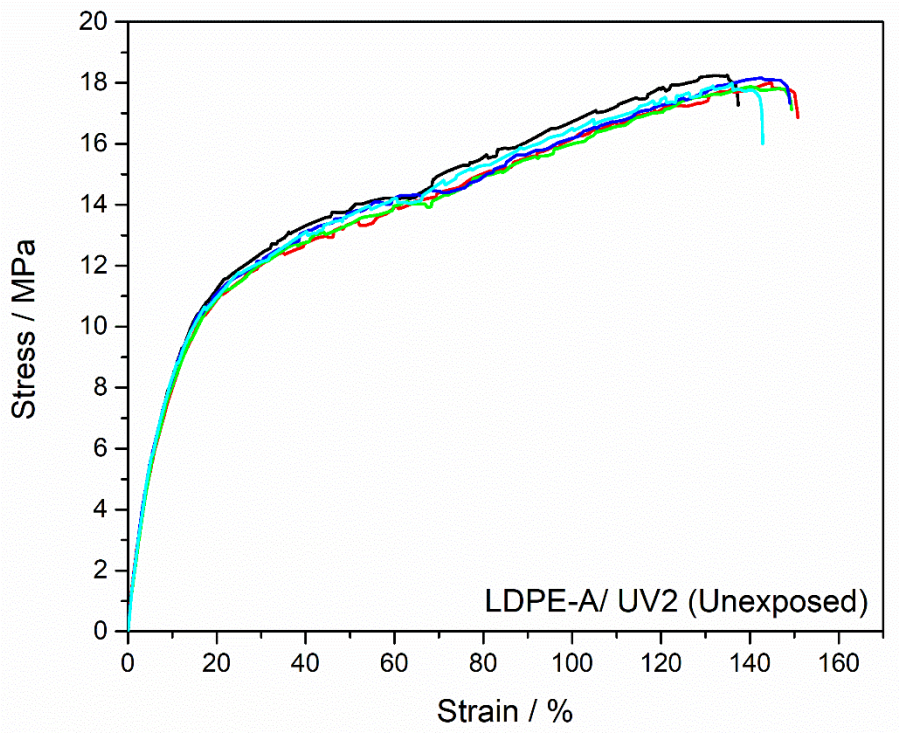
Stress / MPa
Strain / %
LDPE-A/ UV2 (Unexposed)
0
2
4
6
8
10
12
14
16
18
20
0
20
40
60
80
100
120
140
160

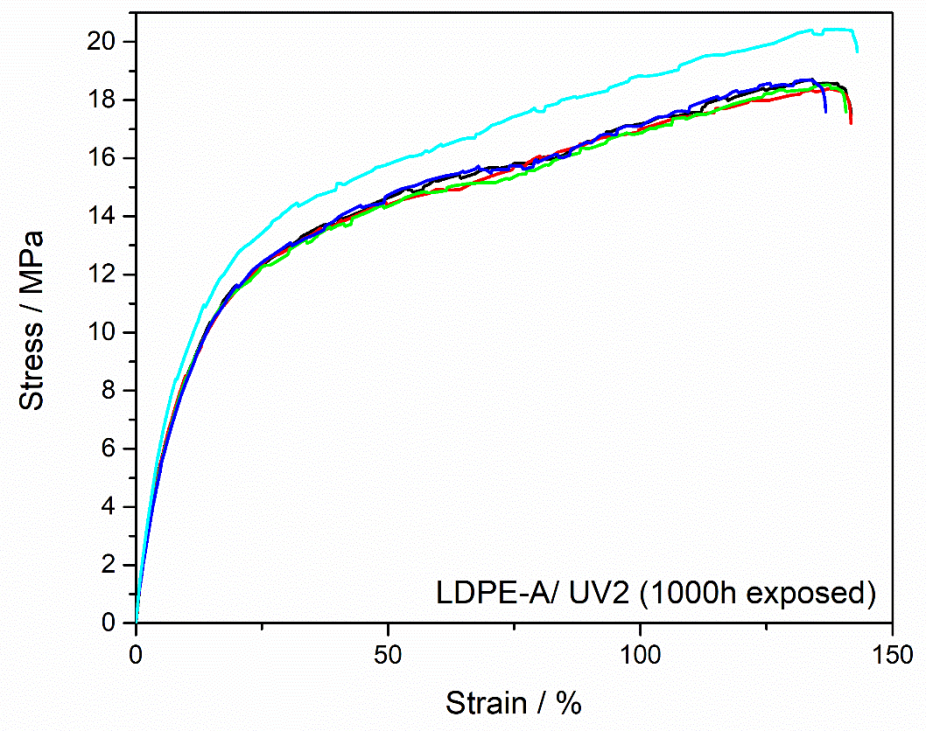
Stress / MPa
Strain / %
LDPE-A/ UV2 (1000h exposed)
0
2
4
6
8
10
12
14
16
18
20
0
50
100
150

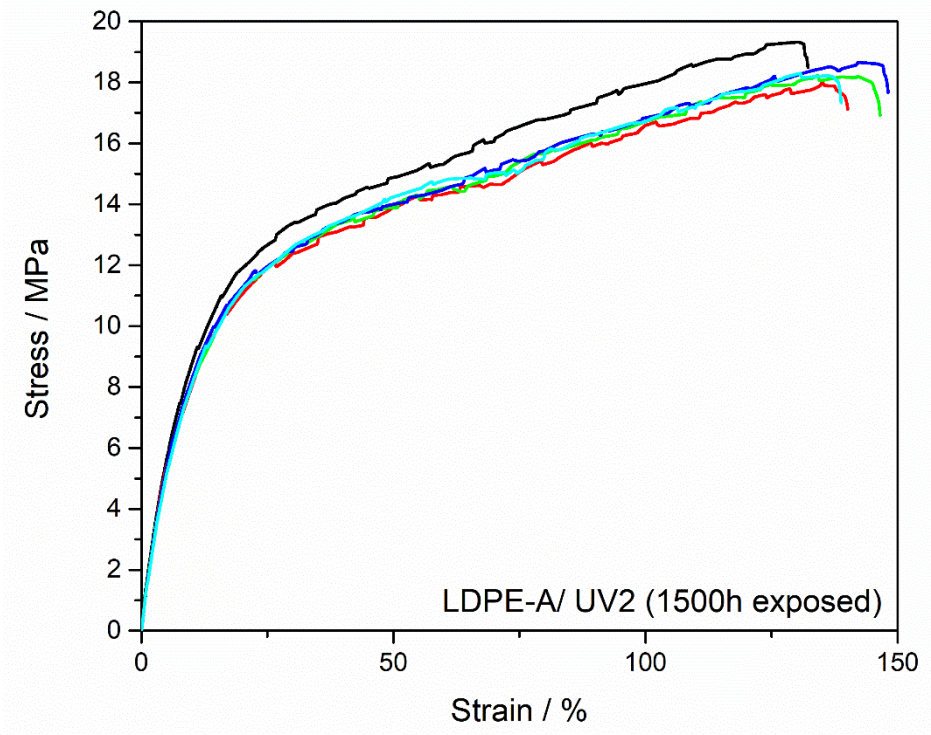
Stress / MPa
Strain / %
LDPE-A/ UV2 (1500h exposed)
0
2
4
6
8
10
12
14
16
18
20
0
50
100
150

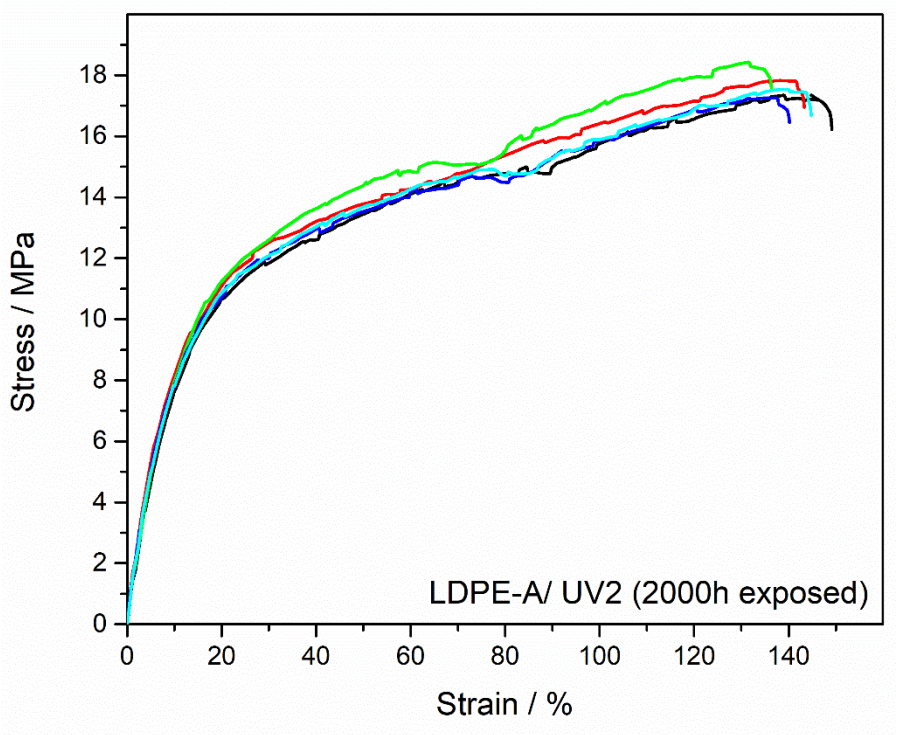
Stress / MPa
Strain / %
LDPE-A/ UV2 (2000h exposed)
0
2
4
6
8
10
12
14
16
18
0
20
40
60
80
100
120
140